Enhanced Cellulose Fiber for Polymer Composites

by

Douglas Casetta

A thesis

presented to the University of Waterloo

in fulfillment of the

thesis requirement for the degree of

Master of Applied Science

in

Chemical Engineering

Waterloo, Ontario, Canada, 2020

©Douglas Casetta 2020

Author's Declaration

I hereby declare that I am the sole author of this thesis. This is a true copy of the thesis, including any required final revisions, as accepted by my examiners.

I understand that my thesis may be made electronically available to the public.

Abstract

In recent years, interest in renewable, environmentally friendly and low-cost materials has grown and has become a global trend. In view of the high consumption of petrochemical plastics that use reinforcing agents such as talc, calcium carbonates, and synthetic fibers to improve their performance, there is an opportunity for cellulose fibers to replace these materials. Cellulose fibers mainly meet this need, as they have very good mechanical properties, low density, high specific resistance, non-abrasive, renewable, ecological and biodegradability characteristics.

Cellulose fiber is produced mainly for the paper and packaging industry. However, cellulose fiber available in regular processes is not suitable for polymer composites because it is highly aggregated. Most studies in literature about cellulose dewatering (filtration) are based on batch processes. To the best of our knowledge, there are no studies in the literature about continuous dewatering (filtration) of cellulose with additives suitable for polymer composites. For this reason, this work studied the variables in a continuous filtration process (rotating drum) that affect the dehydration (filtration rate) of the mixture of cellulose and additives for polymer composites applications. It also correlated the process variables and formulation with the dispersion of cellulose fibers in the polymer matrix and the performance of the polymer composites.

The results showed that vacuum pressure and consistency were the parameters with higher influence in the quality of the cake. The addition of PP fibers and surfactant reduced the aggregation of cellulose fibers allowing to produce injection moulded samples without the need of pre-extrusion. The composites produced via direct injection moulding (without pre-extrusion) showed similar results to the ones produced using the traditional method (extrusion followed by injection moulding) with substantial increase in stiffness and a small reduction in the impact strength.

Acknowledgements

First, I would like to extend my deepest appreciation and gratitude to my academic advisor Dr. Leonardo Simon for his constant support and guidance during this incredible journey. I also would like to thank my committee members Dr. Luis Sandoval and Dr. Tizazu Mekonnen for generously giving their time to be part of my thesis reading committee.

I would like to thank my colleagues in the laboratory in particular Abdulelah Hakami, Andrew Finkle, Chong Meng, Dinesha Ganesarajan, Franciele Turbiani, Gurkamal Saggu, James Kim, Mirela Vanin, and Ryan Park for making this journey more enjoyable.

I want to express my thanks for Department of Chemical Engineering's administrative and technical staff, especially to Judy Caron for helping me in decisive moments and to Bert Habicher for all the support in my project.

I owe a huge debt of gratitude to my dear friends, Adriana Casali, Alexandre Francis, Charles Dal Castel, Guilherme Drechsler, Hassan Moussa, Mariana Beauvalet, and Rosane Rech for all of their encouragement and support. I will be forever grateful.

I am grateful for the support of my family members: Carmelina (mother), and Tania (sister); and my great friends Edson Aleixo, Lucianno Colombo, and Manoel Lisboa, who supported me from a distance and encouraged my development. Thank you very much!

Last but not least, I owe a huge debt of gratitude to my wife Adriana. This work would not be possible without her patience and everlasting support. Thank you always!

Dedication

I want to dedicate this thesis work to both my sons, Davi and Dante, who were always happy to help me practice my oral presentations. I hope that my dedication and enormous effort to complete this important work can be an inspiration for their academic lives.

Table of Contents

List of Figures

List of Tables

Chapter 1: Introduction

1.1 Background and Motivation

Due to economic, political and environmental issues, research on materials based on sustainable sources has grown significantly in recent years. Therefore, there is a market trend towards a considerable increase in the use of natural fibers in reinforcement for plastic materials. This is due to factors such as the fluctuation of prices in petrochemical plastics and the increasing pursuit of low-cost, renewable and environmentally friendly raw materials. Natural fibers mostly fulfil that need as they have fairly good mechanical properties, low cost, low density, high specific strength, non-abrasive, renewability, eco-friendly and bio-degradability characteristics. Natural fibers are exploited as a replacement for other synthetic fibers such as glass, aramid and carbon [1], [2]. In this way, with so many positive characteristics that natural fibers can put into effect to improve the performance of plastic materials, their use has been increasingly explored. Thus, many plastic composites have a percentage of one or more types of natural fibers that can be obtained from flax, hemp, jute, sisal, kenaf, coir, kapok, bananas, henequen and many other sources. Table 1 lists the most common natural fibers used commercially in the world [2]. These composite materials are appropriately relevant for aerospace, leisure, construction, sport, packaging and automotive industries, as shown in Figure 1. The need to improve fuel efficiency in transportation has driven major efforts to produce lightweight materials with reasonable cost. Glass fiber has been dominant in the reinforcement of composites for automotive applications because it presents an excellent balance of properties and cost. Carbon fiber has been extensively investigated for use in composites in the automotive industry, but its elevated cost has limited its application in high volume affordable vehicles. The use of natural fibers has swiftly increased in the automotive industry. Figure 2 shows examples of several car parts and components containing natural fibers.

Table 1: The most common natural fibers used commercially, adapted from [2].

Fiber Source	Global Production (10^3 ton)
Sugar cane bagasse	75000
Bamboo	30000
Jute	2300
Kenaf	970
Flax	830

Despite their excellent properties and the advantages of utilizing them, natural fibers also present certain disadvantages when used as fillers in polymeric composites, such as limited processing temperature, high moisture absorption and incompatibility with more common thermoplastics like polypropylene. Most of the problems related to natural fibers are due to the hydrophilic groups present in their chemical structure and the intrinsic morphology of the fiber owing to its origins as plant material.

Developing new technologies for high performance applications is the challenge for specialists to improve the use of natural fibers with petroleum-based materials. So far, the automotive industry has adopted several types of bast fiber (hemp, sisal, knaf) in thermoplastic and thermoset composites. These fibers are used as non-woven mats, woven mats or chopped short fibers (2-10 mm). On the other hand, the cost of cellulose pulp is lower than that of bast fibers, but its use as a feedstock in automotive composites has not been explored to the same extent. The constant search for technologies to accelerate production processes and reduce costs is also a motivation for researchers and scientists globally. In this scenario, the use of cellulose pulp in the fabrication of automotive composites may result in novel materials that are lightweight, sustainable and cost effective, while maintaining the necessary characteristics required by the injection moulding process widely used in automotive manufacturing.

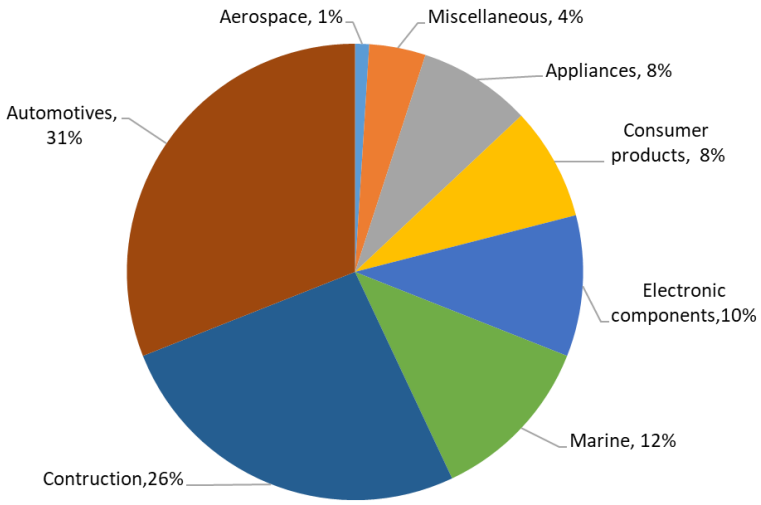

Figure 1: Fiber reinforced plastic composite by commercial segments, adapted from [2], under the Creative Commons Attribution License.

Figure 2: Automobile components made of natural fiber composites [2], under the Creative Commons Attribution License.

1.2 Scope

The dispersion of cellulose in a polypropylene matrix followed by a drying step is a major challenge for the use of cellulose pulp in thermoplastic composites. Other materials like glass fiber and talc, for example, do not require any substantial amount of drying before compounding with polypropylene. The process of compounding polypropylene and cellulose using an extruder requires either drying the cellulose fiber prior to feeding the extruder or removing the moisture during extrusion. This research developed lab-scale continuous drum filter system and correlated the filtration operation variables with the quality of cellulose aiming polymer composite fabrication. These hybrid composites combine cellulose fiber in a polypropylene (PP) matrix to improve the overall properties of the composite. In particular, this study will assemble and evaluate a continuous filtration rotary drum that carries out the dehydration (filtration rate) of the cellulose blend as a viable option for reinforcing polypropylene.

The specific objectives of this research were:

- To assemble a lab-scale continuous drum filter system as a research tool;
- To evaluate the effect of the operational conditions on the filtration rate and visual aspect of the cake;
- To obtain different blends of cellulose and PP using the lab-scale continuous drum filter system;
- To evaluate the processability of the cellulose-PP blends in injection moulding (with or without prior extrusion).

The composites were produced with various cellulose fillers obtained through the filtration system. These fillers were composed of cellulose fibers, PP fibers and additives. These fillers were mixed with PP

pellets through injection moulding (with or without prior extrusion by means of a twin-screw extruder). The filtration system variables (pressure, consistency and rotation) were investigated to optimize the filtration rate and deliver a continuous and uniform pulp. This research also assessed the effect of combining cellulose loading on composite properties (microscopy and mechanics) to investigate strategies for optimizing the performance properties of compounds.

This research attempts to provide a comprehensive study on the development of continuous cellulose dehydration (filtration) with additives suitable for polymer composites. The cellulose fiber available from regular processes is not suitable for polymer composites because it is highly aggregated. Another challenge of incorporating cellulose in polyolefins, such as polypropylene, is surface compatibility, given the hydrophilic nature of the cellulose and the hydrophobic nature of polypropylene. Adhesion of the filler to the polymer matrix is critical because the role of the matrix in a fiber reinforced plastic structure is to transfer the load to the rigid fibers through shear stresses at the interface; this requires strong adherence [3]. Good fiber dispersion and strong bonding capabilities between the filler material and the matrix are desirable. Moreover, weak binding sites promote empty structures and particle agglomeration. Therefore, it is essential to design and maximize interfacial dispersion, filler and matrix interaction to obtain better processability and material properties.

1.3 Structure of the Thesis

This thesis is organised in 6 Chapters, as summarized in Figure 3. Chapter 1 presents the research problem, research approach and project goals. Chapter 2 consists of a literature review to provide a background of past research relevant to this thesis. Chapter 3 describes the materials and experimental procedures used in this research project. The experimental results are organized and discussed in Chapters 4 and 5, with Chapter 4 focusing on the newly created filtration system and Chapter 5 on the polymeric composites. Finally, Chapter 6 describes conclusions as well as recommendations for future work.

<table>
<tr><td colspan="3">1.0 Introduction</td></tr>
<tr><td colspan="3">2.0 Literature Review</td></tr>
<tr><td colspan="3">3.0 Materials and Methods</td></tr>
<tr><td colspan="3">4.0 Filtration System Assembly and Cake Samples</td></tr>
<tr><td>Materials</td><td>Processing</td><td>Characterization</td></tr>
<tr><td>Dry Cellulose + Water (CW cake)</td><td rowspan="3">Mixer

Filtration

Dry</td><td rowspan="3">Filtration Rate
Visual Rate</td></tr>
<tr><td>Dry Cellulose + Water + PP (CWPP cake)</td></tr>
<tr><td>Dry Cellulose + Water + PP + Additives (CWPPS cake)</td></tr>
<tr><td colspan="3">5.0 Polypropylene Compounding with Sample from Filtration System</td></tr>
<tr><td>Materials</td><td>Processing</td><td>Characterization</td></tr>
<tr><td>PP + Dry cellulose</td><td rowspan="4">Cut

Extrusion

Mill

Injection</td><td rowspan="4">Flexural Tests
Impact Tests
SEM</td></tr>
<tr><td>PP + CW cake</td></tr>
<tr><td>PP + CWPP cake</td></tr>
<tr><td>PP + CWPPS cake</td></tr>
<tr><td colspan="3">6.0 Conclusions and Recommendations</td></tr>
</table>

Figure 3: Thesis diagram.

Chapter 2: Literature Review

In the last few years, environmental concerns have stimulated the replacement of composites reinforced with synthetic fibers by composites made with natural fibers. This was due to the many advantages of composites with plant fibers, such as biodegradability, renewable sources, the relatively low cost of raw materials used to manufacture them, as well as the fact that such materials are lightweight. According to recent studies, cellulose fibers have an appealing potential to reinforce polypropylene composites and the resulting mechanical properties [4].

This chapter describes past research as it pertains to composites of polypropylene as well as properties of polypropylene and its relevance in manufacturing automotive parts, cellulose fibers and its properties (cellulose pulp), surfactants and solid-liquid filtration process.

2.1 Composites

Composites are formed by the combination of two or more materials or phases of different natures called matrix and filler material. The matrix (continuous phase) and filler (discontinuous, dispersed or load phase) combine to constitute a multiphase material that exhibits a significant proportion of the properties of both constituents. The objective when producing a composite is to achieve superior performance properties compared to that of its individual constituents [5], [6].

The properties of a composite material are determined by the properties of its constituents, i.e. the geometry of the reinforcements (filler), their distribution, orientation and concentration in the matrix (the latter usually being measured by the volume fraction or fiber volume ratio), as well as the nature and quality of the matrix-reinforcement interface. Figure 4 shows examples of composite materials with different forms of constituents and distributions of the reinforcements. Composites can be classified according to the form and distribution of their constituents. Particulate reinforced composites are formed by large particles or by

dispersion. Fiber reinforced composites are formed by continuous or discontinuous fibers, which are either aligned or randomly oriented (see Figure 5) [5]–[7].

The type of reinforcement used can be chosen to meet all or some of the requirements for the new material, such as strength, rigidity, heat resistance, corrosion and conductivity. However, for the reinforcement to be advantageous, it must be stronger and more rigid than the matrix. Therefore, strong interaction between matrix and reinforcement can be guaranteed by creating an interface between both where the stiffness of the reinforcement is adapted to the ductility of the matrix [5], [6].

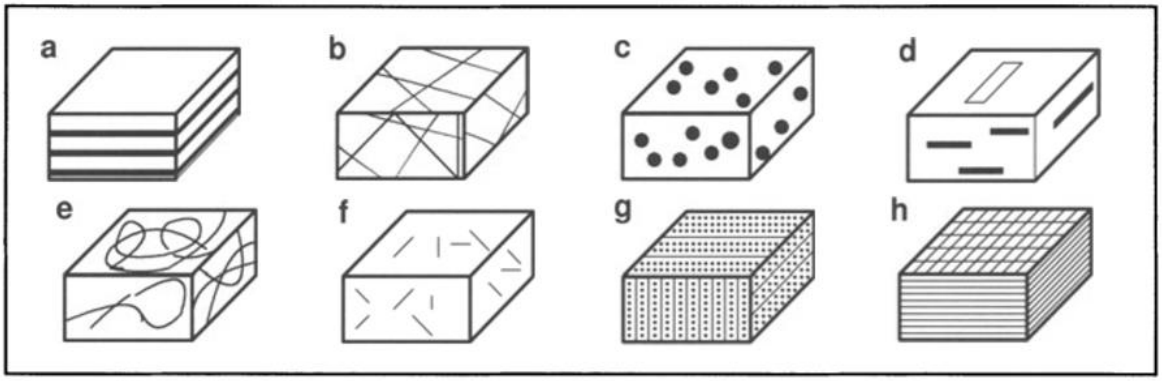

Figure 4: Examples of composite materials with different forms of constituents and distributions of the reinforcements. a) laminate with uni or bidirectional layers; b) irregular reinforcement with long fibers; c) reinforcement with particles; d) reinforcement with plate strapped particles; e) random arrangement of continuous fibers; f) irregular reinforcement with short fibers; g) spatial reinforcement; h) reinforcement with surface tissues as mats, woven fabrics, among others [5], under the Springer Nature and Copyright Clearance Center.

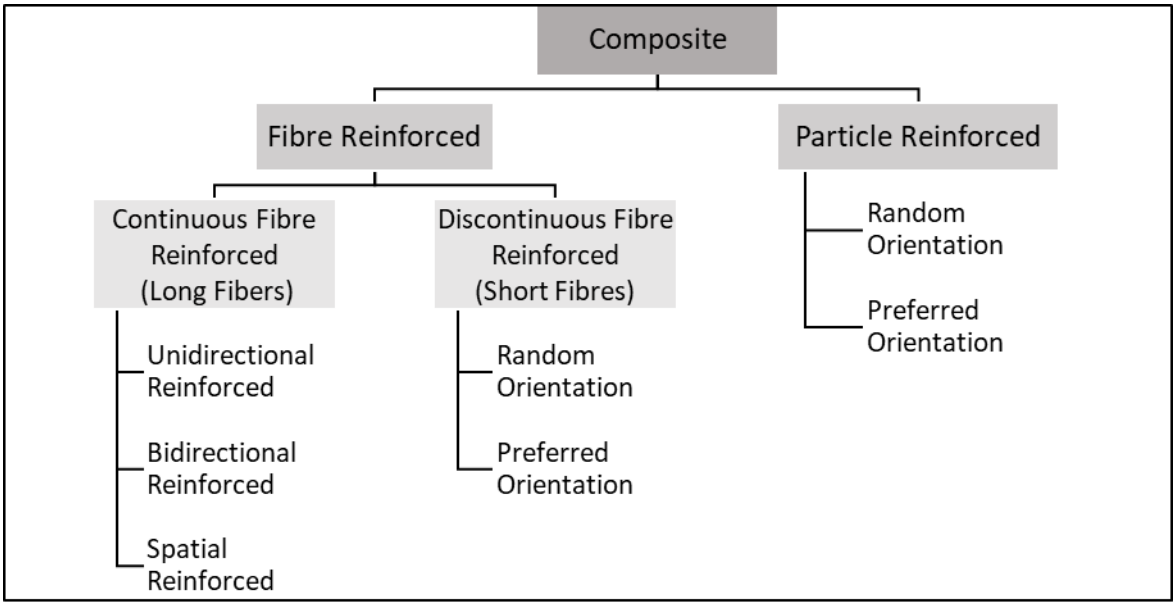

Figure 5: Classification of composites, adapted from [6], under the Springer Nature and Copyright Clearance Center.

Plastics composites are developed to improve the performance of products and meet specific applications to attend the necessity of society [5]. The critical purpose of composite material is to improve the properties by combining two or more different materials together. The idea of composite is applied not only to plastics but also to metals and ceramics.

A prerequisite to form an adhesive bond between fiber and polypropylene matrix is that they have to come into close molecular contact. For fiber-reinforced polymer composites, the ability of a given polymer melt to wet a fiber surface depends on the surface tension of both materials. A general condition that must be fulfilled for wetting exist when the polarities of the two phases match each other. The mechanisms that cause two materials to adhere one to another are not well understood and various mechanisms for stress transfer across the interface are possible. The most accepted theories are adsorption

and bonding, diffusion, electrostatic attraction and mechanical interlocking. Figure 6 shows schematics of these theories [8], [9].

Adsorption and attraction may be the result of relatively weak interactions or primary bonds (ionic, covalent and covalent) across the interface. Primary bonds represent one of the strongest types of interaction and thus an important interfacial adhesion mechanism. Electrostatic attraction is the result of concentration of particles charged with opposite polarities on each surface attracting one to another. Mechanical interlocking adhesion is the result of mechanical interlocking and consequently is strongly influenced by surface roughness. This requires micro-voids and micro-cavities of fiber. Interfacial adhesion can be the result of combined effects of more than one of these mechanisms, consequently interfacial bond strength interpretation is complicated [8], [9].

Some of the difficulties in using natural fibers as reinforcement in polymer matrix composites are related to a few things such as, the relatively low thermal stability of natural fiber, susceptibility to moisture and the fiber decomposition during compounding with the polymer matrix, which leads to significant fiber breakage and alteration of the morphology and the final properties of the composite. However, one of the biggest and fundamental problem in natural fiber reinforced polyolefin composites is the low adhesion between the fiber and the polymer matrix. Bonding between the matrix and the fiber is dependent on the atomic arrangement and chemical properties of the fiber and on the molecular conformations and chemical constitution of the polymer matrix. Therefore, the interface is specific to each fiber-matrix system [1], [10].

In addition, adequate fiber dispersion in the polymeric matrix is a significant factor in the performance of composites. Mass production polymeric materials must be cost-effective, accessible and proven. Appropriate composites can be produced using PP with glass fiber, talc, clay or cellulose fiber and applying processing methods such as injection moulding [11].

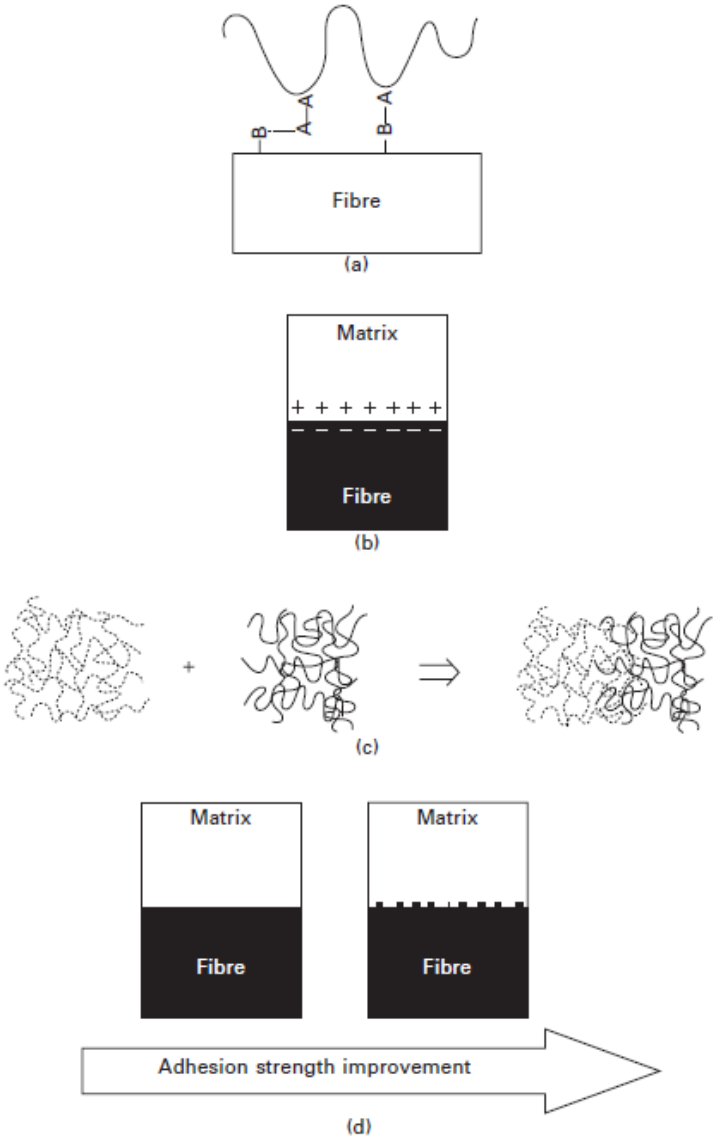

Figure 6: Schematic drawings of the most accepted adhesion mechanism theories of fiber-polymer composite materials: (a) adsorption and bonding, (b) electrostatic attraction, (c) diffusion or interpenetrating network, (d) mechanical interlocking [7], under the Elsivier and Copyright Clearance Center.

2.1.1 Polypropylene with Glass Fiber and Talc

Several inorganic fillers have been used to improve mechanical properties in Polypropylene. Among these fillers, glass fiber has been used as reinforcement for decades [6]. Glass is a great reinforcing agent because it has a high tensile strength (above 3.6 GN / m^2) and a high Young's modulus (94 GN/m^2).

Glass fibers have high dimensional stability, do not undergo creep and these characteristics are passed on to composites reinforced with these fibers. Since glass is a relatively inert material, fibers are also immune to biological attacks and are resistant to attacks by solvents and chemicals. Glass fibers are non-flammable and have good electrical properties [12], [13].

Glass fibers are generally 5 to 20 μm in diameter and their surfaces are not flaw-free. When compounds are processed, the fibers become shorter especially in the case of injection moulding in which great stress is applied to melt [13].

Himani and Purnima [14] studied the mechanical properties and morphology of glass fiber reinforced polypropylene. As shown in Table 2, the mechanical behaviour of glass fiber reinforced PP composites is significantly better than that of non-reinforced PP.

Table 2: Mechanical properties of PP and GF, adapted from [14].

Mechanical Properties	PP Neat	70 PP/ 30 Gf (wt%)
Tensile Strength (MPa)	31.0	35.3
Tensile Modulus (MPa)	336.4	565.4
Elongation at maximum force (%)	12.2	7.1
Flexural Strength (MPa)	39.2	53.1
Flexural Modulus (MPa)	1076.7	3229
Impact Strength (J/m)	25.5	32.2

Among many different mineral fillers for the dispersed phase in composites, talc stands out given that its particle geometry is different, which allows improvements in other mechanical properties of the composites through changes in the fracture mechanism of these materials [5], [15], [16].

Talc is sourced from mineral deposits known as hydrous magnesium silicate, which can be found around the world. The typical composition of talc consists of 31.7% MgO, 63.5% SiO_2 and 4.8% H_2O, but this can vary depending on the ore. Talc is a very soft mineral (Mohr's hardness=1) and it is highly hydrophobic in nature. Its particle size typically ranges from 1 μm to 30 μm [17], [18].

When added as a filler with thermoplastics (polypropylene), talc increases the stiffness of the composite and improves its dimensional stability [17]. The amount of talc also affects composite stiffness [19], [20]. Several studies on talc composites based on PP matrices have shown improvement of mechanical properties such as tensile strength and modulus, as well as reduced impact strength [17], [21].

The study of polypropylene composites with a dispersed talc phase has evolved significantly, given that it has been widely used in the automotive industry for many years. For example, it is employed in under-the-hood components, dashboards, bumpers, as well as interior and exterior trim and other automotive parts [21]. It stands out because of its numerous advantages, due to its low cost and because it promotes the modification of mechanical properties, such as increased modulus of elasticity [17], [21].

2.1.2 Polypropylene with Cellulose

Although conventional reinforcing fillers such as glass fiber and talc were able to overcome dimensional stability issues and effectively improve mechanical properties, bio-based fillers have received increased attention due to their unique characteristics. Many bio-based fibers can be used as fillers in polypropylene. Examples include wood pulp, jute, kenaf, sisal, hemp and many others. Not only do these cellulosic fibers have high specific strength and stiffness, low density, high aspect ratio, but they also have

the advantages of being biodegradable, nontoxic, renewable, low cost and nonabrasive to equipment [22], [23]. Polypropylene-based composite with cellulose fibers can be especially interesting for the automotive industry. They are lightweight, which improves fuel efficiency, and have better sound abatement capability and shatter resistance than glass fiber composites [24].

Cellulose fibers are hydrophilic and polar, whereas polypropylene is hydrophobic and non-polar in nature. The weak bonding between the polymer matrix and fiber is caused by a large difference in the respective surface energies of the two materials, which is linked to the existence of the hydroxyl groups and C-O-C links on the surface of the cellulose fiber. This fact results in poor bonding between the fibers and the matrix, which prevents the necessary wetting of the fibers by molten polymer leading to poor dispersion of the fibers, insufficient reinforcement and poor mechanical properties. Moreover, a weak interface means deficient stress transfer from the matrix to the fibers through shear stresses at the interface [9], [10].

Suzuki *et. al.* [25] investigated the dispersion of cellulose pulp fibers into the matrix to examine the engineering process and the microfibrillation of the cellulose pulp. Two processes were used to prepare the polypropylene reinforced composites (shown in Figure 7). The first consisted in disintegration of the pulp using a bead mill followed by a melt-compounding process with PP (B-MFC-reinforced PP). The second was disintegration of the pulp mixed with PP using a twin screw extruder followed by a melt-compounding process (T-MFC-reinforced PP).

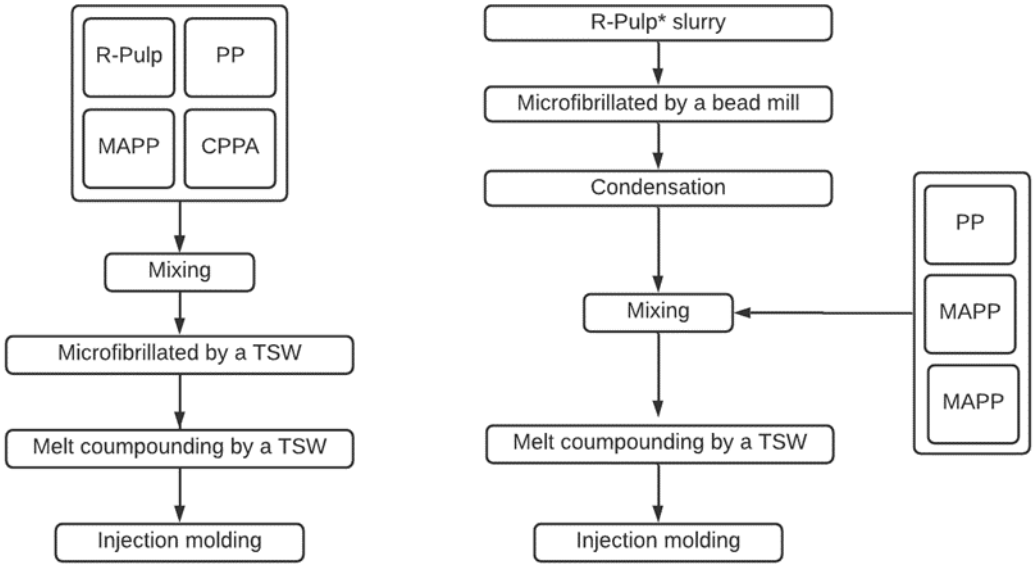

Figure 7: The composite preparation procedures, adapted from [25], under the Springer Nature and Copyright Clearance Center.

Scanning electron microscopy showed that the B-MFC method enabled a more uniform microfibrillation of the pulp, while the tensile modulus and strength of T-MFC composite were about 30% and 40% higher than those of the B-MFC composite. X-ray CT showed that B-MFC was more aggregated, while in T-MFC the fibers were longer and more aligned in the direction of injection. The manufacturing process of the T-MFC composite is more efficient than that of the B-MFC composite, which requires a concentrating process for the MFC slurry [25].

Huang *et. al.* [26] developed a process where acetic-oleic anhydride reacts mechano-chemically with cellulose in a ball mill. The reaction was successful for both ester residues (acetyl and oleic groups) and the degree of substitution was increased with longer milling time. Several composites were prepared using surface modified cellulose particles with different DS values and in a range of ratios from 10 to 90 % with PP. Surface modified cellulose particles cause a decrease in the melting torque value and complex viscosity of composites, improving melt processability. Modified surface particles showed lower water

absorption and improvement of elongation at break, compared to unmodified ones; this can be attributed to better particle dispersion, improved particle/matrix interfacial bonding and presence of crystal B phase. Also, high DS particle composites presented better processability, higher toughness, lower modulus and better water repellency. Employing a solvent-free method based in mechanochemical reaction in a ball mill avoided the use of toxic organic solvents and the necessity of drying, purification and recycling, thus eliminating process steps and generating less waste, making the process less expensive and greener.

Maleic Anhydride Grafted Polypropylene: usage of Maleic Anhydride Grafted Polypropylene (MAPP) is very common tool to enhance the interfacial bonding between the two phases. There are many studies that have proven the improvement in physical properties using maleate polyolefin in composite materials. The MAPP provides covalent bonds across the interface Figure 8 and understood the surface energy of the fibers rises [11]. The strong crystalline structure can be disrupted by substituting the hydroxyl groups with other chemical functionality. This process helps to improve the thermoplasticity of the cellulose since the new substituent acts as plasticizer. There are many techniques on thermoplasticization of natural fibers including alkali treatment, graft copolymerization, usage of coupling agents such as maleated polyolefin, etc. Through the treatment, better wettability and interfacial adhesion is reached. The optimum MAPP concentrations are determined experimentally to get the best results. There are various MAPP available commercially. Theoretically, very long chains of coupling agents (MAPP) with high contents of maleic anhydride would yield excellent covalent bonding to fiber surface. This is because a really long chain of MAPP would have a hard time migrating to the surface because of short processing times. However, if the chain length is too long, coupling agents have difficulty in finding the hydroxyl groups on the fiber surface [27], [28].

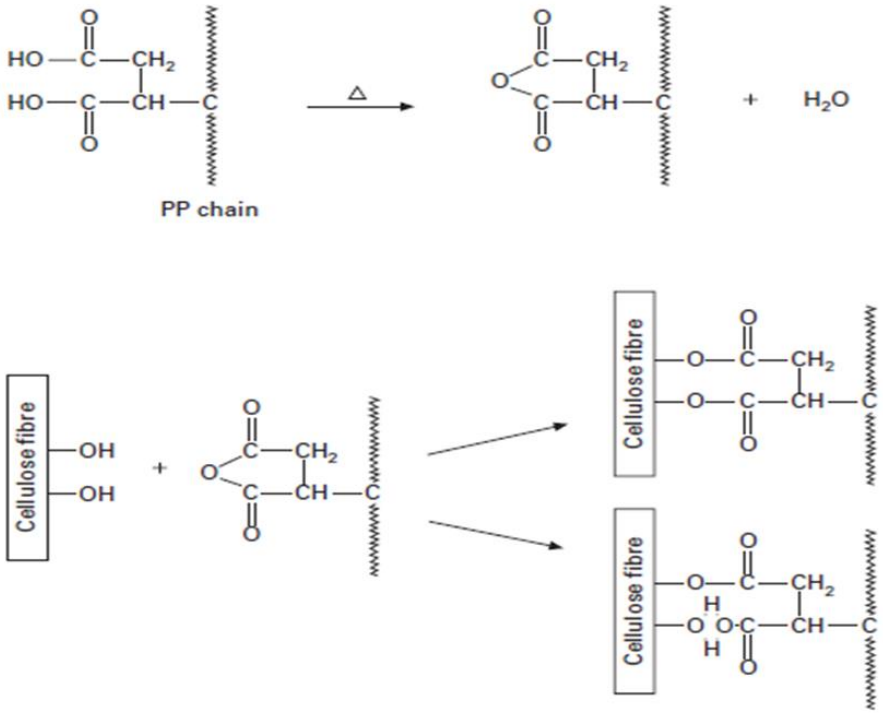

Figure 8: Model of reaction between cellulosic fibers and PP–MAPP copolymer [11], under the Elsevier License and Copyright Clearance Center.

Sullins *et. al.* [29] studied the flexural and tensile properties of hemp fiber reinforced polypropylene composites after material treatment. The addition of a maleated coupling agent, as well the alkaline fiber treatment, improved the interfacial adhesion between the hemp fiber and the PP matrix, and this caused an increase in the flexural and tensile properties of the resulting composites. The higher load of hemp fiber (30 wt%) leads to higher mechanical properties compared with a lower load (15 wt%) or neat PP, using the same material treatment. Adding 5 wt% of maleic anhydride grafted polypropylene (MAPP) and 15 wt% of hemp fiber to the PP caused an increase of 37 % in flexural strength, 37 % in flexural modulus, 68 % in tensile strength and 213% in tensile modulus compared with neat PP. The composite with 5 wt% MAPP and 30 wt% hemp fiber presented an increase of 91 % in flexural strength, 132 % in flexural modulus, 122 % in tensile strength and 297 % in tensile modulus. Absence of gaps between the fiber and the matrix

after fiber breakage and strong interfacial adhesion due to fiber wetting can be observed with SEM imaging (see Figure 9). This tends to lead to favorable mechanical properties.

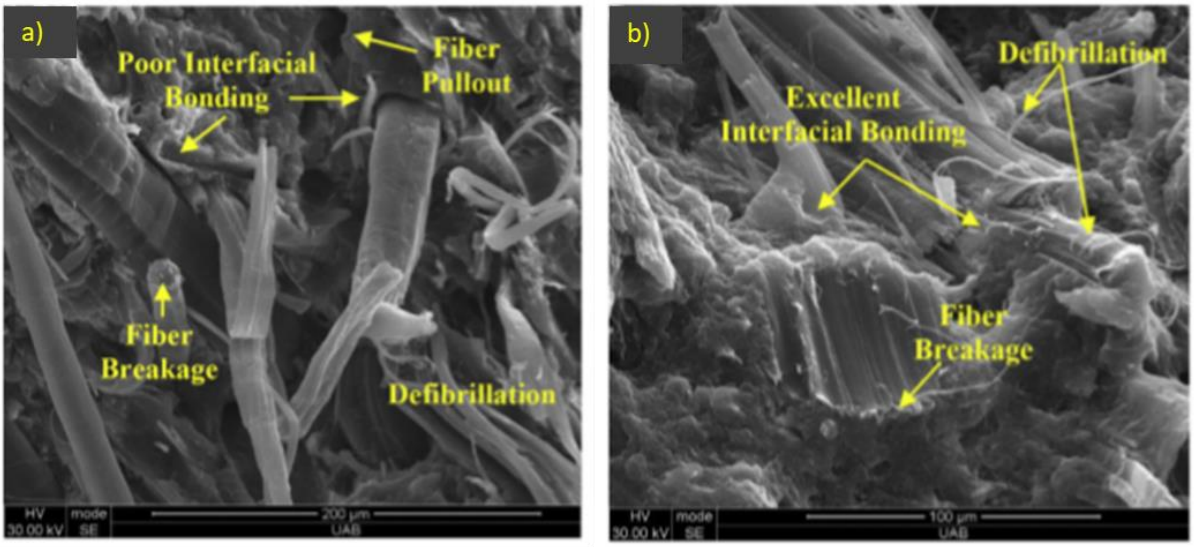

Figure 9: SEM images of 30 wt% hemp fiber reinforced PP composite fiber fracture surfaces of (a) without MAPP and (b) with 5 wt% MAPP, adapted from [29], under the Elsevier License and Copyright Clearance Center.

2.2 Polypropylene

2.2.1 Properties of Polypropylene

Polypropylene (PP) began to be produced in the early 50's and became commercially viable at the end of that decade. Among commodity plastics, PP is one of the most widely used in the world. It is employed in a variety of domains, and especially in the automotive, construction and packaging industries. PP is under the category of thermoplastics, which can be easily processed and re-processed. It can be reshaped effortlessly numerous times at high temperatures. Given this advantage, it is applied in many areas by means of various processing techniques. Polypropylene originates from the monomer called propylene (C_3H_6), which is polymerized by a poly-addition reaction process consisting of a polymerization technique

where unsaturated monomer molecules are added one at a time to a polymeric growth chain. Propylene monomers combine through a covalent bond resulting in the polymer chain shown in Figure 10. The molar mass is generally between 80,000 and 500,000 g/mol. It is a semi-crystalline polymer with a density of approximately 0.90-0.91 g/cm^3 and a refractive index of 1.45. It can be produced in three forms: isotactic, syndiotactic and atactic. Isotactic PP comprises approximately 99 % of all manufactured PP. Polypropylene exhibits strong hydrophobic and non-polar characteristics. For example, PP's water contact angle is as high as 90 to 110^o [30], [31].

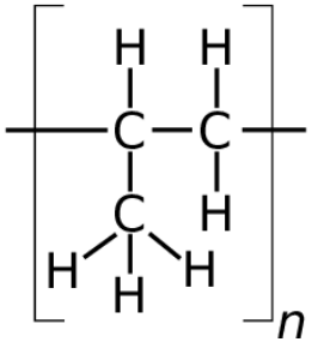

Figure 10: Chemical structures of polypropylene, image by author.

The mechanical properties of polymeric materials are determined by polymeric chain mobility, which is a function of atom agitation and is directly proportional to temperature. Consequently, polymer behaviour at elevated temperatures is related to dominant molecular structure and, as previously mentioned, PP is classified as a thermoplastic. Such plastics soften when heated and then harden when cooling, following reversible and repeatable processes. This is because secondary bond strength decreases when temperature is increased, which allows for greater molecular motion. If, however, temperature is raised beyond a critical threshold, polymer degradation becomes irreversible. The majority of thermoplastics are

linear polymers and have branches with flexible chains. Examples include polyethylene, polystyrene, and polypropylene [32], [33].

The crystallinity of polymers varies with their crystalline domain and chain configuration, but also depends on the cooling rate as they solidify; this is because chains must be brought into an orderly configuration during crystallization and this alignment requires sufficient time to occur [32], [33].

The most assessed properties of semi-crystalline polymers are rigidity and resistance. These are directly related to the elastic and plastic (viscous) deformations that such materials suffer [32]. Figure 11 illustrates the stages of these elastic and plastic deformations. Elastic deformation is the result of a lengthening of chain molecules in the amorphous domain in the direction of the tension applied to the material. This is stage 1 of the deformation, wherein there are two adjacent lamellas with folded chains and the amorphous domain is between them. In stage 2, changes occur in both the amorphous and crystalline domains. The amorphous chain continues to lengthen and the strong covalent bonds within the crystallites are folded and stretched. This generates a small, reversible increase in crystallite thickness. In stage 3, the deformation goes from being elastic to plastic, wherein adjacent chains within the lamellas slide away from each other, causing them to incline in such a way that the chain folds become more aligned. In stage 4, the crystalline blocks separate from the lamellas and the blocks stay tied to one another through the bond chains. In the last stage, the blocks and bond chains become oriented in the direction of the axis of traction. Reversibility of the processes illustrated in Figure 11 is possible if the deformation is interrupted or the temperature is raised and approaches the material's fusion point; said material will thus recrystallize, forming a spherulitic structure again. Various structural and processing factors intervene in the mechanical behaviour of polymers. Therefore, one can observe with Figure 11 that any restriction imposed on the processes occurring during the 5 stages described above will increase the resistance of the material [32].

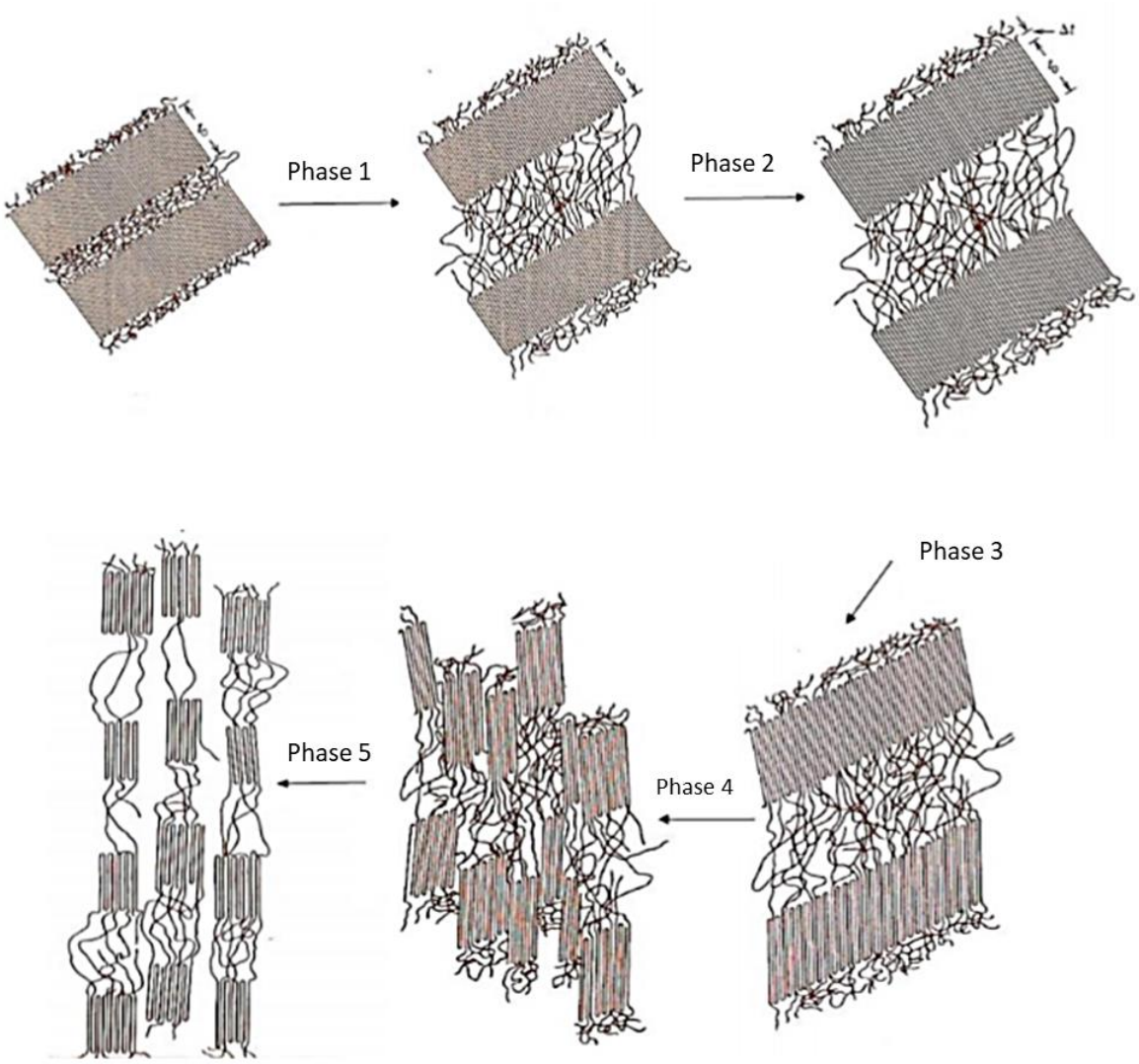

Figure 11: Stages of elastic and plastic deformations of a semi-crystalline polymer, adapted from [32], under the John Wiley and Sons and Copyright Clearance Center.

Along these lines, several semi-crystalline polymer properties depend on the crystallinity and morphology of the crystalline domains. The greater the crystallinity, the greater the density, rigidity, dimensional stability, chemical resistance, abrasion resistance, fusion point (T_m), glass transition

temperature (T_g), etc. In contrast, impact resistance, elongation at break, and optical clarity will decrease [32], [34]. Table 3 describes typical properties of PP compared to other polymer matrices [35].

Table 3: Typical properties of polymer matrices, adapted from [35].

Property	PP	LDPE	HDPE	Nylon 6
Density (g/cm^3)	0.899-0.920	0.910-0.925	0.94-0.96	1.12-1.14
Glass Transition *(T_g)*	-10 to -23	-125	-133 to -100	48
Melting Temperature *(T_m)*	160-176	105-116	120-140	215
Tensile Strength (MPa)	26-41.4	40-78	14.5-38	43-79
Elastic Modulus (GPa)	0.95-1.77	0.055-0.38	0.4-1.5	2.9
Elongation (%)	15-700	90-800	2.0-130	20-150
Izod Impact Strength (J/m)	21.4-267	>854	26.7-1,068	42.7-160

2.2.2 Relevance of Polypropylene in Manufacturing Automotive Parts

According to the American Composites Manufacturers Association (ACMA), the thermoplastic industry is expected to grow 4.9 % over the next years and reach an estimated $8.2 billion by 2017, with even larger opportunities in emerging economies [6]. In the 1970s, the automotive market became the most important market, surpassing the marine market, and it maintains this position to this day.

Polypropylene is one of the most commonly used plastics, in particular in the automotive industry [36]. PP accounts for more than 50 % of all the plastic components employed in vehicles, given its low cost, excellent mechanical properties and mouldability. Table 4 lists common plastics used for automotive parts.

Table 4: Engineered plastics used in a typical vehicle, adapted from [36].

Component	Main types of plastics	Average Weight in car (kg)
Bumpers	PS, ABS, PC, PC/PBT	10
Seating	PUR, PP, PVC, ABS, PA	13
Dashboard	PP, ABS, SMA, PPE, PC	7
Fuel systems	HDPE, POM, PA, PP, PBT	6
Body (incl. panels)	PP, PPE, UP	6
Under-bonnet components	PA, PP, PBT	6
Interior trim	PP, ABS, PET, POM, PVC	20
Electrical components	PP, PE, PBT, PA, PVC	7
Exterior trim	ABS, PA, PBT, POM, ASA, PP	4
Lighting	PC	5
Upholstery	PVC, PUR, PP, PE	8

2.3 Cellulose Fibers

2.3.1 Plant Fibers

Natural fibres can be obtained from various sources; the majority of its production is sourced from forestry or algae. The main chemical structures of plant fibers are cellulose, hemicellulose, pectin and lignin, and their percentage differs from fibre to fibre [37]. The concentration of these constituent varies according the source, age and moisture, playing a major role for the mechanical and chemical properties of end products. Figure 12 shows the chemical structure of main components of natural fibers, which are polysaccharides with five and six carbon rings. The hydroxyl groups attached to the structure generally give strong hydrophilic character to natural fibers.

Opposite to the majority of natural fibres components, lignin is hydrophobic and its content has a strong influence on fiber wettability and adhesion characteristics performances as a cementing agent to increase the stiffness [31], [37]. Though lignin also plays a role in structural support, it may cause problems when fibers are mixed with plastic. This is because lignin has low thermal stability and can contribute to thermal degradation when processing polymer composites. Natural fibers, when incorporated into plastic products, can be processed through virtually all conventional plastic processing methods such as extrusion, injection, calendering and pressing [2], [31]

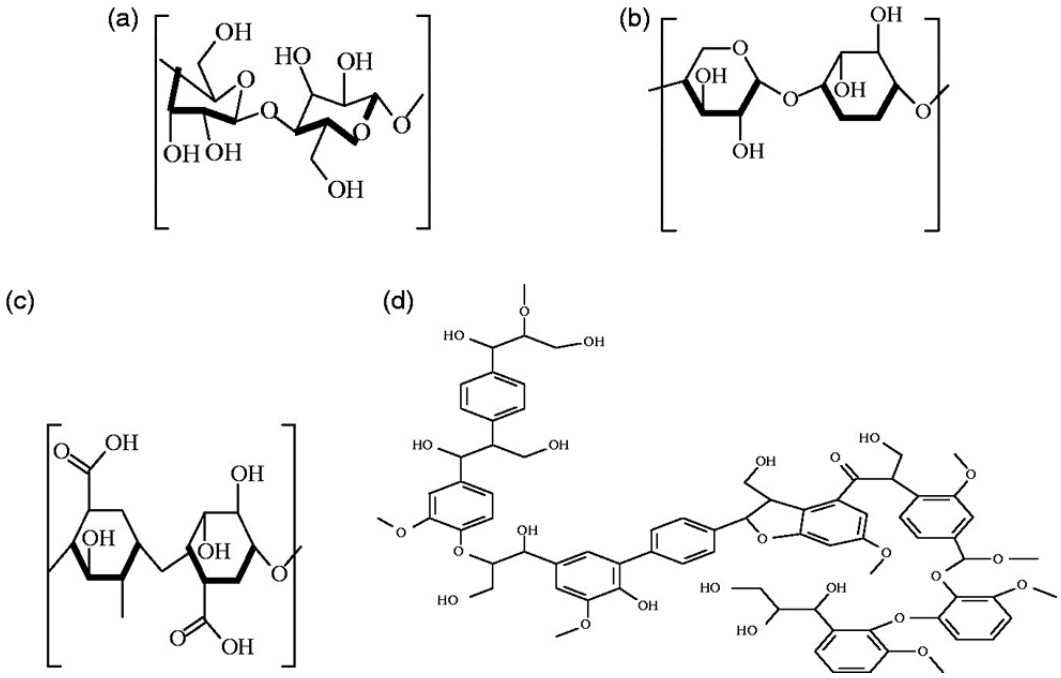

Figure 12: Structural representations of (a) cellulose, (b) hemicellulose, (c) pectin, and (d) lignin [37] under the Sage Publishing and Copyright Center.

2.3.2 Properties of Cellulose

Cellulose is responsible for the hydrophilic nature of the plant fiber, is semi crystalline, its content is crucial for good strength, stiffness and stability, whereas hemicellulose is amorphous polysaccharide, partially soluble in alkaline solution and water, and also contributes to structural stability [37].

The cellulose polymer chain can be very long. Its length (D.P.), i.e. the number of the anhydroglucose units in the cellulose molecule, can range from 15 to 15,000, with an average value of around 3,000 units. Chemically, cellulose can be represented (see Figure 13) as a linear homopolysaccharide composed of repeat d-anhydroglucose $(C_6H_{11}O_5)_n$ ring units joined by glycosidic linkages, between the C-1 of one pyranose ring and the C-4 of the next ring, also known as β(1-4) configuration, leaving just the hydroxyl from carbons C-2, C-3 and C-6 free to react with modifier agents or each other. This configuration allows a linear configuration of the polymeric chain with the hydroxyl groups in equatorial to the sugar rings. The equatorial arrangement of the hydroxyl groups makes them prone for inter-chain hydrogen bonding, causing a parallel stacking of a bundle of chains, forming elementary crystals and nanofibrils, that further aggregate into larger microfibrils [38], [39].

The cellulose molecule has regions with ordered, rigid and inflexible structures (crystalline cellulose) and other regions with flexible structures (amorphous cellulose) [40], [41]. These structural differences are responsible for certain variations in physical behaviour, which can be observed in a cellulose molecule. For example, water absorption and swelling of a cellulose molecule is limited to the amorphous regions of the molecule. The strong network of hydrogen bonds in the crystalline regions prevent the swelling process from occurring in these areas [37], [40], [42].

The hydrogen bonding network gives cellulose high stability, axial stiffness and make the polymer insoluble in the majority of the solvents. The high energy necessary to break these interactions makes the melting point of cellulose much higher than the degradation temperature [38], [43]–[46]

Cellulose fiber sourced from plants is essentially composed of cellulose itself, but depending on the process employed to obtain the fiber, it may contain small fragments of hemicellulose and lignin [47], [48]

Wood has cellulose as one of its main components, which can be extracted through several different methods to obtain wood pulps, i.e. mechanical, thermal and chemical, or combinations thereof [39]. These processes modify lignocellulose materials by disrupting the cell wall structure of plant biomass through removal, solubilization or depolymerization of the lignin. The method through which wood is processed into compoundable wood fiber has a significant effect on its composition and material properties [39], [40].

Chemical pulping is the process relevant to this thesis, with the most used and better-known method being the ‘Kraft’ process, developed by the German chemist Carl F. Dahl in 1879. Currently, this process is associated with 90% of all cellulose pulp produced worldwide [40], [41]. It uses sodium hydroxide and sodium sulfide to break down and remove most the lignin, resulting in a high-strength pulp with only 3-5% lignin content. This process’s pulp yield ranges between 45-70 %, depending on how much bleaching is required. The Kraft pulp production process is based on the transformation of wood into fibrous material (cellulose pulp) and includes the following steps: peeling; chipping; classification; cooking; liquor purification, bleaching and recovery. Some of this process’s advantages include production of a high-performance cellulose pulp and viability of used reagent recovery. One notable disadvantage would be the relatively large investment required for the installation of factories utilizing this process [39]–[42].

The selection of an appropriate type of wood for the production of cellulose pulp is a decisive factor in the production of favorable characteristics and performance for the final products, e.g., paper bags, printing paper. The types of wood used in the production of cellulose pulp can be classified into two groups: hardwood and softwood. Table 5 lists the technological characteristics of the species most used for pulp and paper production [39]. The first comprise species such as Eucalyptus, Acacia, Propulos and Betula. Their pulp fibers are designated as short, varying from 0.5 to 2 mm in length, and are used to produce printing, writing and sanitary tissue paper. Softwood is sourced from conifers, such as the Pinus genus, which has fiber lengths of 2 to 5 mm. Its cellulose is designated as 'long fiber' and is used to produce paper

with greater resistance, such as packaging papers [39]. Table 6 describes average fiber dimensions and wood densities for several wood species [47], [49]–[52].

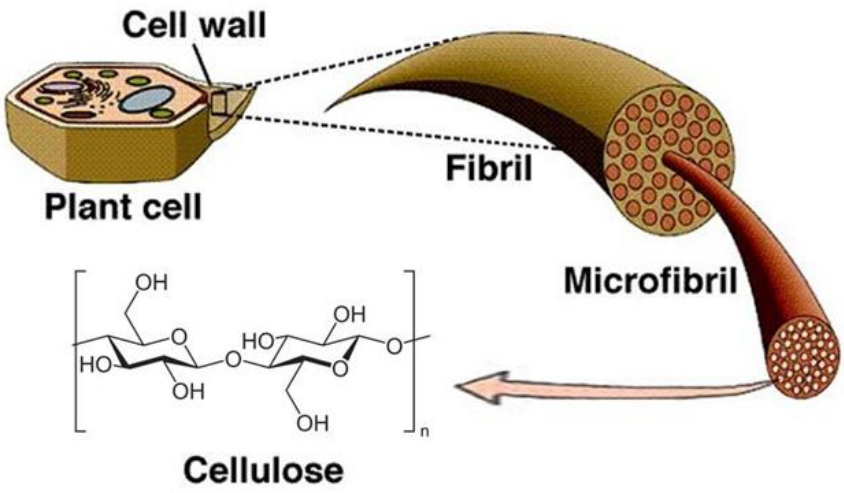

Figure 13 - Chemical structure of cellulose adapted from [38], under the terms of the Creative Commons Attribution 3.0 License.

Table 5: Characteristics of wood species most used for pulp and paper production, adapted from [39].

Type of wood	Species	Location	Characteristics				
			A	BD	TE	TL	HL
Hardwoods	*E. grandis* x *E. urophylla*	Brazil	6	0.47	3.1	28.1	68.8
	Eucalyptus globules	Chile	12	0.63	5.6	25.9	68.5
	Eucalyptus nitens	Chile	12	0.52	4.5	27.1	68.4
	Acacia mangiun	Indonesia	6	0.52	5.2	28.0	66.8
	Acacia crassicarpa	Indonesia	6	0.57	4.1	29.4	66.5
	Populus tremuloides	Canada	55	0.37	6.9	22.1	71.0
	Betula pendula	Finland	67	0.50	4.8	17.4	77.8
Softwood	*Pinus taeda*	Brazil	21	0.43	2.8	26.7	70.5
	Pinus silvestris	Finland	45	0.43	6.4	25.6	68.0

A: age in years; BD: basic density in g/cm^3; TE: total extractives in %; TL: total lignin in %; HL: holocellulose content in %.

Table 6: Average fiber dimensions and wood densities, adapted from [47], [49]–[52].

		Wood Properties			
Type of wood	Species	Length (mm)	Diameter (µm)	Cell wall thickness (µm)	Wood density "dried" (kg/m^3)
Hardwoods	*Eucalyptus globules*	1.0	16	3.8	820
	Populus tremuloides	1.0	20	3.2	550
	Betula pendula	1.1	21	3.8	640
Softwood	*Pinus taeda*	3.3	30	2.9	540
	Pinus silvestris	3.1	30	3.0	550

2.3.3 Challenges in Mixing and Dispersion of Cellulose in Polypropylene

Cellulose fibers usually have low density, making the extrusion feeding process difficult. A common method to avoid the light fibers handling is pelletizing. Pelletization allows for a much easier and

safer feeding process of cellulose in extrusion compounding, but it also has a negative effect on fiber dispersion. Mechanical entanglement and increase in inter-fiber hydrogen bonding can cause irreversible stiffening and prevent fiber re-dispersion. Another challenge is fiber shortening caused by shear forces applied during compounding. The high aspect ratio of cellulose fibers is among the most important properties making this material a good reinforcement filler. Avoiding fiber breakage during the dispersion process is essential to achieve superior enforcement [53], [54].

Hietala *et. al.* [53] used a lubricant to improve fiber dispersion and reduce hydrogen bonding They employed a twin-screw extrusion to compound pelletized cellulose fiber on a polypropylene matrix. The addition of 4-6 wt% of a lubricant to the cellulose pellets allowed the production of a 50 wt% composite with enhanced mechanical properties. The lubricant did not have an effect on fiber breakage but was found to be a promising method to enable the use of a low bulk density cellulose fiber.

Subasinghe *et. al.* [54] compounded kenaf fibers with polypropylene adding maleic anhydride. Fiber length and distribution after each stage of the processing were evaluated. The authors found that processing twin-screw extruded causes considerable damage the fibers but achieves good distribution. They also observed an increase in strength and stiffness when maleic anhydride is used as a compatibilizer.

2.4 Surfactants

Surfactants are commonly used in engineering practices to tailor surface and interfacial interactions of such immiscible substances as oil and water. The term “surfactants” refers to molecules that are “surface-active”, usually in aqueous solutions. Surfactants also called amphiphilic or amphipathic, consist of a nonpolar tail and a polar head, as show in Figure 14 [55]. The polar ends are attracted to water (hydrophilic), while the nonpolar ends are attracted to oils (lipophilic) or repelled from water (hydrophobic). The nonpolar region can vary in number of chains, chain length, composition and chain saturation/branching. The head groups can be either polar, ionic, and zwitterionic. The latter is also referred to as amphoteric, when a single

surfactant molecule exhibits both anionic and cationic dissociations. Figure 15 shows examples of amphiphilic molecules, which are commonly used in several industries such as petroleum, household detergents, concrete additives, agro and food processing, etc [56], [57].

The concept of surface energy can be more easily understood by using a liquid as an example. Atoms and molecules of the liquid can move freely, seeking to occupy a position of lower potential energy a that is, a place where the forces (attractive and repulsive), acting in all directions, are in balance. The particles on the surface of a material, however, only experience forces directed into the liquid as shown in Figure 16 [58], [59].

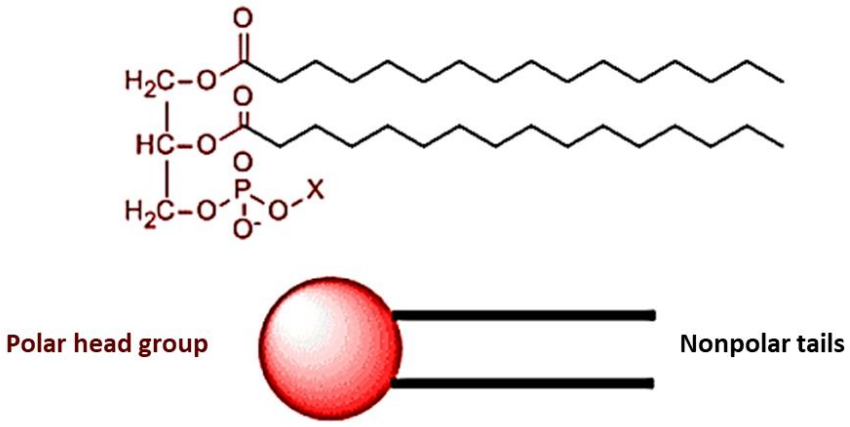

Figure 14: Double chain amphiphilics, x represents a polar group containing a charged phosphate adapted from [55], under the permission of College of Saint Benedict / Saint John's University.

Quaternary ammonium cations, also known as quaternary ammonium salts, quaternary ammonium compounds or "quats", are cations of quaternary ammonium salts with an anion. Most applications of quats are related to their very strong surface affinity, which makes them powerful surfactants [57], [60].

Quats are positively charged ions with an NR_4^+ structure, where R is any alkyl radical. Unlike the NH_4^+ ammonium ion itself and the primary, secondary and tertiary ammonium cations, quaternary ammonium cations are permanently charged electrically, regardless of the pH of the medium. They are synthesized through the complete alkylation of ammonia or other amines. Figure 17 shows the general formula for quaternary ammonium salt [57], [60].

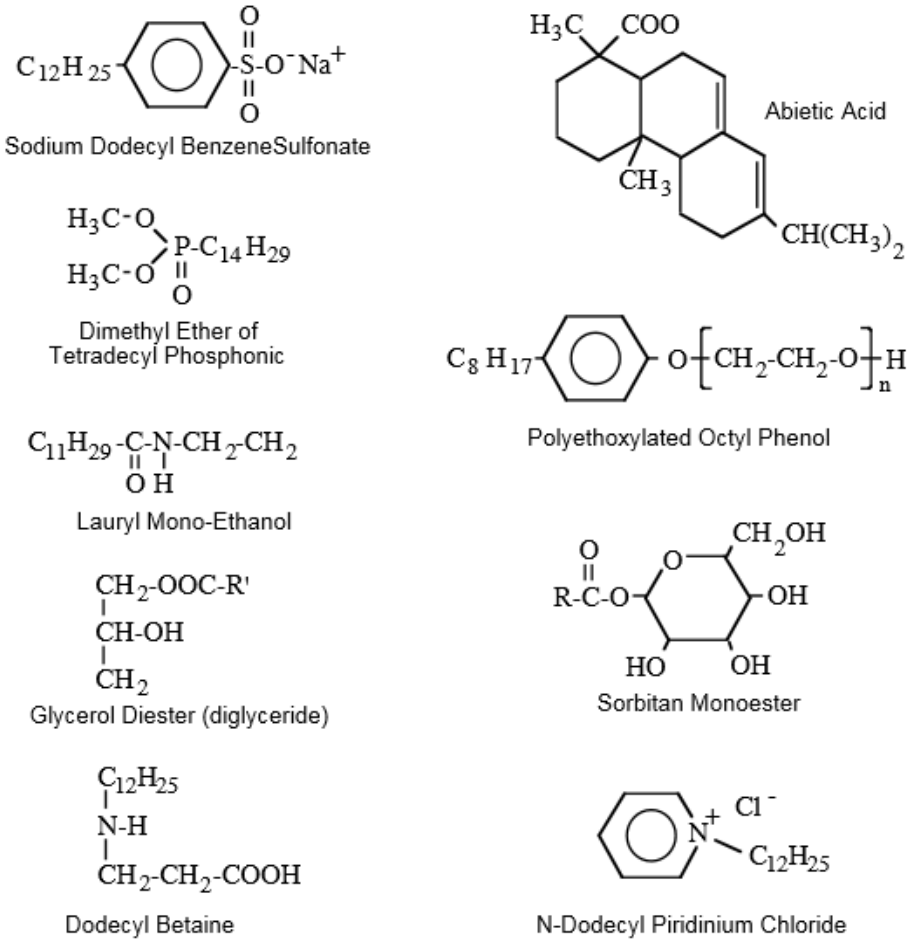

Figure 15: A few commonly used surfactants [56], under the permission of FIRP Booklets.

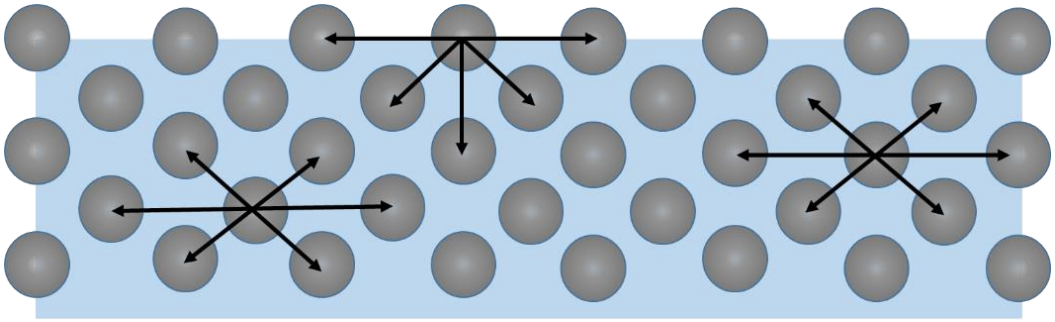

Figure 16: Behaviour of surface energy in a liquid, image by author.

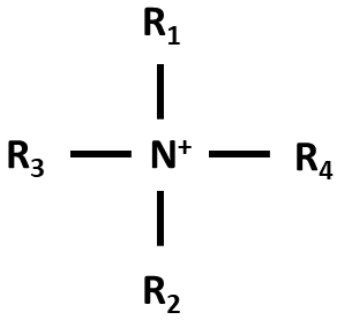

Figure 17: Representation of the general formula of quaternary ammonium salt [60], image by author.

A study conducted by T. Seyidoglu [61] evaluated a modification and characterization of bentonite with quaternary ammonium and its use in polypropylene nanocomposites. This research was developed with four different quaternary alkyl salts to produce organoclays. The results indicate that the d-spacing of the organoclays increased as a consequence of the exchange of Na^+ ions in the clay galleries with the cation of the surfactants with long alkyl tails. The analysis of the organoclays showed that the decomposition temperatures of the organoclays were higher than the melt processing temperature of PP, permitting the use of these organoclays in melt processing of PP. Transmission electron microscopy analyses established the intercalation of surfactant molecules through the organoclay layers. X-Ray Diffraction analyses showed enhanced basal spacing of the bentonite after alteration showing intercalation.

According to Peter and Croft [60], the use of a surfactant (debonder) can lessen inter-fiber bonding during composites manufacturing. As will be described in section 3.5 of the next chapter, a surfactant will be used in the experimental portion of this project.

2.5 Filtration

2.5.1 Overview

Filtration is a unitary operation whose objective is to mechanically separate a solid or fluid, regardless of whether this fluid is a liquid or a gas, with the aid of a porous media. When the suspension is forced through the media, the solid in the suspension is retained by the filter, forming a deposit called cake, whose thickness increases during the operation. The liquid that passes through the filter media (or 'filter bed') is called filtrate [62], [63]. Thus, filtration is also the process of removing particles from the liquid suspension, resulting from the mechanisms of transport, adhesion and detachment existing in filter beds. These mechanisms are influenced mainly by the physical and chemical characteristics of the particles that constitute the filter bed and the filtered fluid, and by rate of filtration [14].

The goals of filtration generally can be categorized into one of the following classifications: clarification for liquor purification, separation for solid recovery, separation for both liquid and solid recovery, and/or separation aimed at facilitating or improving other plant activities [14].

In 1865, the French engineer Henry Darcy experimented with flow through a porous bed and demonstrated that the flow rate is correlated to the pressure drop over the bed. From this, he developed Darcy's law, which is commonly used to describe most filtration processes [14], [63]–[65].

Filtering is the process of separating one or more distinct phases from each other in a procedure where there are physical contrasts between phases such as molecule size, density and electrical charges. A phase separation spectrum is described in Table 7 [66].

Although other separation mechanisms may coexist with filtration in filtering systems, this literature review will focus on solid-liquid filtration, given that in this research project, cellulose dewatering requires the use of this mechanism.

Table 7: The separation spectrum, adapted from [66].

Completely mixed phases	Separation types
Vaporization	Distillation
	Evaporation and drying
	Sublimation
Condensation	
Sorption	Absorption
	Adsorption
Phase transfer	Diffusion
	Leaching and Extraction
Distinct phases	Separation types
Solid from solid	Screening and Elutriation
Solid from liquid	Filtration
	Sedimentation
	Flotation
	Scrubbing (wet or dry)
	Electrostatic precipitation
Liquid from Liquid	Sedimentation
	Coalescing
Liquid from gas	Demisting
	Sedimentation
Gas from liquid	Defoaming
	Sedimentation

2.5.2 Industrial Liquid Filtration Equipment

Three main filtration techniques are used in different industrial sectors: (1) mechanical, (2) chemical and (3) thermal [63]. Within these three categories, there are a number of well proven and developed processes that could also be used for specific applications [63].

The mechanical "solid-liquid" filtration technique is one of the oldest and widely used methods, even though such a separation technique is not economically suitable for all applications. Three standard units are used in the solid-liquid separation: filter press, belt press, and rotary vacuum filter [63]. The latter will be further examined in the next section given that it is the most commonly used equipment in the cellulose pulp industry.

2.5.2.1 Rotary Drum Vacuum Filters

A drum filter is a large, cylindrical device typically used in industrial applications to filter liquids that carry a high concentration of suspended solids. The rotary drum filter acts by drawing the liquid to the outer surface of the filter through the interior space by means of an internal vacuum [67]. The suspended solids in the solution are attached to the external surface of the cylinder, and the filtrate is then pumped out [67], [68]. The filter process may be a continuous or batch process flow.

These machines typically consist of a large barrel that rotates inside a slurry-filled compartment. The inside of the drum is equipped with a vacuum duct in its center and a pumping system for the filtrate. Once the system has started, a power vacuum is created inside the rotating drum that draws the slurry from the filter vat through the filter media. Suspended solids are attached to the outer surface of the filter device to be discarded or used, depending on their use. The key highlights of a rotational drum vacuum filter are represented in Figure 18 [63].

This type of filtration system deals with an extensive range of materials and a range of solid yield. The capacity of such a system varies between 5 and 200 lb/(h ft²). Cakes will accumulate at rates ranging from 0.0013 m/min to 0.0013 m/s. Cylinder diameters normally are 6 to 12 ft, but can sometimes be larger. The formation of the cake solid depends on the type of discharge used. There are five types of discharge: Scraper, Endless Belt, String, Roll, and Precoat. In fact, these five kinds of discharge let the rotary vacuum filter treat a varied range of process sludge [63].

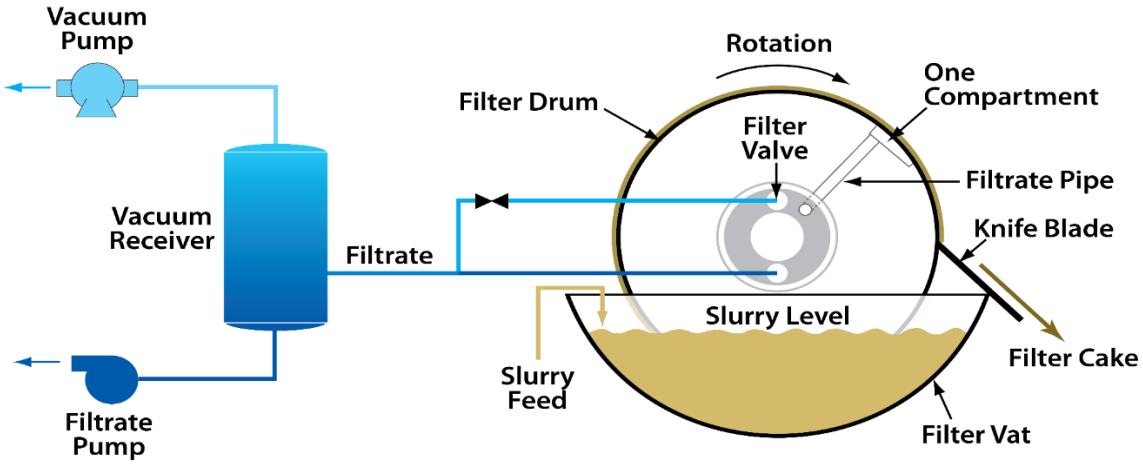

Figure 18: Rotary drum vacuum filter machine [69], under permission for Non-commercial Use.

Rotary drum filters with scraper discharges are outstanding for managing large quantities of solid. It has high filtration efficiency and a simple configuration for the release of the cake; the discharge can be equipped with “air blow-back.” The filter cloth is commonly a synthetic woven fabric. A schematic of this filter system is displayed in Figure 19. This is the type of filter commonly used in industry [63].

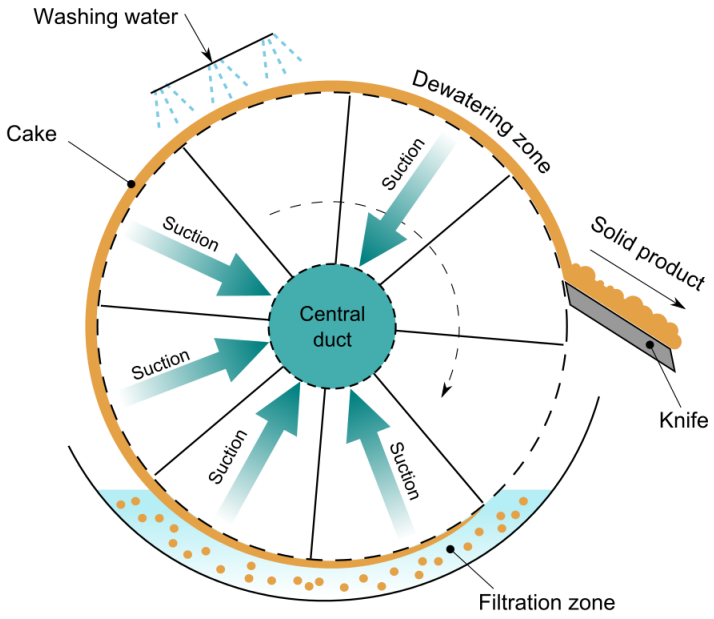

Figure 19: Rotary drum filter with a scraper discharge [63], under GNU Free Documentation License.

2.5.3 Mechanisms for Particles Removal

The filter medium may be classified as a surface or depth filter. The first retains solid particles on its surface, as illustrated in Figure 20a [64]. During filtration, the pore size of the media should be smaller than the diameter of the smallest particle present in the suspension to be filtered. All filtration then occurs on the filter media surface [66]. Depth filters retain the solid within the bed of the filter medium as shown in Figure 20b [64].

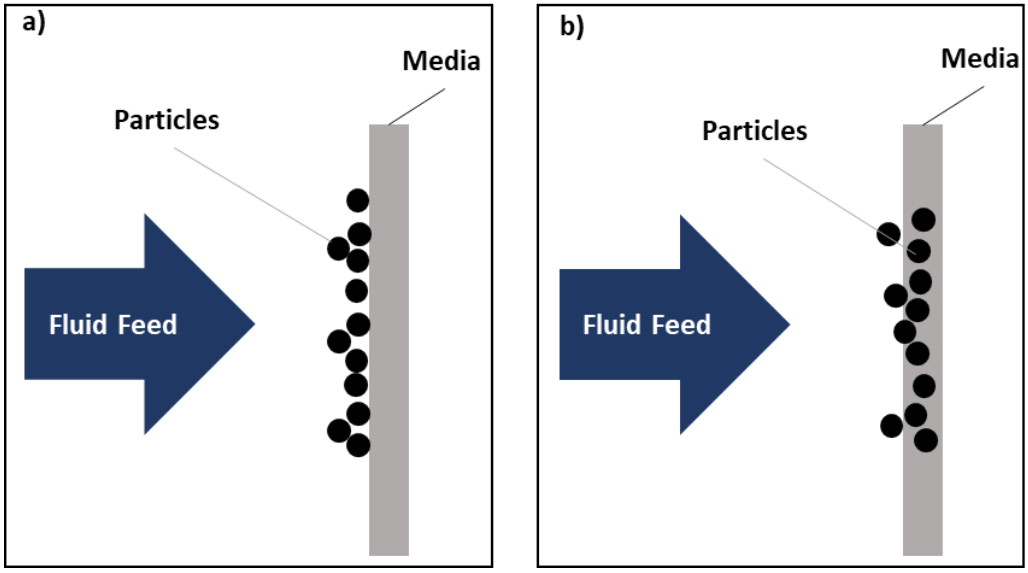

Figure 20: Example of how particles are retained on the surface filter (a) and within the depth filter (b) [64], figure by author.

Size, mass and surface area of the particles influence the three mechanisms of particle removal in solid-liquid filtration. These mechanisms are diffusion interception, inertial impact and direct interception [62], [66]. In diffusion interception, Brownian motion allows particles to make contact with the fiber wire. This mechanism applies to tiny particles. The principle is that particles slam into the fluid atoms, then the repetitive impacts force the particles to move in an arbitrary manner around the liquid streamlines. Movement makes the smaller particles escape the liquid streamlines improving the probability of the particles striking the fiber surface and being expelled, as shown in Figure 21. This phenomenon merely plays a minor part in fluid filtration [64], [66].

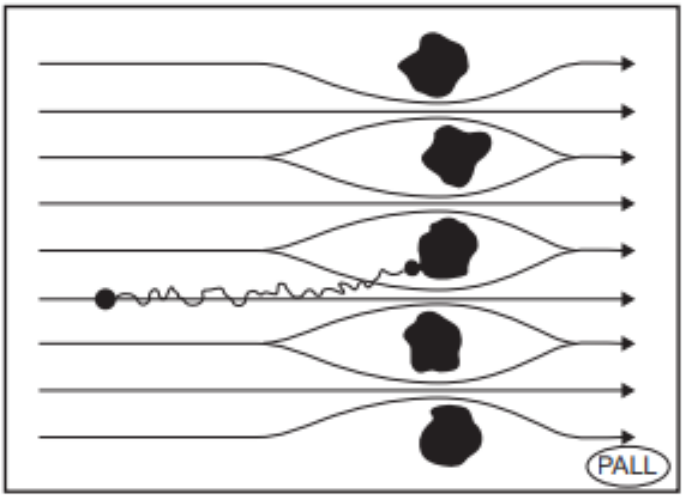

Figure 21: Particle removal in diffusional interception [62], under the Elsivier and Copyright Clearance Center.

Inertial impact occurs when larger or fast-moving particles cannot make the curve current and inertia collide against the fiber and are retained, as shown in Figure 22 (Perlmutter 2015). Since the degree of particle and fluid density difference is small, this system is less powerful for fluid filtration [64], [66], [70].

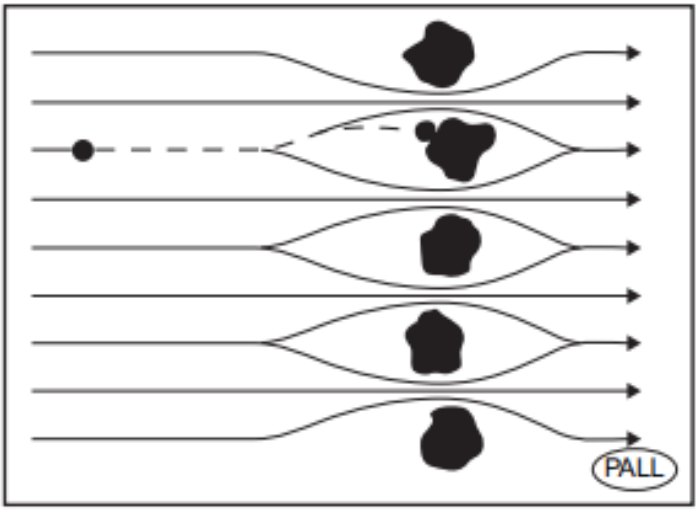

Figure 22: Particle removal in inertial impact [62], under the Elsivier and Copyright Clearance Center.

Direct interception occurs when the radius of the particle is larger than the distance from the stream to the surface of the fiber. That is, the pore size is smaller than the size of the particle retained, as shown in Figure 23. This mechanism extends through most filter designs and is entirely related to the diameter of the particle, media arrangement, and media compactness [62] [64], [66], [70].

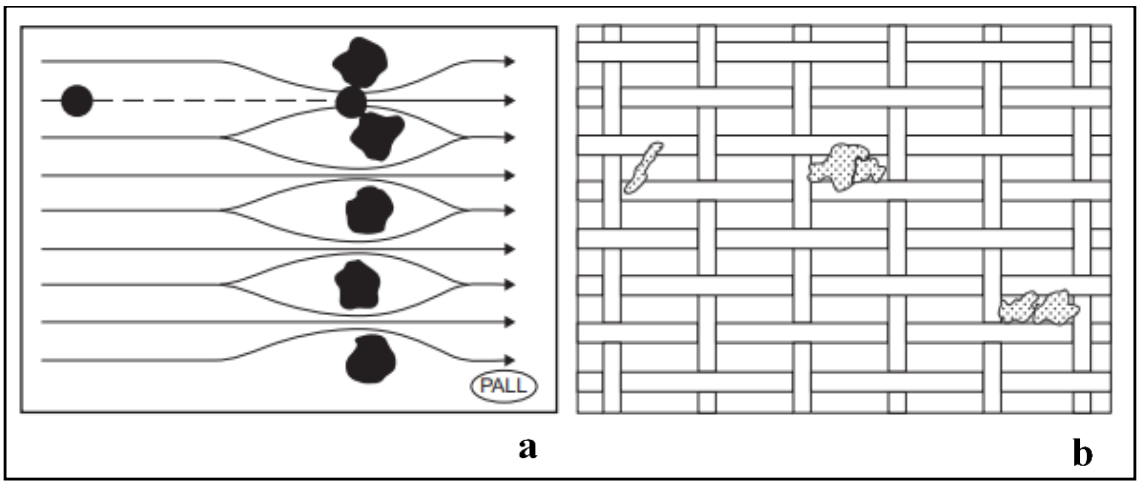

Figure 23: Particle removal mechanism in direct interception (a) and front view of particles striking a pore in direct interception (b) [62], under the Elsivier and Copyright Clearance Center.

2.5.4 Types of Filter Media

There are two main types of filter used in solid-liquid separation: synthetic cloth and metal. The selection of media relies upon various factors; this selection can be determined by filtration removal efficiency, procedure necessities and filter technology, features of the solids and liquids, as well as other parameters.

2.5.4.1 Synthetic Cloth Filter Media

A range of different materials can be used to produce synthetic cloth filters, such as polypropylene, nylon, polyester, polyether ether ketone, polyvinylidene fluoride or fluoropolymers. The degree of openness of the media can be classified as plain, where square weaves have visible or nearly visible weave openings typically bigger than 200 µm, or as closed weave filter cloth, where the openings can vary from 1 to up to 200 µm [62], [64], [66].

Synthetic cloth filters can be weaved using two different types of fibers: monofilaments and multifilaments. Monofilaments are single strand threads with smoother surfaces, which are less prone to solid adherence and simpler to wash multifilaments are textures made of fine strands woven together into strings. They are more difficult to clean and can confine certain solids. There are filter media that can be both mono and multifilaments [66].

Ultimately, there are various types of open regions, as well as ranges of string sizes and pore sizes. Filtration rates can be correlated with the relationship between the total open surface and the region that occupied by the strings themselves. A larger open region yields higher filtration rates. A greater string size provides higher quality, yet reduces the size of the open zone. Filtration media suppliers use various complex descriptions and classifications of synthetic cloth media.

Figure 24 shows the main types of weaving and characteristics of synthetic cloth filter media. The plain square weave (Figure 24a) is made of monofilament fibers, with a large open area and high penetrability, allowing easy cleaning, but providing low stability in the dynamic processes. The twill weave (Figure 24b) is made of monofilament fibers. The cloth is calendered to adjust pore size and air permeability. This weave has dense patterns, as well as favorable strength and durability. The plain reverse Dutch, or PRD (Figure 24c) is made of monofilament fibers with a symmetrical weave, which yields a complex flow and an exceptional high flow rate for a given pore size. Finally, the double layer weave, known as DLW (Figure 24d), can be made of monofilaments or combinations of mono and multifilaments. It is robust, durable and presents great strength in both directions. This weave also provides a smooth cake side and backside flow feature [62], [64], [71].

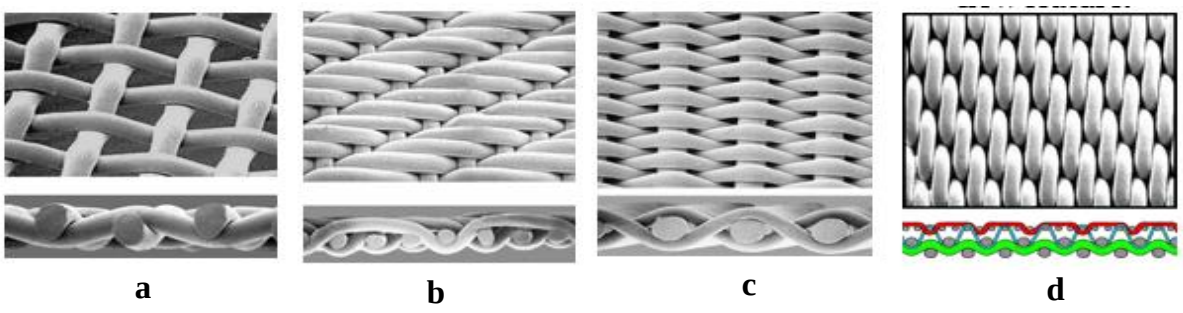

Figure 24: Front and side views of the main types of weaving: a) plain square weave, b) twill weave, c) plain reverse dutch weave and d) double layer weave [62], under the Elsivier and Copyright Clearance Center.

2.5.4.2 Metal Filter Media

Metal filter media can be a formed by a single layer or multilayers and are made of various sorts of tempered steel and metal combinations, such as titanium, nickel, Monel, Inconel, and others. Single layer metal work weaves are like the fabric weaves. As far as multilayers, these can be sintered or un-sintered. With un-sintered materials, the wires do not move due to the interlocking of the weft. When a sintering process is applied, it fully restricts the motion of the wires, which makes the spacing between them fixed.

This type of material is built with different layers of wire work and is intended for precise control of permeability, static pore dimensions, and distribution. The overlays are permanently reinforced under exact dissemination holding conditions during the sintering process. The standard structures can be formed by two, three, or five layers. The inside layer usually provides the evacuation proficiency while the top layer is a defensive layer, and the base layers are for draining. Below, we describe the main types of metal filter media and their characteristics.

Figure 25 shows the main types of metal filter media. The plain weave (Figure 25a) is the most commonly used type of weave. In this weave, a weft wire passes alternately over and under each warp wire; additionally, each warp wire passes alternately over and under each weft wire. In the twilled weave (Figure 25b), every weft wire passes over two, then under two successive warp wires and the warp wires do the same in relation to the weft wires in a staggered composition. In the plain Dutch weave (Figure 25c), the weft wires are plain woven to lie as close as possible against each other in a linen weave forming a dense and strong material with small, irregular and twisting paths. In the twilled Dutch weave (Figure 25d) , the weave is twilled, enabling a weft wires doubled layer, with no “straight-shot” openings through the mesh, and the filtrate passes through a convoluted path [62], [63].

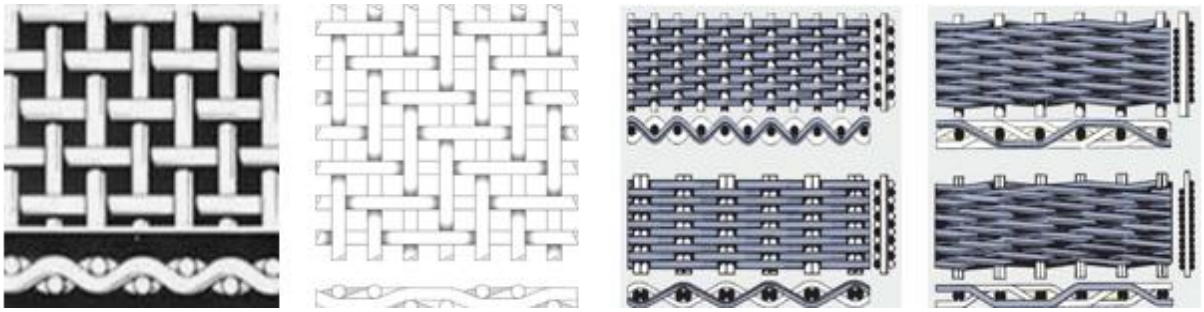

Figure 25: Front and side views of the main types of weaving: a) plain square weave, b) twill weave, c) plain dutch weave and d) twilled dutch weave [62], under the Elsivier and Copyright Clearance Center.

2.5.5 Filtration Theory

In 1856, working on unconsolidated granular media, Henry Darcy proposed that for the horizontal flow of a single-phase fluids, the leakage of the fluid (volume per time unit) flowing through a sample of a porous medium of length L and area A, is given by Darcy's equation (Eq. 1) (m^3/s) [62].

$$Q = -\frac{kA}{\mu}\frac{\Delta P}{L} \tag{1}$$

Where Q is the superficial flow velocity (m^3/s), k is the permeability of the bed (m^2), A is the area of the bed (m^2), ΔP is the total pressure drop over the bed (Pa), μ is the viscosity of the fluid (Pa·s), and L the length of the bed (m).

Permeability is a property of the bed and therefore can be used to formulate an expression for the specific filtration resistance for the bed [72]. Permeability is expressed by Equation 2.

$$\alpha = \frac{1}{k\ \rho_s\ \ \phi} \tag{2}$$

Where α is the specific filtration resistance (m/kg), ρ_s the density of the solid material and ϕ is the solidosity.

The solidosity is a description of the amount of mass in the filter cake (Equation 3).

$$\phi = \frac{V_{solid}}{V_{total}} \tag{3}$$

Where V_{solid} is the volume of the solid material in the porous bed and V_{total} is the total volume of the bed.

Thereby, Equation 4 shows Darcy's law in differential form.

$$u = \frac{Q}{A} = -\frac{k}{\mu}\frac{\partial P}{\partial x} \quad (4)$$

Where u is the superficial velocity of flow (m/s) and the negative sign of this expression indicates that the pressure decreases in the direction of the flow.

According to these equations, one can observe that for the same geometry, same pressure differential, and the same fluid conditions, the outflow is directly proportional to the permeability coefficient k. Therefore, the permeability of a porous medium can be defined as the ability or capacity to allow the flow of the fluid through its pores. As mentioned, the pressure difference (ΔP) is the driving force for the filtration process [62], [72].

It is important to note that Darcy's law was created in a very specific context: laminar flow in a saturated porous medium under steady-state flow conditions, considering a homogeneous, isothermal, and incompressible fluid, and neglecting kinetic energy [62], [73].

The most restricted form of Darcy's law considers laminar flow, the movement of flow being overwhelmed by viscous forces. That is, when fluids move slowly, and their molecules move along parallel streamlines. As the speed of the flux enhances, the particles move chaotically and no longer follow parallel lines. In this case, flux, turbulence, and inertial forces are more significant than viscous forces.

Compressible materials as a result of a filtration process cannot be obtained by directly applying Darcy's equation. In 1935, Ruth defined an essential filtering condition based on Darcy's law, where the flow through the filter cake was described, which is expressed by Equation 5:

$$\frac{dt}{dV} = \frac{\mu(\alpha_{av} cV + R_m A)}{A^2 \Delta P} \quad (5)$$

Where α_{av} is the specific filtration resistance (m/kg), c the mass of solid per unit of filtrate volume and R_m is the resistance of the filter (kg/m^3).

The average specific filtration resistance (m^{-1}) shown in equation 6 described by Ruth is the main value of the local specific filtration resistance and is formulated through integration of the pressure drop over the filter cake, expressed in Equation 6:

$$\frac{1}{\alpha_{av}} = \frac{1}{P_c} \int_0^{Pc} \frac{1}{\alpha} \, dP_s \quad (6)$$

Where P_c is the pressure drop (Pa) over the filter cake and P_s is the solid compressive pressure (Pa). It is problematic to isolate and measure the pressure drop over the filter cake, and therefore it is more convenient to use the total pressure drop over both the cake and the medium as Ruth does with Equation 6.

One limitation of the basic filtration equation proposed by Ruth is the assumption of an incompressible filter cake and, therefore, it is only suitable for materials that form incompressible filter cakes. Tiller and Shirato [74] presented a modification of the classical filtration equation that compensates for the compressibility of the filter cake. Equation 7 introduces a factor that varies with concentration and suggests an approach for low slurry concentrations.

$$\frac{dt}{dV} \equiv \frac{\mu(\alpha_{av} J_R cV + R_m A)}{A^2 \Delta P} \quad (7)$$

Where J_R (correction factor) is represented by Equation 8.

$$J_R = \frac{Adt}{dV}\int_0^1 \left(v - \frac{1-\emptyset}{\emptyset}v_s\right) d\left(\frac{w}{w_c}\right) \quad (8)$$

Where v is the superficial velocity (m/s) along the drainage chamber, v_s sis the superficial velocity (m/s) of the solid, w is the surface weight (kg/m^2) and w_c is the surface weight of the filter cake (kg/m^2).

2.5.5.1 Permeability and Pressure Drop

Permeability (m^2) describes the ease with which a fluid will flow through a porous medium, including inside the cakes. Variables influencing permeability include porosity as well as the size of the particles size make up the porous medium. Equation 9 expresses permeability as established by Kozeny in 1927 [75].

$$K = \frac{\varepsilon^2}{k(1-\varepsilon)^2 S_v^2} \quad (9)$$

Where S_v is the specific surface area per unit of volume of particles, ε is void ratio, and K is the Kozeny constant. Substituting the previous equation into Darcy's law (Equation 1) results in the Kozeny-Carman equation 10 in 1937 [75]:

$$\frac{\Delta P}{L} = \mu\left[\frac{K(1-\varepsilon)^2 S_v^2}{\varepsilon^2}\right]\frac{dV}{dt}\frac{1}{A} \quad (10)$$

Then it is observed that permeability is inversely proportional to the filter's resistance to the flow. Along this line, low permeability leads to higher resistance and the opposite is true as well. Permeability can be defined using a permeability coefficient. This coefficient is proportional to the fluid viscosity, flow rate, and filter medium thickness, and inversely proportional to fluid density and filter area. The consequence is that the permeability coefficient has the dimension of a length. However, this expression is difficult to use. The permeability behaviour is more easily visualized by a progression of curves linking

pressure drop from one side of the filter medium to the other with the fluid flow rate through it. A different arrangement of pressure drop curves can be set up with regard to medium filter size, fluid temperature and filtration time (for example, level of medium contamination) [62], [75], [76].

The consequence of a longer filtering time is the creation of a buildup on the surface of the media, thereby reducing permeability and increasing filtration as the amount of solids retained increases, as shown in Figure 26. If the medium depth is augmented at the same time as its area, then a distinct set of curves will be created in light of the fact that the medium additionally restricts the flow of fluid. Every individual filter component will, in this way, have its own curve relating pressure and drop flow rate which will depend on medium depth, area and permeability [62], [75], [77].

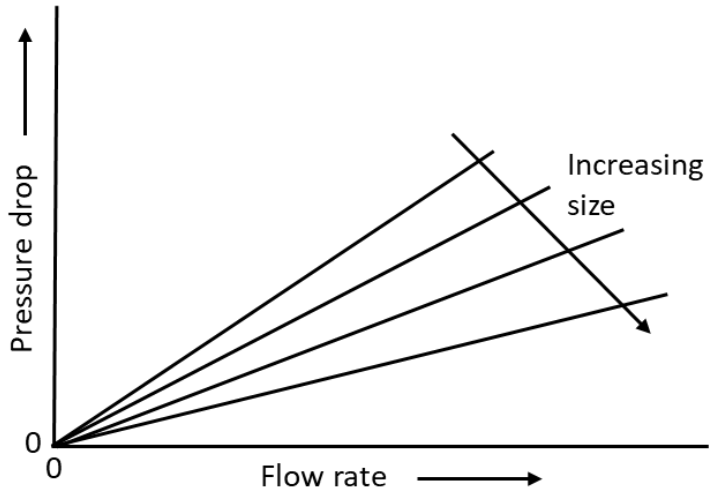

Figure 26: Filter size curves related to pressure drop and flow rate variation [62], figure by author.

The total pressure drop (ΔP) in a filter is the pressure difference between the inlet pressure of the fluid and the outlet pressure after passage through the filter medium, which must be a porous medium to allow the liquid to pass through. For a given mass flow, the enhanced filter area will decrease the pressure drop in light of the fact that the amount of fluid flowing through the filter per unit area will be reduced and

the pressure loss will be inversely proportional to the filter area. Such a relationship results in a standard of design of the area of a filter using the value of the pressure drop (in any fluid-dynamic design). Nevertheless, the rise in pressure drop will lengthen filtering time as the media becomes obstructed, as seen in Figure 27 [62], [75], [77]

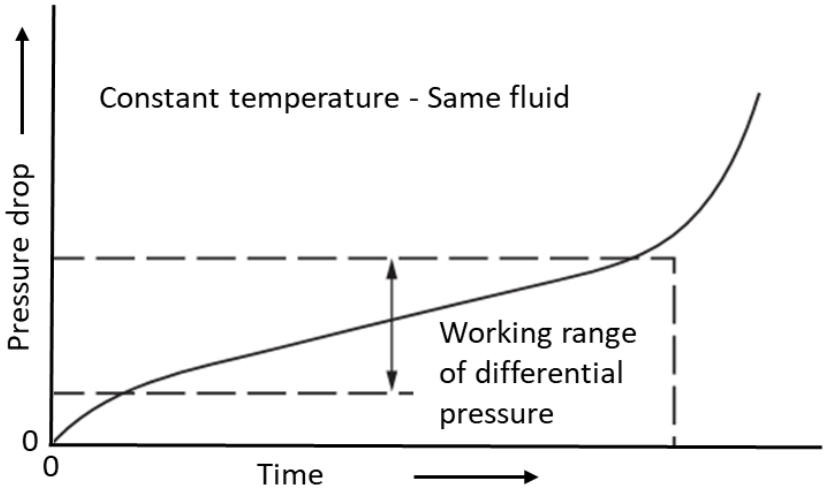

Figure 27: Variation of pressure drop as a function of filtration time [62], figure by author.

The operating temperature of the fluid will influence the pressure drop in the filter because the fluid viscosity will undergo a modification. A less viscous fluid will be subjected to less resistance through the filter medium, and therefore an inferior pressure drop [62], [75].

As shown in Figure 28, the pressure drop is contrariwise proportional to the temperature, and a reduction in the temperature causes a rise in pressure drop. The change in fluid velocity is not the only possible factor being impacted by temperature. At lower temperatures, some fluids may undergo phase transition (solidification). For example, the water contained in an oil can freeze obstructing or even partially blocking the filter and consequently generate an abnormally high drop in pressure. A similar phenomenon may take place with waxes dissolved in oil [62], [75], [77].

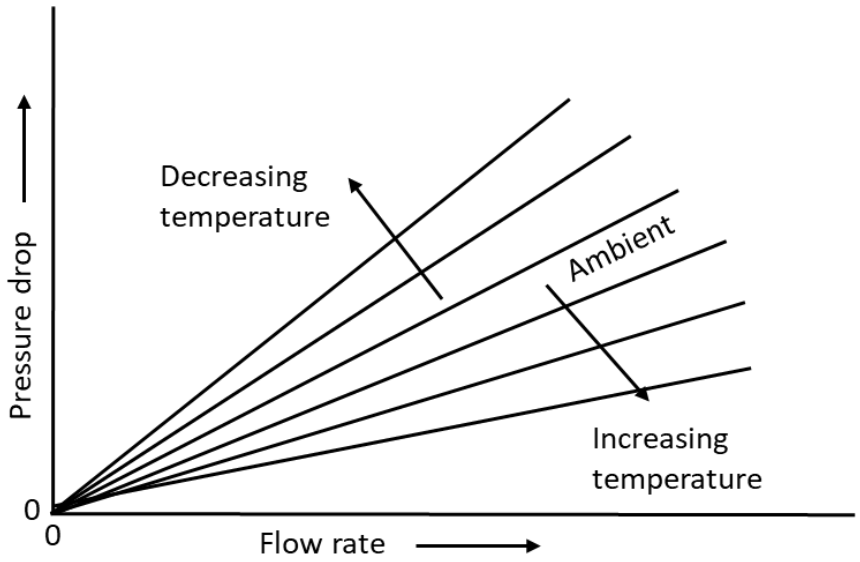

Figure 28: Effect of temperature in the relation of pressure drop and flow rate [62], figure by author.

2.5.6 Filtration Testing Approaches

Testing is essential for choosing the most appropriate filtration technology. Many parameters can influence the filtration process and should be considered and revisited in the tests. These include, but are not limited to: pressure, viscosity, solid content, particle size distribution (PSD), form and size of particles, compressibility, deformability, agglomerate building behaviour, zeta potential, and others [62].

Most cases of filtration testing can use Darcy's law. The focus of this equation is obtaining the filtration system total discharge. To increase the latter, one can increase pressure, permeability, or filter area, or alternatively, decrease viscosity or filter length [64]

In dealing with suspensions, decisions should be made about pressure or vacuum system testing. Table 8 lists characteristics of each system that can support testing choices depending on use [62].

Table 8: Comparison between the pressure and vacuum systems, adapted from [62].

Pressure system experiment	Vacuum system experiment
Can be applied to elevated temperatures or super-saturated solutions.	Commonly used for rapid filtering of suspensions and settling of solids.
Useful for hazardous/nonhazardous suspensions, given that the system is completely closed	Not recommended for hazardous products, given that the system is open.
Completely closed systems.	Open filter systems.
Batch system and restricted to a continuous process.	Are normally used in a continuous process.
The range of operation for pressure is usually 6 - 16 bar	The range of vacuum operation is normally between 0.4 - 0.6 bar.
High pressure systems, above or equal to around 25 bar, which requires more energy and a more complex design, thus raising cost	Increasing vacuum from 0.6 to 0.9 bar requires a huge effort – for a filtration effect that increases only by 22 %

2.5.6.1 Commissioning and Operation

The commissioning and preventive maintenance plan, as well as a training plan for system operators and mechanics, play an important role in avoiding or solving problems and challenges that may arise in a filtration process. The formats and requirements of these plans differ according to industrial domains. However, each filtration equipment provider and each operator ought to have explicit arrangements for plant acceptance testing, site acceptance testing, mechanical start-up, and start-up as such. Table 9 lists common elements involved in all processes [62], [66].

Table 9: The common topics to be involved in process, adapted from [62].

Protocol approvals	Signature
Introduction	Purpose
	Scope
	Responsibility
General	Equipment description
	Auxiliary equipment descriptions
	Process functions
Specific reviews	Nameplates
	Installation and lifting
	Fabrication, assembly, and quality control plan
	Material certificates and finishes
	Verification of P&ID
	Utilities
	Wiring
	Controls
	Seals
	Calibrations
	O&M manuals
	Spare parts
	Maintenance
	Cleaning
Operations	Start-up
	Shut-down
	Normal process
	Mechanical
	Controls

2.5.6.2 Process Challenges - Rotary Pressure Filter

Actual filtration systems are affected by changes that would appear to be small and seem to have little impact on operation, but which in fact end up having great impacts on the systems. Two cases

describing changes and related challenges identified for industrial vacuum filtration systems are discussed next.

The first case dealt with a continuous rotary pressure filter used in a specialty chemical application. Preliminary experiments with sampling carried out on the batch reactor revealed that there was a dual distribution in the particle size distribution of the filter. With the aim of achieving a continuous process, the batch system was converted to a continuous system, assuming the same particle size distribution. However, the continuous system yielded a very different particle size distribution, which necessitated modifications to the filter media [62].

In another case, preliminary experiments had indicated that a continuous rotary pressure filter would satisfy requirements with respect to filtration, cake washing and drying. Once the system was installed and activated, filtration flux rates turned out to be much lower than in the preliminary experiments, such that the continuous process could not be carried out. Even after reviewing all the process parameters, the engineers were unable to correct the issue. They then analyzed the data for a long period and concluded that the slurry's zeta potential had been altered by the process flow, and that agglomeration was taking place in the filter itself. A slight modification to the pH was sufficient to resolve the process issues with no impact to the reaction chemistry [62].

Chapter 3: Materials and Methods

In this chapter a description is made about the materials used for the preparation of the filtration system, the cellulose samples prepared by filtration and the preparation of the composites. The methodology used for this purpose and the methods of characterizing these materials are also described.

3.1 Dry Cellulose Pulp

The dry cellulose fibers were supplied by West Fraser from British Columbia. The fibers were produced primarily from lodgepole pine and white spruce using the thermo-mechanical pulp process followed by bleaching (trade name QRP). The cellulose fibers were provided in the form of dry sheets around 1 mm thick. The cellulose content was 99.6% dry base minimum.

3.2 Polypropylene

Polypropylene (PP) homopolymer was supplied by Sabic (PP 500P). The type of PP used was a medium flow, multipurpose grade for injection mould and extrusion with density of 0.905 g/cm^3 and a melt flow index (MFI) of 3.1 g/10 min at 230 °C and 2.16 kg.

3.3 Polypropylene Fibers

Chopped polypropylene fibers were supplied by Ecofabril (Brazil). The PP fibers were around 64 mm long, round shape with 15 μm diameter, and melting point of 160 ºC.

3.4 Compatibilizer

Polypropylene-graft-maleic anhydride (MAPP) was supplied by Eastman. The selected grade was G-3015 which is a maleic anhydride grafted polypropylene recommended as a coupling agent for polypropylene composites. This grade has molecular weight of 47,000 g/mol, acid number of 15 mg KOH/g and viscosity of 18,000 cP at 190 ºC.

3.5 Surfactant

Arquad 2HT-75 was used a surfactant. Its composition informed by the supplier is di(hydrogenated tallow) dimethylammonium chloride (~75%) containing 14% of 2-propanol and 11% of water as impurities. Hidrogenated tallow is a hard saturated fat consisting of glyceryl esters of oleic, palmitic, and stearic acids (16–18 carbon chains) and extracted from fatty deposits of animals, especially from suet (fatty tissues around the kidneys of cattle and sheep). This surfactant does not have an accurate molecular weight because of the impurities and homologs present in it [78]. This material was purchased from Sigma Aldrich and used as received.

3.6 Cake Production with the Lab-Scale Rotary Drum Filtration System

The procedure used for the preparation of all filter cakes was the same: the components were stirred for two minutes in a blender and then transferred to the slurry vat. The blades of the blender were slightly dulled in order to avoid cutting the cellulose fibers.

The results measured for the evaluation of the runs were the filtration rate (g/cm^2.min) and visual aspect. The filtration rate was calculated by the mass of dry solids (M_s, g) divided by submerged filtration area (A_s, cm^2) multiplied by vacuum time (when the filter was submerged, t_V, min) as indicated by Equation 12. All sample cakes were collected during the initial 60 seconds after activation of the vacuum pump.

$$Filtration\ rate = \frac{M_s}{A_s \times t_V} \tag{12}$$

The visual aspect of the cake was ranked as “good” or “poor” as described in Table 10.

Table 10: Criteria for visual aspect ranking of the cakes

Cake ranking	
Good	Poor
- Discharged from drum filter continuously (no ruptures) - Cake is easily removed from drum filter - Uniform thickness - Cake has flat surface	- Breaks and disintegrates when discharging from drum filter - Difficult to removal from drum filter with the scraper - Non-uniform thickness - Gaps in the cakes

3.7 Pelletizing of Cakes

The cakes prepared using the continuous filtration device developed in this research were pelletized using a manual paper guillotine trimmer. The pellets where shaped in the form of approximately 5 mm squares, as shown in Figure 29

Figure 29: Pelletized cellulose cake, image by author.

3.8 Extrusion Process

The composites were extruded using a Haake MiniLab Extruder. This model is a benchtop twin screw conical extruder. Pelletized sample cakes, PP and MAPP pellets were manually forced in the extruder. The extruder temperature was 200 ˚C with a screw speed of 80 rpm.

3.9 Pelletizing of Composites

A laboratory wiley mill (Thomas-Wiley model 4) was used to grind the composite samples after extrusion. The samples were ground until they pass the mesh opening of 1/8" (3.1 mm).

3.10 Injection Moulding

The bars for mechanical testing were prepared using an injection moulding machine Ray-Ran RR/TSMP injector. Sample pellets were injected using 200 ˚C and 80 ºC in the barrel and mould respectively.

3.11 Apparent Consistency Method

The apparent consistency test was designed to observe the behaviour and interaction of PP fibers and cellulose fibers in an aqueous medium. This test aims to follow and measure the formation of two phases (separation) in the water-fibers mixture as a function of time without the influence of stirring

The test was carried out with a consistency of 0.7 wt% for all mixtures, using PP fibers, with and without cellulose, and demineralized water. The mixture was stirred in a mixer for 2 minutes and then immediately placed in the graduated cylinder (500 mL). The mixture was allowed to settle without any mixing or stirring in any way. To obtain apparent consistency results, the fiber phase volume (as shown in Figure 30) was measured after 1 min, 3 min, 10 min, 30 min, 60 min, 90 min, 120 min, 180 min, 240 min, 300 min and 1440 min (24 hours). The results were measured as the proportion of total volume occupied by the volume of water with fibers according to Equation 11.

$$Apparent\ consistency\ (\%) = \frac{Fibers\ phase\ volume}{Total\ mixture\ volume} \quad (11)$$

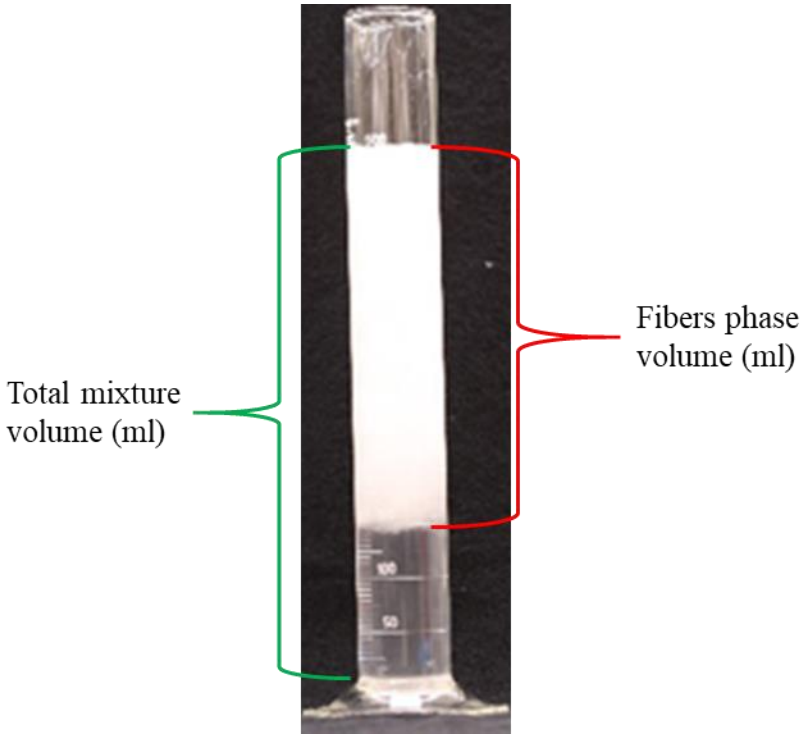

Figure 30: Apparent consistency results: total mixture volume (mL) and fibers phase volume (mL), image by author.

3.12 Morphology

A scanning electron microscope Zeiss LEO 1530 Gemini operating at 5 kV was used to observe the morphology of the cakes and resulting composites. For the cross-sectional imaging of the samples, the cakes were cut using a fresh razor blade and the composites were cryofracturated using liquid nitrogen. All samples were gold coated before the SEM analysis.

Optical microscopy images were obtained using a Leica MDG36 connected to a digital camera. The magnification used was 12.6 times.

3.13 Mechanical Test

Flexural and Izod notched impact tests were conducted using a universal testing machine (TestResources 120R,) and a pendulum tester (Monitor impact tester from Testing Machines Inc) in compliance with ASTM D790 and D256, respectively. The samples were conditioned prior to testing at 23 °C ± 2 °C and 50 ± 5 % relative humidity for at least 40h. All mechanical tests were run in an environmentally controlled room using the same conditions.

Chapter 4: Filtration System

4.1 Overview

The objectives of this chapter are:

1) to design and assemble the lab-scale continuous filtration system,

2) to evaluate the filtration of pulp and

3) to evaluate the effect of PP and additives on the filtration process.

The research tasks (Section 4.2) for the first objective included the creation of a flowchart describing the lab-scale filtration system, the selection of components (filter, screen, pump, pipes, etc.) and the assembly and commissioning of the continuous filtration system. The results of a filtration system built in the laboratory (Lab-Scale Rotary Drum Filtration System) are presented in Section 4.3. The research tasks for objective 2 were to evaluate the behavior of this device characterized by the influence of pressure, rotation speed and consistency. The goal was to obtain the highest filtration rates while producing a filtrate (cake) with relatively good homogeneity. The characteristics of the filtrate (cellulose cake) were evaluated with qualitative aspects (visual aspect ranking). The research tasks for objective 3 are described in Sections 4.4 and 4.5. The goal was to evaluate the filtration when PP fiber was added to the components, first without any additives in Section 4.4 and then with a surfactant in Section 4.5.

4.2 Filtration System

The objective was to build on a laboratory scale system to operate similarly to the industrial vacuum drum system that is often employed in the dewatering process of the cellulose industry. These rotatory drum systems for dewatering cellulose pulp in laboratory scale are not readily available for purchase. Therefore, a research task was to devise a new system. It started with the purchase of the laboratory scale vacuum

drum filter used for waste water. The system was purchased, evaluated and then later it was modified. An image of the original filtration system is shown in Figure 31. An auxiliary package was designed and added to the drum filter. This package was comprised of a slurry vat (plastic bucket), a submersible pump, and a vacuum pump. The drum filter was modified to better suit the process and to match filter media used in the pulp industry. Several type of filter media were evaluated. In the end the most suitable filtration media was an actual filtration media donated by a pulp and paper company, which was the same filtration media used in their cellulose dewatering drum filtration system.

Figure 31: Original laboratory scale vacuum drum filter, image by author.

The experimental system is comprised of three parts: (1) feeding system, (2) filter media and vacuum, and (3) discharge system. The design and construction of each part is explained below.

1) The feeding system was initially constructed, as shown in Figure 32a, that is with a rectangular slurry vat, a mechanical mixer (to maintain the homogeneity of the system), and a submersible pump to push the slurry towards the drum filter. One-inch pipes, fittings and globe valves were used since the entry orifice of the drum filter vat is one inch in diameter. The flow entering into the drum filter vat was controlled by means of a globe valve. The flow rate supplied by this pump was not measured due to the difficulty of measuring flow of cellulose slurries. The flow rate was controlled to assure a constant level of slurry in the drum filter vat.

The problems that arose and modifications were made to improve the feeding system (shown in Figure 32) are described respectively below:

- Issue: Opening the feed flow control valve to the full position caused the drum filter vat to overflow. Moreover, the feed pressure was so high that the drum filter was "washed off" by the slurry, which then prevented cake formation on the filtration media located in the cylinder surface. Opening the valve partially caused clogging of pipes due to the intrinsic nature of the cellulose slurry. It is well known that pumping cellulose slurry is a common challenge in the cellulose manufacturing industry.

  Solution: Substitution of pipes, fittings and valves with 1-inch for 2-inch parts to enable improved slurry flow, which in turn minimized clogging of the pipes.

- Issue: Dead spots in the rectangular slurry vat accumulated material due to rapid sedimentation of the cellulose slurry, thus impeding homogenization. Moreover, after operating for a few minutes, the mechanical mixer became jammed by cellulose fibers entangling its impeller.

Various impeller types and configurations were tested with no or little success to attempt to resolve this issue.

Solution: Addition of another valve to create slurry reflux before feeding the drum filter vat. This way the reflux homogenized the slurry eliminating the need for a mechanical mixer. The use of two valves also allowed for improved manual control of the feed flow. To maintain a constant flow into the drum filter vat, a plate was placed in the vat to stabilize the flow and prevent the cylinder from being "washed off" by the slurry itself. The measure enabled a homogeneous cake formation over the filtration media. The rectangular slurry vat was replaced by a cylindrical one, which eliminated the so-called "dead spots" with no homogenization and prevented sedimentation of the cellulose fiber.

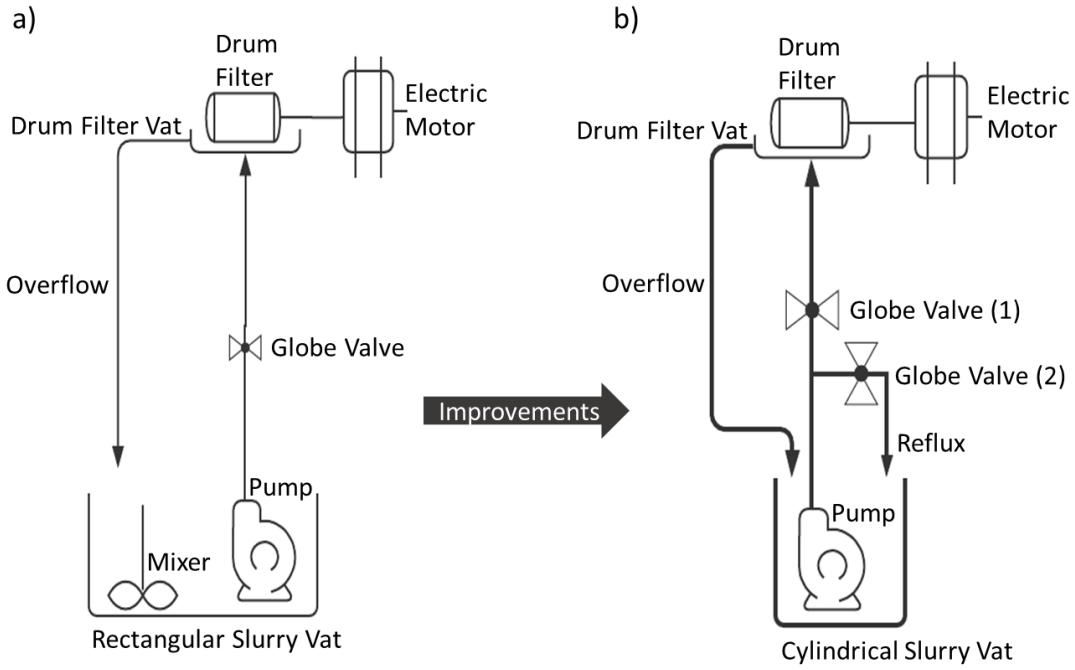

Figure 32: Simplified diagram of the feeding system setup - a) initial and b) final, with improvements.

2) Filter media and vacuum: the drum filter system, as purchased, had a filter media that was different from that employed in the pulp industry. The system was encapsulated in acrylic material, which prevented direct access to the drum and filter media. To access the drum filter, which allows one to change filter media and makes internal cleaning easier, the upper part of the acrylic capsule was removed. To simulate industrial conditions, the filter media was substituted with a filtration media supplied by an industrial partner. This company provided four different types of filters (shown in Figure 33 and Figure 34). Comparative flow tests were carried out with the four filters media. The highest flow rate was obtained with filter media (d) in Figure 33. The filter media were also tested in the drum filter with respect to cake formation. However, it was only possible to obtain cake samples with filter media (d) in Figure 33. This filter media was therefore selected for this project.

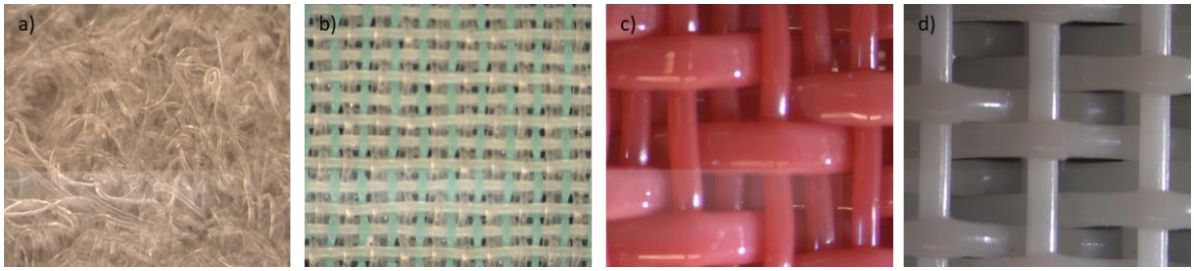

Figure 33: Microscopic optical images of filter element used in industrial scale.

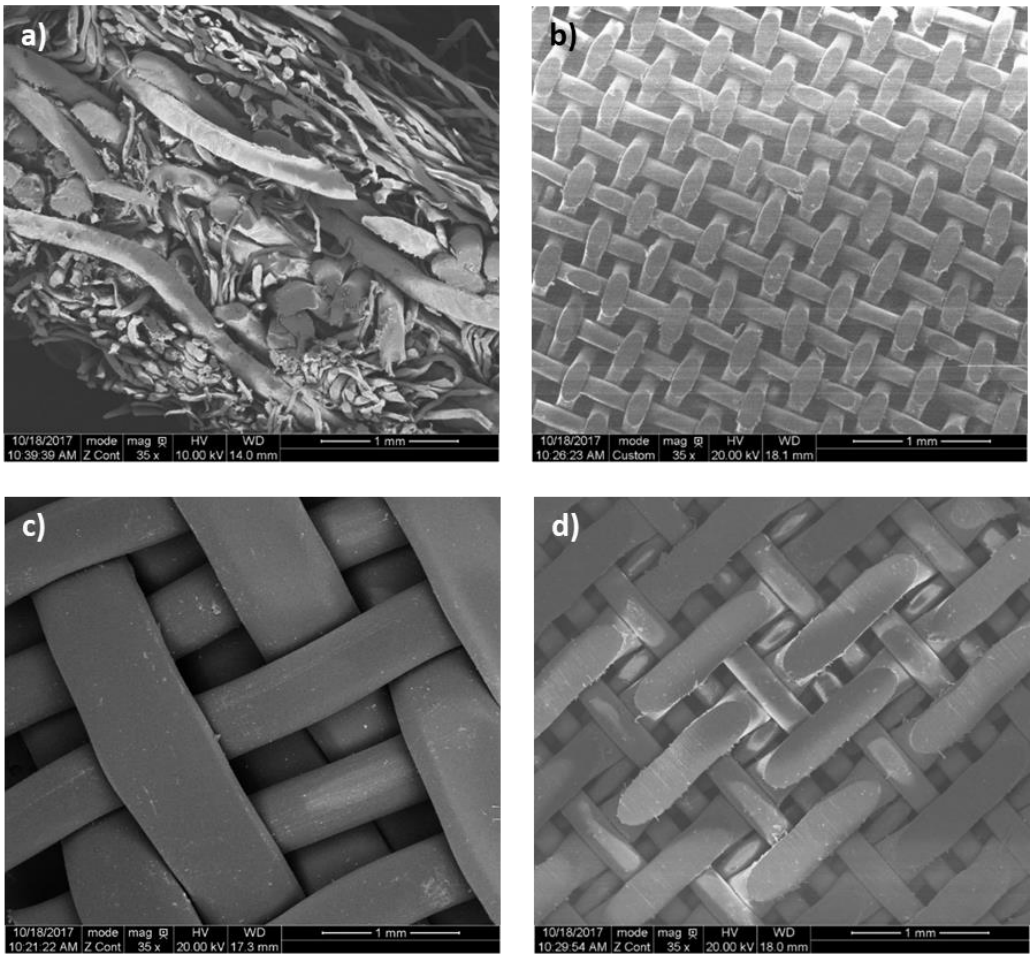

Figure 34: SEM images of filter element used in industrial scale.

3) Discharge system: For removal of the solids from the cylinder, a fixed scraper was provided with the original drum filter's discharge system. However, after substitution of the filter media, the distance between the fixed scraper and the drum filter became much greater, making it impossible to discharge samples. The fixed discharge scraper was therefore removed and resized with a new acrylic plate. This altered scraper was fitted with screws allowing adjustment of the distance from the drum filter and contact angle. The discharge scraper was thus installed and adjusted to enable the collection of cakes.

Figure 35 shows a simplified diagram of the final lab-scale drum filter and Figure 36 shows the entire system itself.

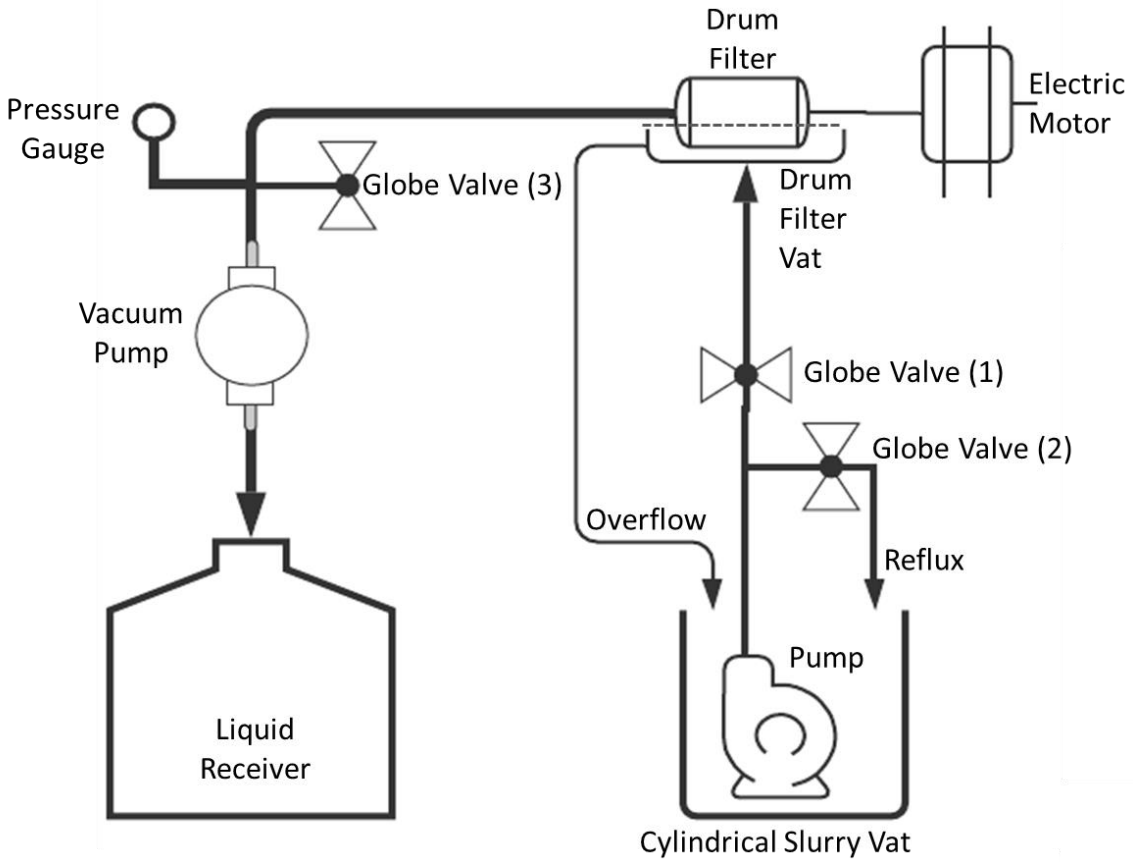

Figure 35: Simplified diagram of the final lab-scale drum filter.

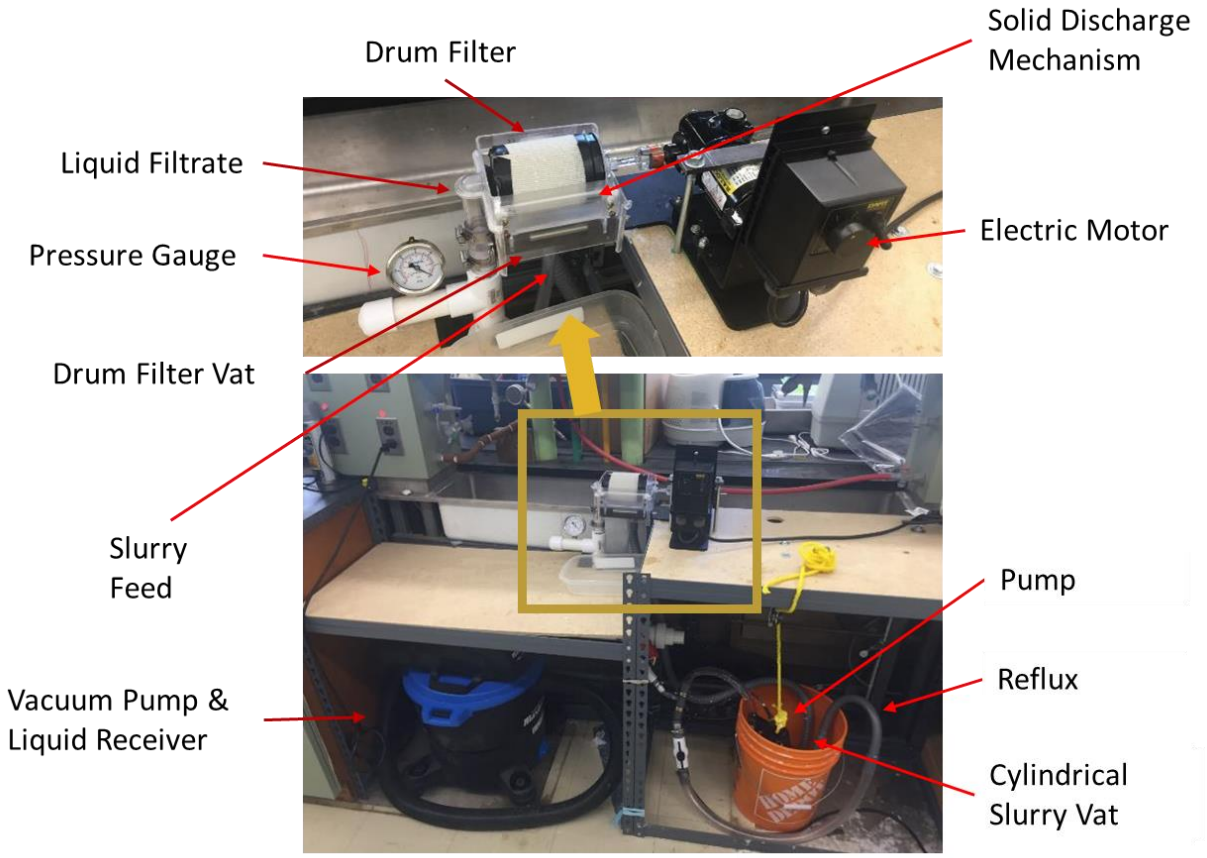

Figure 36: Laboratory scale filtration system.

4.3 Filtration with only Cellulose and Water – CW Cakes

The initial tests of the filtration equipment aimed to establish the best operational conditions – vacuum, rotation speed and slurry consistency – for the system. In this phase, all runs were performed using dry cellulose and demineralized water (which are labeled as CW cakes below). Figure 37 illustrates the steps of the process.

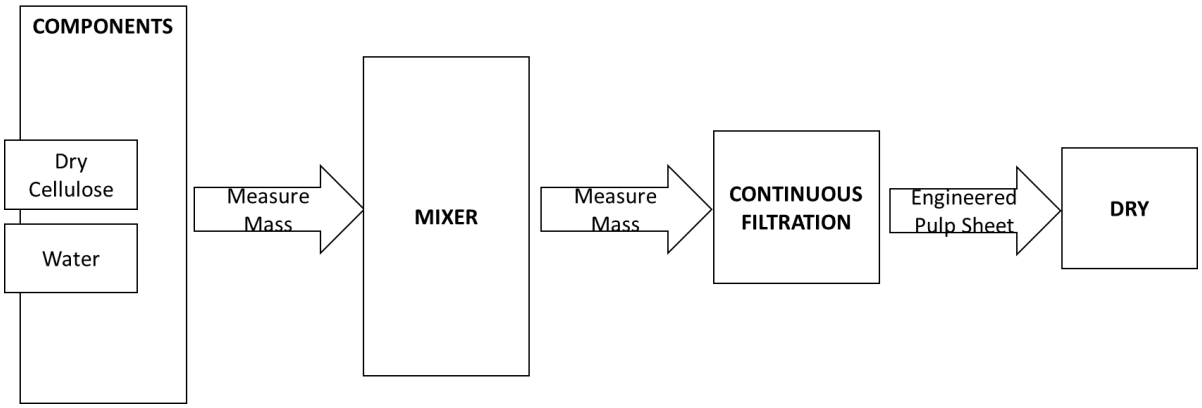

Figure 37: Process to obtain CW cakes.

The experiment was designed according to a 2^3 factorial design with central points to evaluate the linearity of the system. The factorial design maximizes the information that can be obtained with a predefined number of runs, to evaluate the effects of main operational parameters of the system as well as interactions among them. The limits for each variable were established in accordance with the system's operational capacity. The main operational parameters studied were:

- The vacuum applied in the system, with a low value of 0.05 bar, central value of 0.08 bar and a high value of 0.11 bar.

- The rotation speed of the drum filter with a low value of 3.8 rpm, central value of 9.4 rpm, and high value of 14.7 rpm.

- The filtration time with a low value of 4.1 s, central filtration time of 6.4 s, and the high filtration time of 4.1 s.

- The consistency: the percentage of cellulose in terms of the total weight (wt%) of the mixture containing water (wt%), with a low value of 0.3 (wt%), a central value of 0.5 (wt%), and a high value of 0.7 (wt%).

Process variability was verified. Several runs were performed before the ones from the final experimental design. These previous runs were analysed and showed large differences among the results of the replicates. The sources of variability were identified and minimized. As a result, the variability among the replicates decreased and it was possible to identify not only the factors with a strong influence on the results (vacuum and consistency), but also the variable with a lesser influence (rotation). The absence of interactions between the factors was also confirmed. By using 2 replicates for the factorial points (CW1 to CW8) plus 5 replicates in the center point (CWCP), totalizing 21 runs, the analysis of variance had 12 degrees of freedom associated to the error term, which is usually high enough [79].

4.3.1 Results and Discussion

The visual aspect ranking of the cellulose sheet was rated as good or poor. A good ranking indicates a continuous and uniform cake (shown in Figure 38). In contrast, a cake was rated as poor when there were gaps, breakage and disintegration of the sheet, and/or non-uniformity of the cake thickness (shown in Figure 39). The highest vacuum value (0.11 bar) resulted in better ranked cake sheets, as shown in Table 11. The other variables (rotation and consistency) did not influence the visual aspect ranking of the cakes.

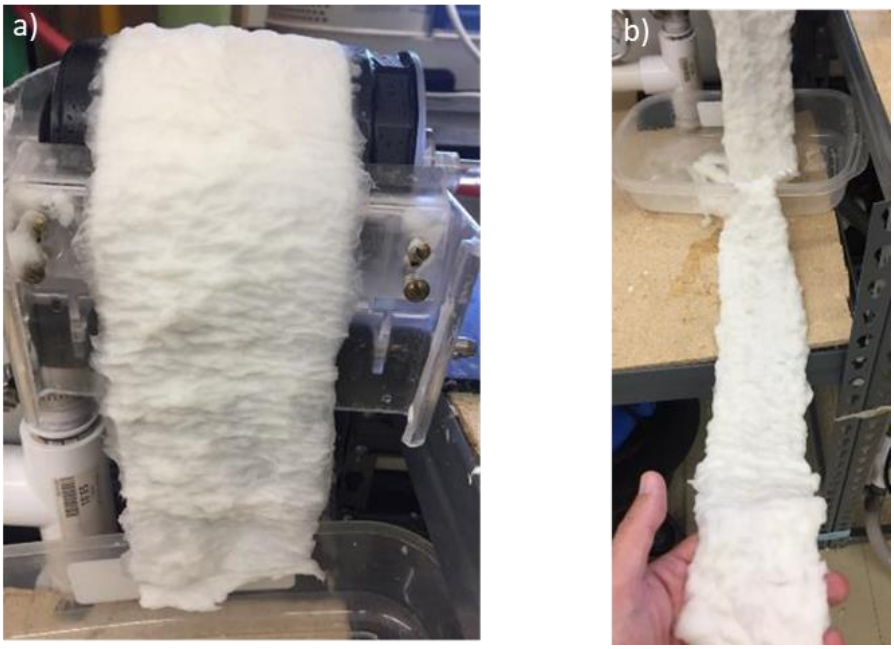

Figure 38: Cakes evaluated as ‘good’ in terms of visual aspect ranking – a) on drum filter and b) discharge cake.

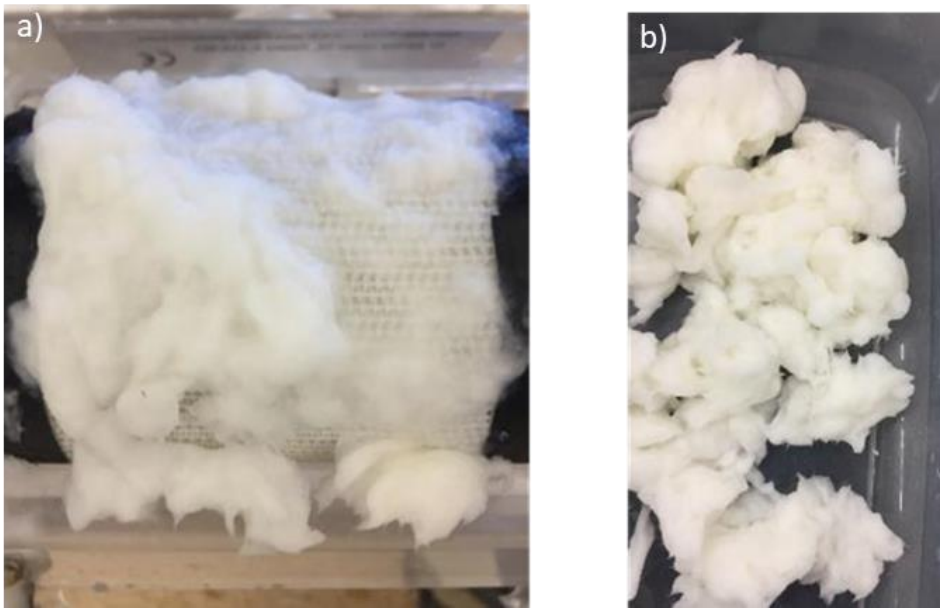

Figure 39: Cakes evaluated as ‘poor’ in terms of visual aspect ranking - a) on drum filter and b) discharge cake.

Table 11: Filtration rate and visual aspect of the cakes.

Cakes	Variables					
	Vacuum (bar)	Rotation (rpm)	Filtration time (s)	Consistency (wt%)	Filtration Rate (g/cm^2 min)	Visual Aspect Ranking
CW1	0.05	3.8	7.9	0.3	0.043 ± 0.001	Poor
CW2	0.11	3.8	7.9	0.3	0.164 ± 0.002	Good
CW3	0.05	14.7	2.0	0.3	0.059 ± 0.001	Poor
CW4	0.11	14.7	2.0	0.3	0.167 ± 0.002	Good
CW5	0.05	3.8	7.9	0.7	0.124 ± 0.010	Poor
CW6	0.11	3.8	7.9	0.7	0.234 ± 0.009	Good
CW7	0.05	14.7	2.0	0.7	0.119 ± 0.013	Poor
CW8	0.11	14.7	2.0	0.7	0.302 ± 0.001	Good
CWCP	0.08	9.4	3.2	0.5	0.170 ± 0.005	Poor

With respect to filtration rate the best result of 0.302 g/cm^2.min was achieved when all operational parameters were set at the highest levels: 0.11 bar, 14.7 rpm, 0.7 wt%. In contrast, with the lowest levels of operational parameters (0.05 bar, 3.8 rpm, and 0.3 wt%) the lowest filtration rate of 0.041 g/cm^2.min was obtained.

The analysis of variance of the results showed that vacuum and consistency had a strong influence on the filtration rate (p < 0.0001), while rotation speed had a weak effect (p = 0.0487). The p-value is defined as the smallest level of significance (α). The traditional approach was to use a fixed significance level, usually $\alpha = 0.05$, and infer that a factor or interaction affected the outcome ($p < 0.05$) or not ($p > 0.05$) at this fixed α by the use of the F test. However, this information is incomplete, since it gives the decision maker no idea if the test result was barely significant (rotation, $p = 0.0487$) or highly significant (vacuum and consistency, $p < 0.0001$). To avoid these difficulties, the p-value approach has been adopted

widely in practice [79]. The system was linear and the interactions among factors were insignificant. All insignificant interactions were excluded. Therefore, only significant factors were considered to obtain the graphs presented below. The Statsoft Statistica software package was used for all statistical analyses of results in this project.

Filtration rate increased as vacuum and consistency increased as shown in Figure 40. When increasing the vacuum from 0.05 bar to 0.11 bar under constant conditions of consistency, the filtration rate increased on average from 0.086 g/cm^2.min to 0.217 g/cm^2.min. That is, increasing the vacuum by 2.2-fold resulted an average rise of 2.5-fold in the filtration rate. Similarly, when increasing consistency from 0.3 wt% to 0.7 wt% the filtration rate increased from 0.108 g/cm^2.min to 0.198 g/cm^2.min under constant vacuum conditions. In other terms, increasing consistency by 2.3-fold resulted in a 2.0-fold change in the filtration rate. The highest vacuum and consistency levels evaluated here resulted in the highest filtration rate. In contrast, the lowest levels of consistency and vacuum resulted in the lowest filtration rate.

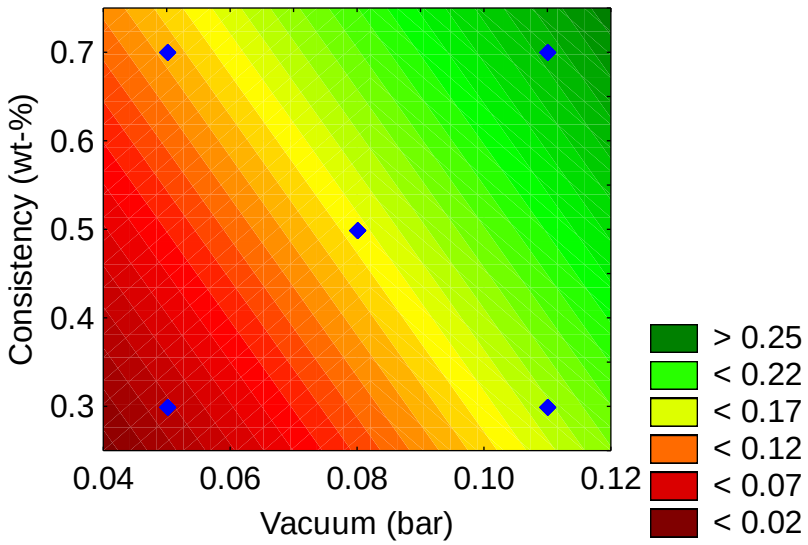

Figure 40: Filtration rate (g/cm^2.cm) shown in color (from dark green to brown) as a function of consistency (wt%) and vacuum (bar).

Rotation speed showed a weak influence on filtration rate compared to the other variables, within the current experimental range. When increasing rotation speed from 3 rpm to 14.7 rpm under constant conditions of consistency, the filtration rate increased by approximately 30 %. That is, a 4.6-fold increase in cylinder rotation speed only resulted in an increase of approximately 30 % in filtration rate, as shown in Figure 41a). Similarly, the influence of rotation was weak under constant vacuum conditions. Increasing rotation speed from 3 rpm to 14.7 rpm (4.6-fold), under constant vacuum conditions, only resulted in an increase of around 30% in filtration rate, as show in Figure 41b).

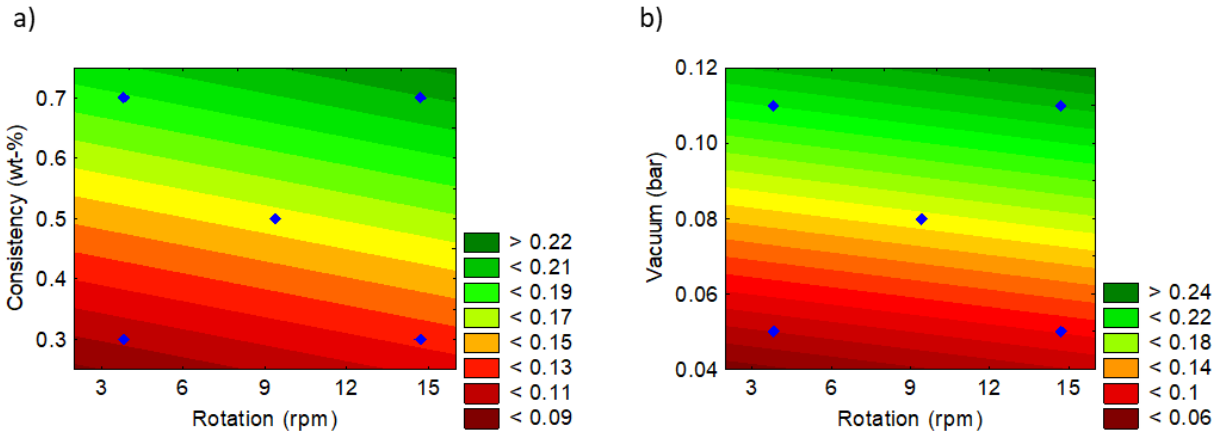

Figure 41: a) Filtration rate (g/cm^2 min) as a function of rotation speed (rpm) and consistency (wt%); b) filtration rate (g/cm^2 min) as a function of rotation speed (rpm) and vacuum (bar).

4.4 Filtration with Cellulose, Water and Polypropylene Fiber – CW6PP Cakes

The results obtained in the cellulose and water tests (CW cakes) made it possible to start the filtration system evaluation using polypropylene fibers. The values obtained in the tests described by Section 4.3 were used to guide this new set of experiments. Knowing that higher filtration rates are obtained with higher vacuum and consistency values, and that rotation speed can be changed without much impact on the filtration rate, a low rotation speed was selected for the experiment. This is because the low rotation

speed should enable easier handling of the filtration system. Thus, the variables for the filtration system were defined as follows: vacuum = 0.11 bar; consistency = 0.7 wt% and rotation speed = 3.8 rpm (i.e. the parameter values for the CW6 cake in Table 11 above). This being the case, filtration rate will no longer be considered in the next section, which focuses on the role of adding PP fibers and additives to the mixture.

As will be described in Chapter 5 (Section 5.2), it was not possible to obtain a viable resulting composite with CW6 through the extrusion/injection process with polypropylene. Therefore, the research strategy investigated here was to add polypropylene to the wet cellulose slurry. This attempt enables missing cellulose fibers and polypropylene before drying the cellulose fibers after filtration. The polypropylene chosen to be mixed with the cellulose slurry was polypropylene fibers. The research hypothesis to be evaluated here is if mixing a certain amount of polypropylene fibers with the cellulose fibers in the slurry could produce a cake of cellulose and polypropylene that would enable improved extrusion and injection molding. The rationale for testing this hypothesis is to create a mixture of polypropylene phase and cellulose phase prior to drying the cellulose.

The polypropylene phase was chosen to be in the shape of polypropylene fibers. The selection of polypropylene fibers was based on whether these fibers would have a high probability of entangling with the cellulose fibers during the continuous filtration process. It is expected that the entanglement of fibers and the fast rate of filtration could create a cellulose cake with a significant amount of polypropylene well mixed together. Moreover, the entanglement of polypropylene fibers and cellulose fibers could contribute to preventing the segregation of each phase apart from each other. This potential segregation of phases could be expected if the phases were powders for example with different specific gravity, poor turbulence and a low filtration rate.

Therefore, the polypropylene fibers were added to the CW6 slurry (which can then be labeled CW6PP). Figure 42 shows the steps of the process through which the CW6PP cakes were obtained.

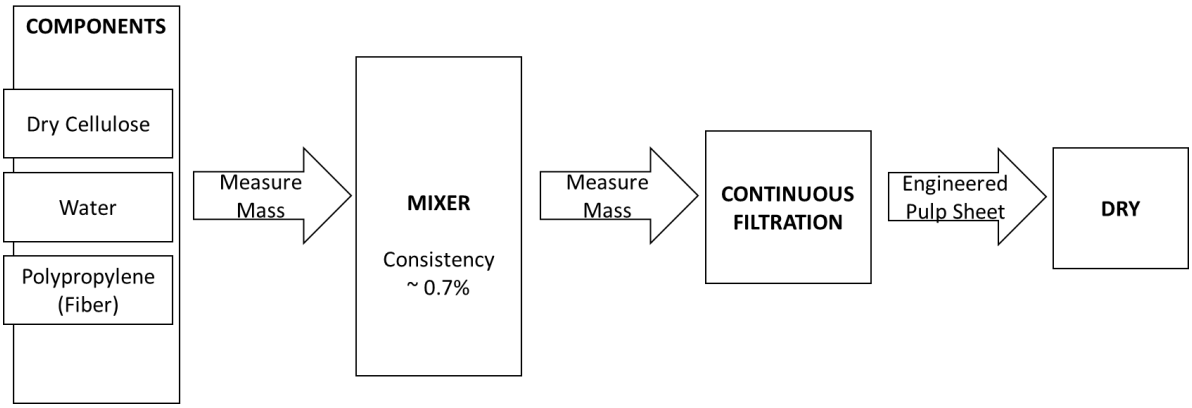

Figure 42: Process to obtain CW6PP cakes.

4.4.1 Results and Discussion

Five mixtures were prepared with different amounts of polypropylene fiber: CW6PP20, CW6PP25, CW6PP33, CW6PP50, CW6PP66, and CW6PP75. The last two digits of each label (20, 25, 33, 50, 66 and 75) refer to the percentage (wt%) of polypropylene fiber (PP fiber) in the solid cakes. For example, the CW6PP-20 cake contains 20% PP fiber and 80% cellulose. For all cakes, a consistency of 0.7 wt% was maintained in the slurry used as a feedstock for the filtration process. Table 12 shows the filtration rate and the visual aspect ranking results for these cakes.

The visual aspect ranking of the CW6PP-20, CW6PP-25, and CW6PP-33 was good, given their continuous and uniform aspect (see Figure 43-a below). The CWPP-50, CWPP-66, and CWPP-75 mixtures were not obtained due to obstruction of pipes in the filtration system. Increasing the amount of PP fiber in the mixtures caused entanglement with the cellulose fiber, which in turn lead to blockage in the pipes. Several attempts were made, but the pipes leading to the drum filter always became obstructed. This is shown in Figure 44. Given this result, an apparent consistency test was designed, using the methodology described in Section 3.11.

Table 12: CW6PP cakes with 0.7 wt% of consistency.

Cakes	Components (g)			Visual Aspect Ranking
	Cellulose	PP Fiber	Water	
CW6PP-20	0.560	0.140	99.300	Good
CW6PP-25	0.525	0.175	99.300	Good
CW6PP-33	0.490	0.210	99.300	Good
CW6PP-50	0.350	0350	99.300	Failed
CW6PP-66	0.233	0.466	99.300	Failed
CW6PP-75	0.175	0.525	99.300	Failed

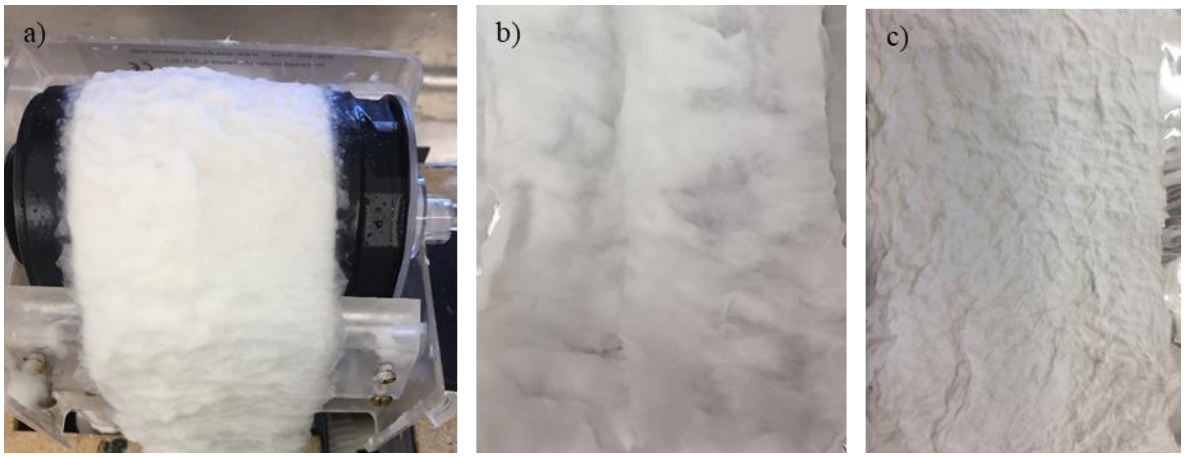

Figure 43: CWPP-33 cakes: a) on rotary drum filter; b) wet; c) dry.

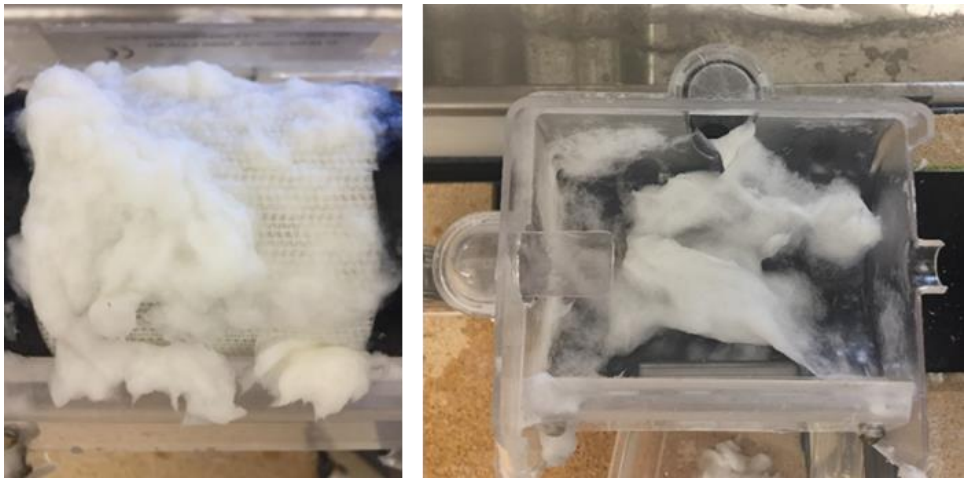

Figure 44: CWPP-50 cake on rotary drum filter.

The apparent consistency test results showed that slurry consistency varies with time according to the amount of PP fiber added to the water-cellulose mixture. In the extreme case, when a mixture of 100% PP fiber and water (without cellulose) was used, the apparent consistency increased rapidly by almost 30% within the first minute. Then it varied more regularly until it reached a peak value of 55% at 24 hours (total test duration). This behaviour can be explained by the density of PP fiber is 0.95 g/cm^3 being smaller than water as well as by the lower affinity of PP with water (hydrophobic). In summary, pure PP fibers have a tendency to float in water quite rapidly in the beginning in the absence of stirring or turbulence, thus leading to accumulation of PP fibers on the surface of the liquid.

In contrast, when no PP was added to the mixture the apparent consistency did not vary at all within 24-hours. That is, even with no stirring the cellulose-water mixture (without PP) remained homogeneous for up to 24 hours. In this case, one could expect the cellulose to settle at the bottom of the cylinder due to its density 1.5 g/cm^3 being higher than water. However, cellulose is highly hydrophilic and forms a stable network of fibers in water. Figure 45 shows a comparison of the test results for the mixture with water and

100% cellulose (0.7 wt% consistency) and the mixture with 100% PP fiber and water (0.7 wt% consistency), after one minute 1 minute and 24 hours without stirring.

For the intermediate mixtures in Table 12, the apparent consistency varied markedly with changes in PP fiber content as shown in Figure 46. The mixtures with higher PP fiber contents have a tendency to float faster, thus increasing the entanglement behaviour between the fibers. This phase separation caused by addition of PP fibers is a significant challenge for pumping the slurry and feeding the drum filter.

Consequently, the stability of the entanglement behaviour of the slurry used for the filtration system is affected by the addition of PP fibers. The obstruction of the pipes was observed when more than 33% of the PP fibers is used in the mixture.

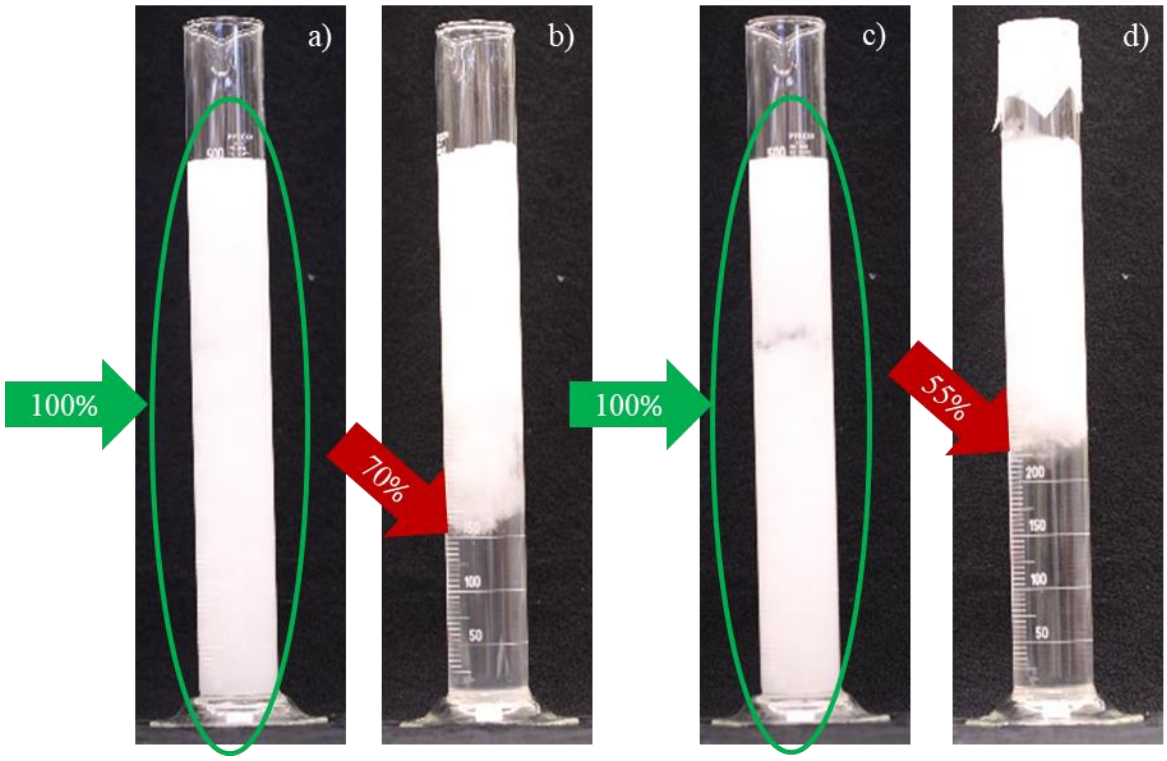

Figure 45: Apparent consistency test - a) 100 % cellulose fibers and b) 100 % PP fibers - both after one minute; c) 100 % cellulose fibers and d) 100 % PP fibers - both after 24 hours.

The formulation CWPP-33 (shown in Figure 43) was selected for use in the remainder of this research based on its performance measured by its good visual aspect ranking and high PP fiber content. This performance of this formulation was better than formulations CWPP-20 and CWPP-25. This selection should increase the chances of obtaining a resulting composite through injection moulding. Results regarding the utilization of sample CWPP-33 for the preparation composites with polypropylene pellets using extrusion and/or injection molding will be presented in Section 5.3 of the next chapter.

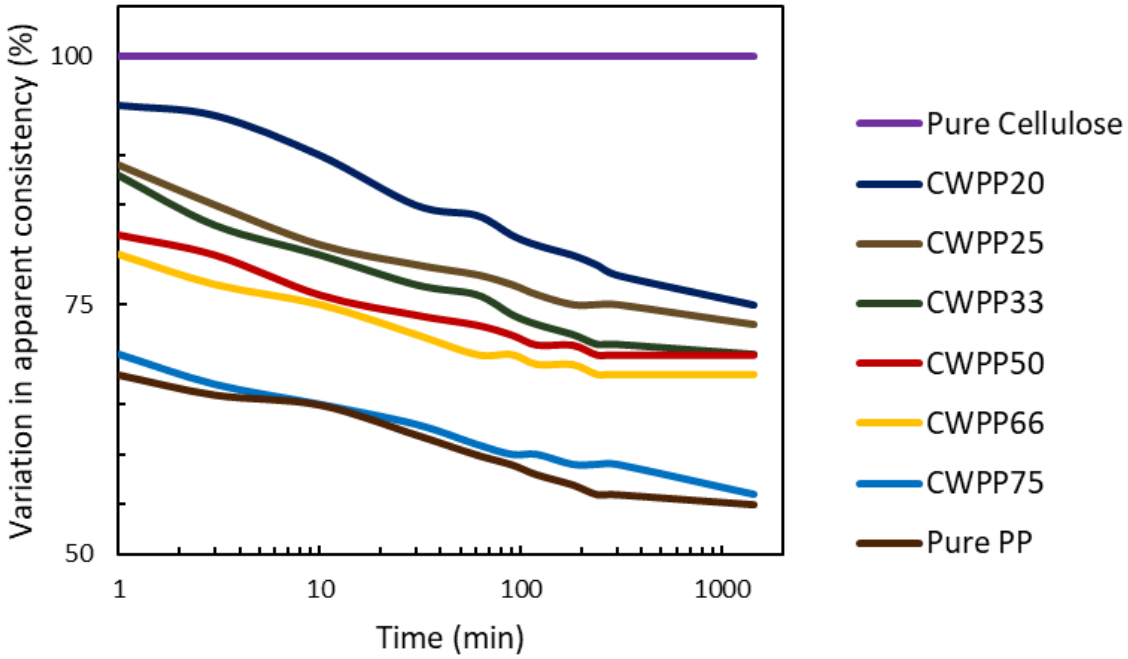

Figure 46: Variation in apparent consistency (%) as a function of time (min).

4.5 Filtration with Cellulose, Water, Polypropylene Fiber and Surfactant – CWPP-33S Cakes

A surfactant (debonder) was used in this project to decrease the cellulose inter-fiber bonding during composites manufacturing. Decreasing the interaction between cellulose fibers is much important because

it enable an improved dispersion of the cellulose fibers within the polymer matrix when manufacturing a thermoplastic composite. A good dispersion of cellulose fibers is likely to produce a composite with higher stiffness and strength.

In an aqueous medium, surfactants can promote the formation of foam, which is undesirable when manipulating mixtures in industrial scale applications. This being the case, two cellulose cake formulations with 0.5% and 1% (total weight) of surfactant content were prepared. The cakes were designated CWPP33S0.5 and CWPP33S1 (see Table 13).

Table 13: CW6PP33S cakes with 0.7 wt% of consistency.

Cake	Components (g)				Visual Aspect Ranking
	Cellulose	PP Fiber	Water	Surfactant	
CW6PP-33S0.5	0.49	0.21	98.80	0.50	Good
CW6PP-33s1.0	0.49	0.21	98.30	1.00	Failed

4.5.1 Results and Discussion

The visual aspect ranking of the CW6PP33S0.5 was good given their continuous and uniform aspect (shown in Figure 47). Cake CW6PP33S1 was not obtained due to the formation of foam in significant amounts which resulted in the overflow of the tank with pulp slurry. The results relating to the CW6PP33S0.5 cake and associated sample composite will be described and discussed in Section 5.5.

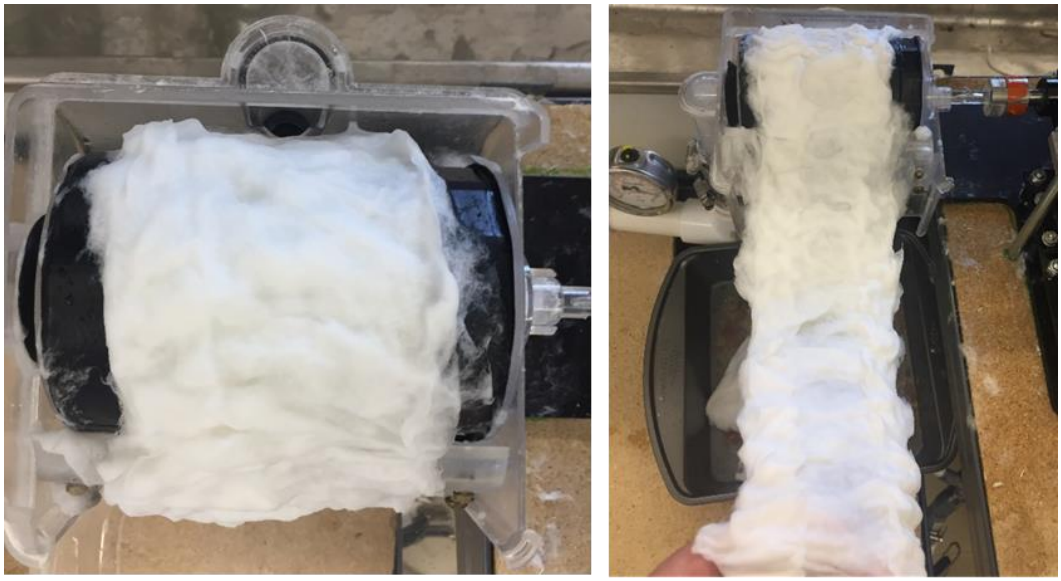

Figure 47: CW6PP33S0.5 cake on rotary drum filter.

4.6 Summary

In conclusion, the laboratory scale continuous filtration system was designed and assembled. It was built with a modified off-the-shelf laboratory scale drum scale filter coupled to a vacuum pump, submersible pump, pipes and valves.

The variables used to evaluate the filtration rate and visual aspect of the cakes were: vacuum pressure, drum filter rotation speed and consistency of the pulp. Filtration rate had a high positive effect by increase in consistency and vacuum pressure. Vacuum pressure also showed a high impact in the uniformity of the cake (visual aspect). Only when a high vacuum pressure was used the cake showed a good visual aspect. Rotation speed showed a weak influence on filtration rate compared to the other variables, within the current experimental range. The best combination of parameters was the following (CW6 cake): high vacuum (0.11 bar), high consistency (0.7 wt-%), and low rotation (3.8 rpm).

When PP fibers were used, the best overall performance was achieved with 33 wt% of PP fiber (CW6PP-33) because it showed good visual aspect ranking and higher PP fiber content. The effect of adding a surfactant to reduce the cellulose inter-fiber bonding strength. was also studied (CW6PP33S0.5 cake).

Chapter 5: Composites

5.1 Overview

This chapter presents the results and the discussion on the research evaluating the processability of selected cakes prepared in Chapter 4 with respect to preparing thermoplastic composites with polypropylene. Chapter 5 does not deal with filtration, it deals with extrusion, injection molding and the measurement of physical properties of the resulting thermoplastic composites. In this research, processability is defined as the ability to obtain viable composites preferably through injection moulding. An attempt is made to eliminate the compounding operation based on extrusion. As stated earlier, the research hypothesis tested here is if mixing a polypropylene fibers with the cellulose fibers in the wet slurry could produce a cake of cellulose and polypropylene that would enable improved processability. The most desirable outcome is to eliminate the compounding processing using extrusion and consequently preparing the thermoplastic composite directly with injection molding. If successful, this approached will led to a new technology that has not been reported in the literature yet.

When manufacturing cellulose, producers can either use cellulose directly to produce paper or store the cellulose. The most common method for preparing cellulose for storage is to produce sheets using a dewatering process (drum filter).

The dispersion of dry cellulose in polypropylene with extrusion is known to be a difficult process. Feeding regular sheets of dry cellulose in an extruder for compounding with polypropylene often clogs the extruder. Most authors in the literature have taken the approach of using a mill to grind the regular sheet of dry cellulose to disintegrate the sheet and produce a fluffy cellulose. This approach has been used by other researchers in our group. Grinding the sheet of dry cellulose produces a fluffy cellulose with aspect similar to cotton balls. The fluffy cellulose have very small bulk density, which creates a challenge to feeding it in

the extruder equipment. Most extrusion systems are design with feeders that can handle plastic pellets (typically around 3-5 mm) or powders (additives).

An attempt to extrude polypropylene pellets and cellulose from dry sheets was made here to replicate previous reports from other researchers in our lab. Although the outcome of this experiment was already known to be unsuccessful, it is presented here to serve as a reference in the context of this thesis.

The dry cellulose sheet was cut with a guillotine in size of approximately 0.5 cm (shown Figure 48) which was appropriate for feeding the lab-scale extruder. Then such cellulose sample was blended inside a beaker with PP pellets to form a mixture; this process is known as dry blend. Then this mixture was fed to the extruder and the injection molder. A diagram explaining this process is shown in Figure 49.

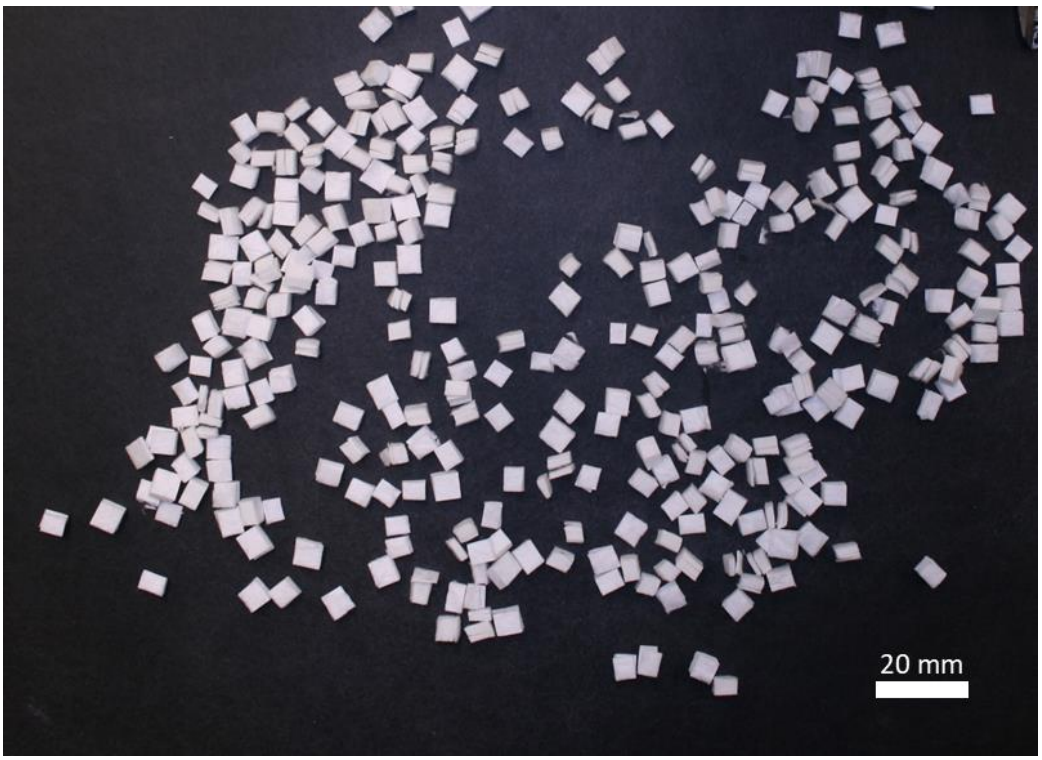

Figure 48: Cut dry cellulose.

An attempt was made to process mixture of polypropylene pellets and pieces of cellulose cut from a sheet using the lab scale extruder and injection molder. This process was not successful. Neither the injection molding nor the extrusion processes were capable of processing the feedstock mixture in a thermoplastic composite. The cut cellulose sheet (approximately 0.5 cm x 0.5 cm) caused the injector nozzle to be obstructed preventing the flow of material. The same occurred in the extrusion process, with cellulose obstructing the outflow opening and preventing the flow of material. An image of the clogged extruder is shown in Figure 50. The behavior can be attributed to the highly packed cellulose fiber present in the cut cellulose sheet. The cellulose sheet displays a high degree of fiber entanglement. The morphology and fiber arrangement in the cellulose sheet can be seen in the SEM image shown in Figure 51. Understanding the outcome of this experiment is important because it represents a significant barrier to developing a technology for manufacturing thermoplastics composites with polypropylene and cellulose fiber. The explanation for this is that the dispersion of the cut cellulose sheet during extrusion with polypropylene did not happen because the shear forces caused by molten polypropylene pellets during extrusion were unable to overcome the attraction forces and entanglement of the cellulose fibers present in the cellulose sheet. Further increasing shear forces during the extrusion could be done by significantly increasing the speed of extrusion screws (rpm). But this solution would not be possible because excessive shear during extrusion would lead to chain scission and thermal degradation of polypropylene resulting in poor mechanical properties.

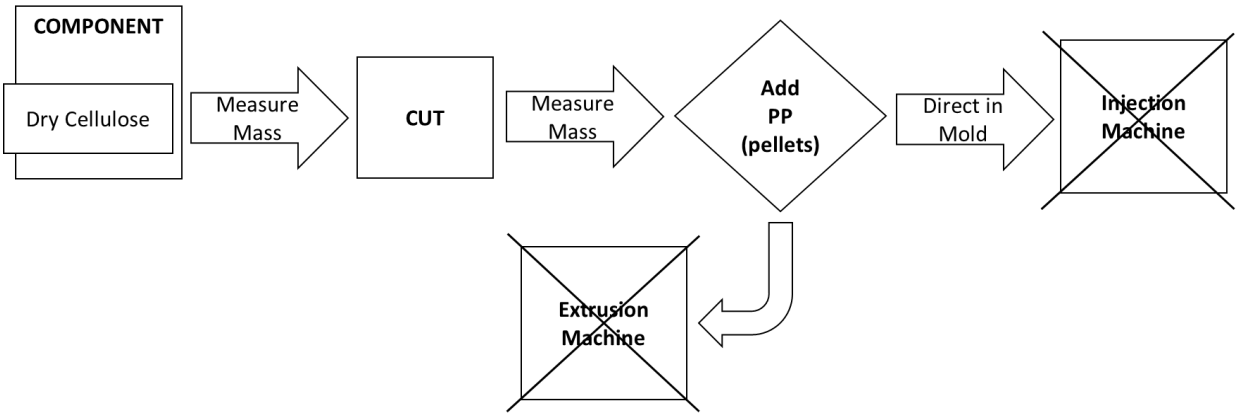

Figure 49: Process for the mixing of dry cellulose (cut) and PP pellets.

Figure 50: Obstruction of the extruder by the dry cellulose and PP mixture.

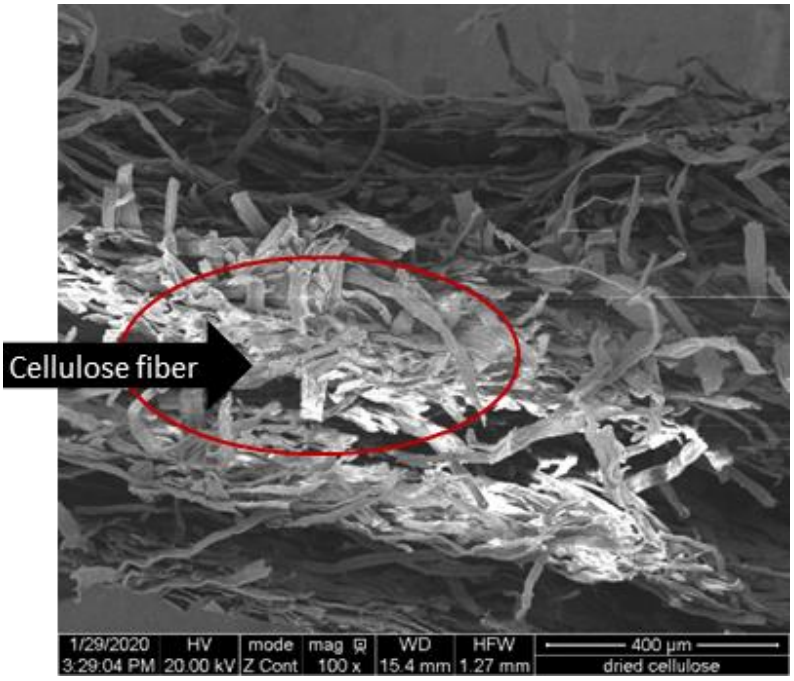

Figure 51: SEM of dry cellulose (cross-sectional view).

5.2 Processing Polypropylene and CW6 Cake

Similar to the process described in the previous section with respect to the cut cellulose sheet, the CW6 cake was mixed with PP pellets and subjected to injection moulding. However, here too, there were blockages at the exit of the injector nozzle. The cake and pellets were also subjected to extrusion, but this also failed due to blockage of the extruder outflow opening. Even with different operating conditions for the extruder (temperature, speed) and for the injector (temperature), it was not possible to obtain composite samples. A diagram for the entire process of attempting to obtain a resulting composite from the CW6 cake is shown in Figure 52. As shown by SEM imaging (Figure 53), the packing of cellulose fibers was reduced when compared to the dry cellulose sample (Figure 51). However, the inter-fiber interactions were still too strong to allow prompt dispersion of the fibers in the extrusion and injection moulding processes.

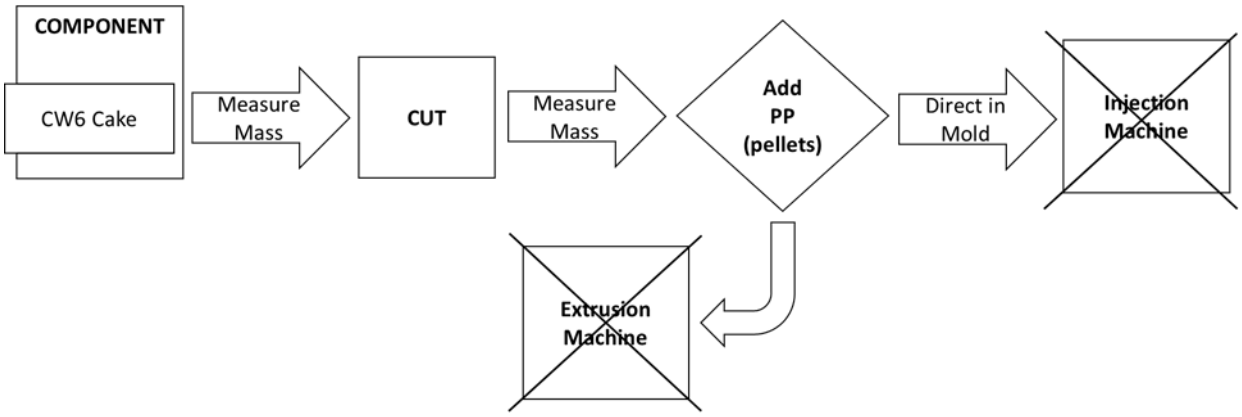

Figure 52: Process for the mixing of the CW6 cakes (cut) and PP pellets.

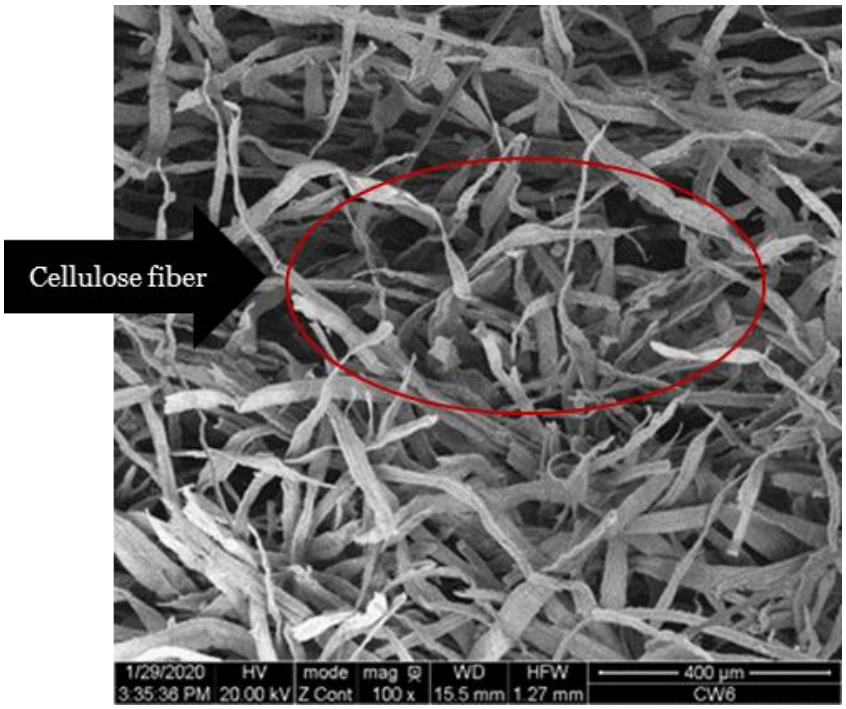

Figure 53: SEM of CW6 cake (cross-sectional view).

5.3 Processing Polypropylene and CW6PP33 Cake

It was possible to obtain a compound sample by first blending it with PP pellets with the CW6PP33 cake using extrusion and injection. The resulting composite was designated CW6PP33-X_I (Figure 55 and Figure 67). The diagram for this process is shown in Figure 54.

The attempt to prepare a composite directly with injection molding without prior extrusion was not successful. Blockage occurred at the injector nozzle. The interpretation of this result is that the presence of PP fibers inside the cellulose cake acted as spacers in between the cellulose fibers reducing the cellulose fiber-fiber interactions thus facilitating the dispersion of the cellulose fibers and mixing with the molten polypropylene during the extrusion process. Figure 56 shows the SEM of the CW6PP33 cake. It is possible to see that the smooth polypropylene fibers were well mixed with inside the cake within the cellulose fibers. The mixture of the polypropylene fibers and the cellulose fibers was facilitated by the low concentration (low consistency) of solids in the slurry prior to the continuous drum filtration process. The speed of the filtration process is also considered a relevant factor because a slow filtration rate could have enabled phase separation between polypropylene fibers and cellulose fibers.

The level of shear forces used here to disperse the CW6PP33 cake inside polypropylene matrix in the extruder was similar to the previous attempts because the same extrusion conditions were used. This clearly demonstrated that the integration of the polypropylene fibers within the cellulose cake has proved to be a successful strategy to enable the compounding of cellulose cakes and polypropylene using extrusion. This approach has not been reported in the literature before.

However, the CW6PP33 cake could not be processed by direct injection, that is, without compounding the CW6PP33 cake with polypropylene using extrusion. The attempt of direct injection molding led to clogging the nozzle of the injection molder. This is interpreted based on the level of mixing

present in the extruder and the injection molder. The extruder has a high degree of mixing and a low degree of shear when compared to the injection molding machine.

Cellulose content was limited to 10 wt% in the final composites. Image analysis was used as an attempt to understand the dispersion of cellulose inside the polypropylene matrix after injection molding. Photography with transillumination (light transmission through the sample) was used to identify the dispersion of the cellulose fibers he PP matrix in the moulded samples. The objective of capturing these images was to identify the phase contrast (dark areas in the image) indicating the presence of cellulose fibers.

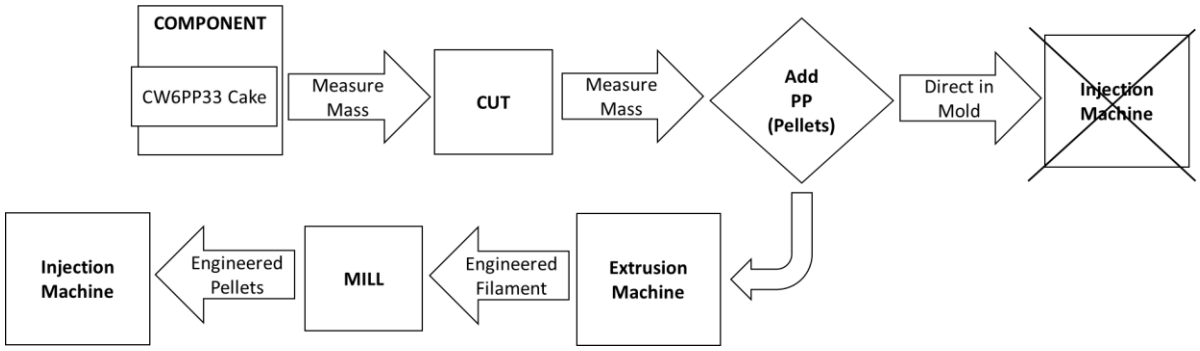

Figure 54: Process for obtaining the CW6PP33-X_I samples.

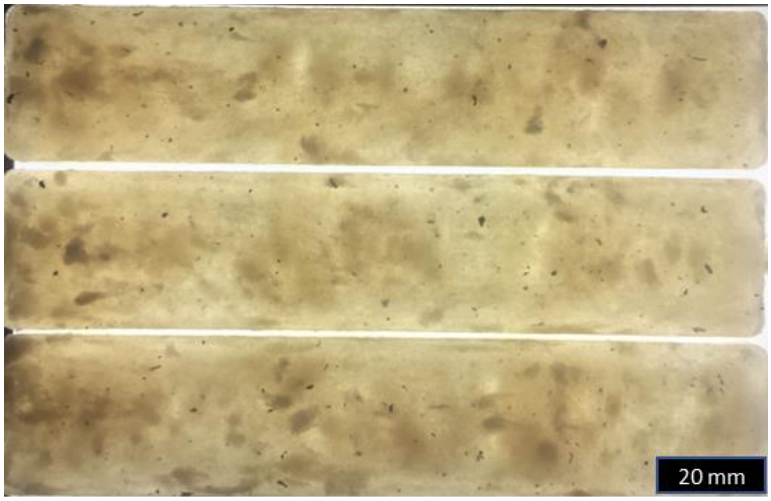

Figure 55: Photography with transillumination of CW6PP33-X_I moulded samples.

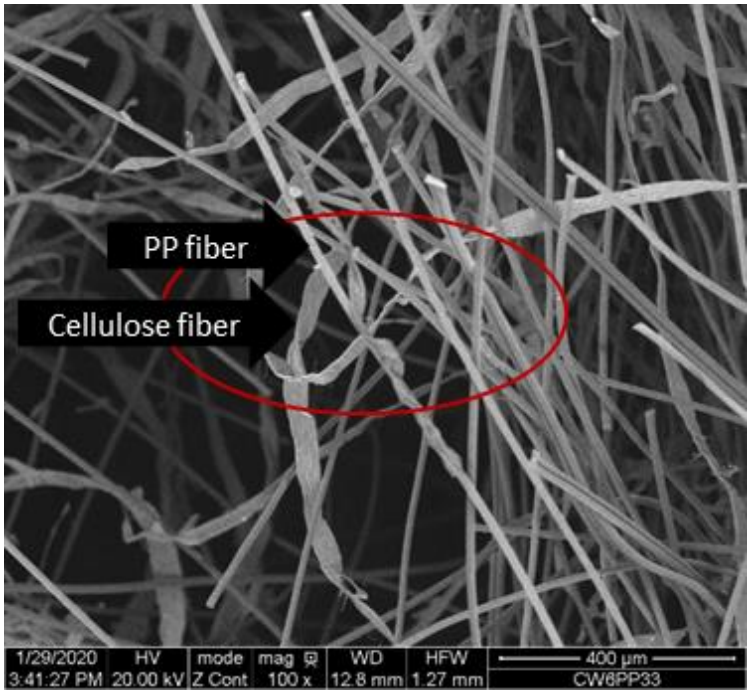

Figure 56: SEM of CW6PP33 cake (cross-sectional view).

5.4 Processing Polypropylene and CW6PP-33S0.5 Cake

The next step in attempt to produce a cellulose cake that would enable direct injection molding with polypropylene pellets was to evaluate the effect of debonder additive. The role of this additive is to work as a surfactant on the interface of cellulose fiber and decrease the level of inter-fiber interaction by replacing hydrogen bonding with other interaction of lesser strength.

The direct injection molding with the CW6PP33S0.5 cake and polypropylene pellets was successful. This is a significant milestone because the resulting composite was prepared without the need to first extrusion compounding.

First blending it with PP pellets through direct injection; this resulting sample was named CW6PP33S0.5_DI. Likewise, injection with prior extrusion was also successful, and the resulting sample was labeled CW6PP33S0.5_X_I. Figure 57 shows the flow of the entire process. As explained previously, the addition of a surfactant reduces the cellulose fiber-fiber interaction allowing the fibers to easily disperse in the PP matrix, when used in combination with PP fibers, as shown by SEM imaging (see Figure 58). The resulting samples obtained in these processes are shown in Figure 59 and Figure 60, and by SEM imaging in Figure 68 and Figure 69.

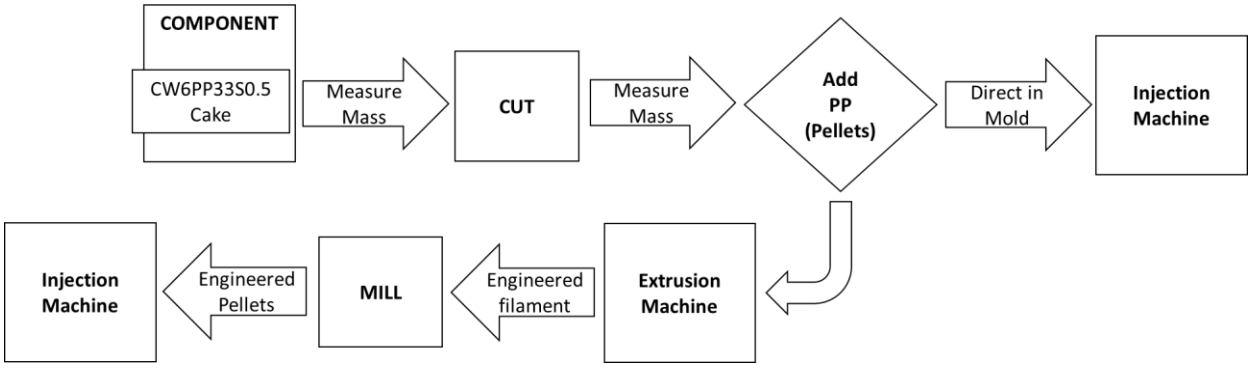

Figure 57: Process for the mixing of CW6PP33S0.5 cakes and PP pellets.

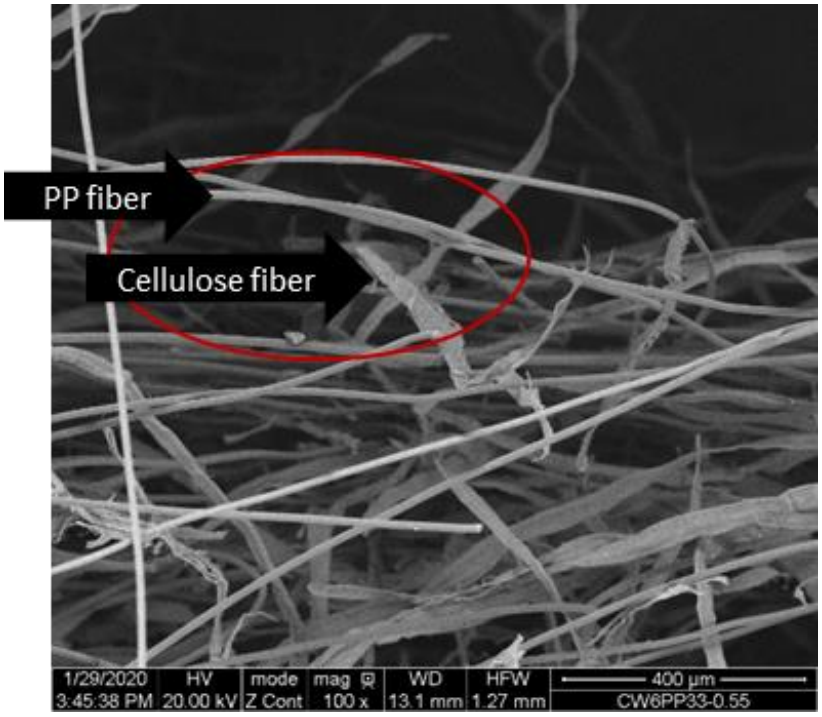

Figure 58: SEM of CW6PP33S0.5 cake (cross-sectional view).

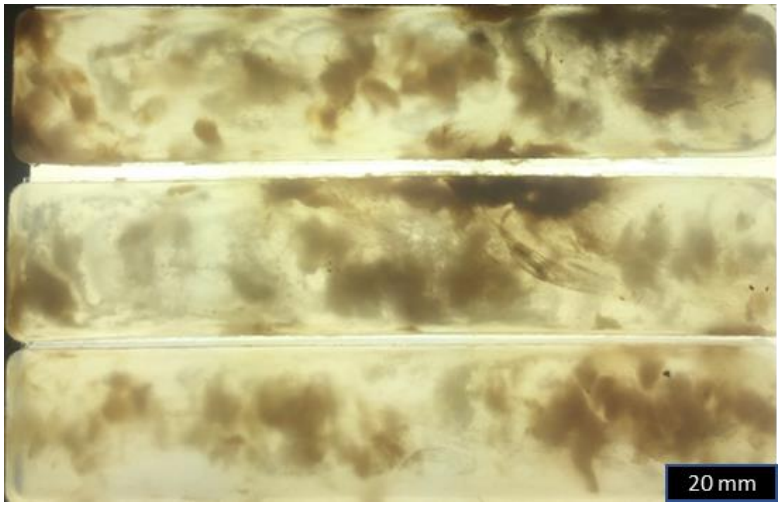

Figure 59: Photography with transillumination of CW6PP33S0.5_DI moulded samples.

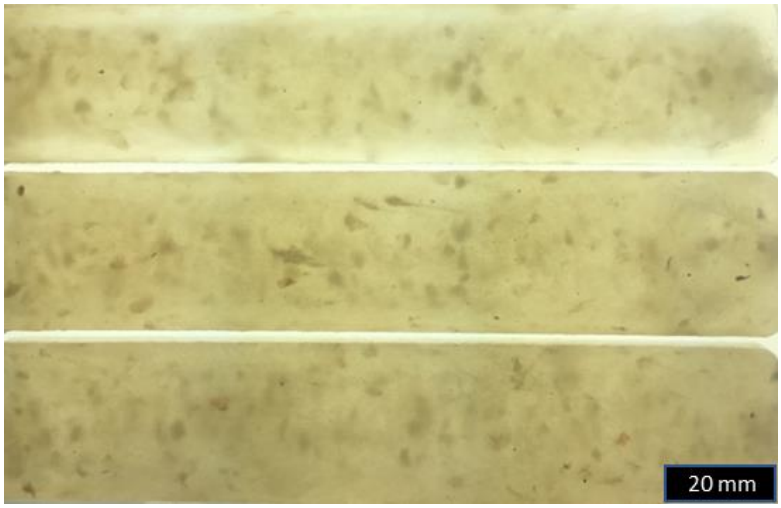

Figure 60: Photography with transillumination of CW6PP33S0.5-X_I moulded samples.

5.5 Processing Polypropylene, MAPP and CW6PP33S0.5 Cake

As discussed in Section 2.1, one of the main challenges for technologies involving composite materials is to obtain strong bonds between the matrix and fibers. The most studied methods of achieving this objective are those that involve chemical interaction through the modification of the fiber, the modification of the matrix, or the addition of coupling agents [37]. These coupling agents include polypropylene grafted with maleic anhydride (MAPP). The interactions between the coupling agent anhydride and the hydroxyl groups on the surface of cellulose fibers increase the adhesion of the fibers to the matrix and can improve composite properties [1].

The effect of MAPP on the processability and properties of the thermoplastic composites was investigated here. A compound was prepared with the replacement of PP pellets by an equivalent amount of MAPP. Table 14 shows the formulation for this sample designated as CW6PP33S0.5-MA. Figure 61 shows the flow of the entire process.

The effect of MAPP was favorable towards the processability of the composite. It was possible to obtain a composite sample using direct injection; the resulting sample was designated CW6PP33S0.5MA-DI (Figure 62). Likewise, processing this sample first with extrusion and secondly with injection molding was also successful; the resulting sample was labeled CW6PP33S0.5MA_X_I (Figure 63).

Table 14: Composite with PP, MAPP and CW6PP33S0.5.

	Components (g)		
Sample	PP	MAPP	CW6PP33S0.5
CW6PP33S0.5MA	84.00	1.00	15.00

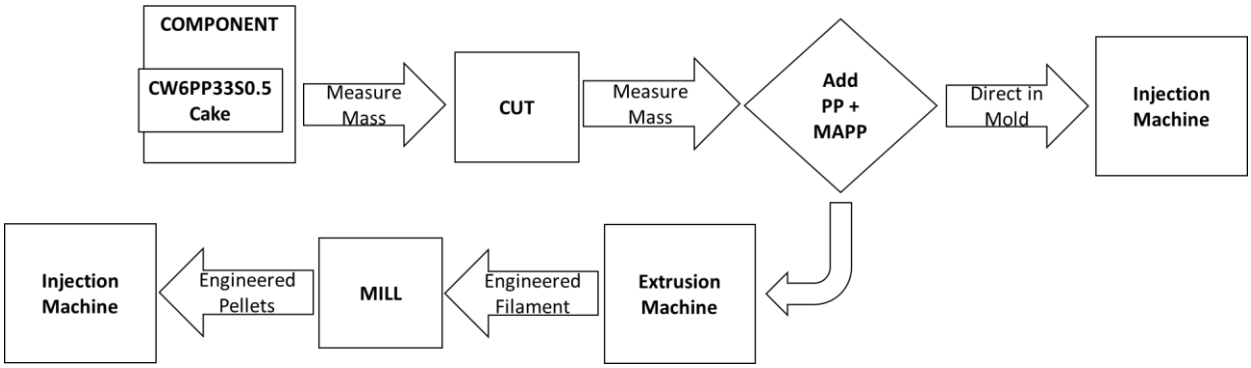

Figure 61: Process for mixing the CW6PP33 cakes, PP and MAPP.

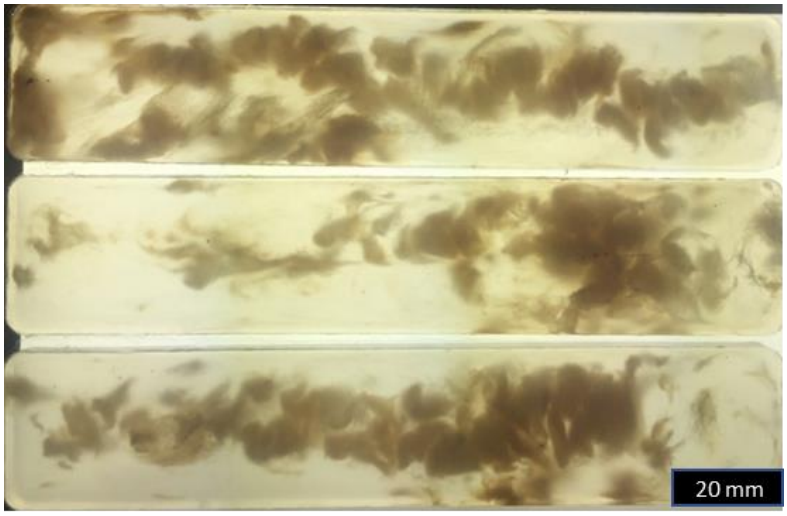

Figure 62: Photography with transillumination of CW6PP330.5SMA_DI moulded samples.

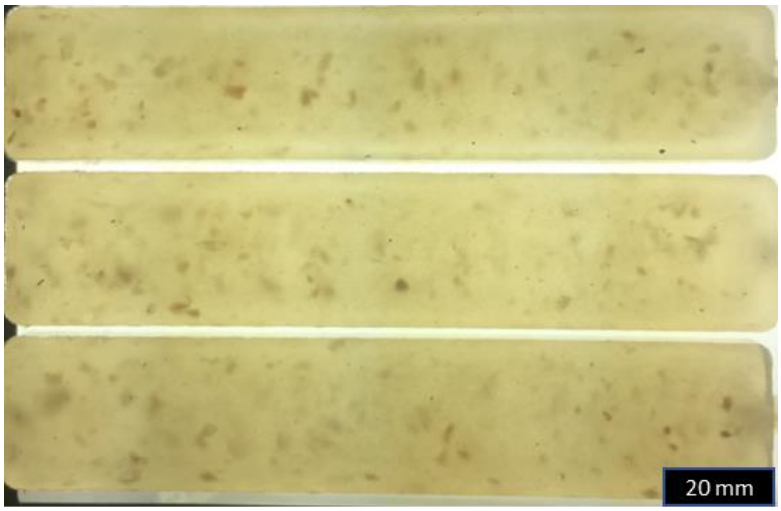

Figure 63: Photography with transillumination of CW6PP330.5SMA_X_I samples.

5.6 Results and Discussion

As mentioned in the previous sections, 5 samples were obtained with 10% cellulose content (wt%) through the injection process with and without extrusion. These samples are described in Table 15 below.

After investigating the processability of the compounds resulting from adding PP pellets to the cakes obtained through the lab-scale drum filtration system, an assessment was performed to evaluate how the cellulose fibers affect the flexural and impact properties of the PP composites. SEM was used to evaluate the dispersion and interaction of fibers with the PP matrix.

Table 15: Sample processability.

Sample	Components	Processability (Yes, Failed, n/a)	
		Direct Injection (DI)	Extruder – Injection (X_I)
Dry Cellulose	Cellulose	Failed	Failed
CW6 Cake	Cellulose	Failed	Failed
CW6PP33_X_I	Cellulose, PP Fiber	Failed	Yes
CW6PP33S0.5_DI	Cellulose, PP Fiber, Surfactant	Yes	n/a
CW6PP33S0.5_X_I	Cellulose, PP Fiber, Surfactant	n/a	Yes
CW6PP33S0.5MA_DI	Cellulose, PP Fiber, Surfactant, MAPP	Yes	n/a
CW6PP33S0.5MA_X_I	Cellulose, PP Fiber, Surfactant, MAPP	n/a	Yes

5.6.1 Mechanical Properties

The flexural modulus and strength for the pure PP and the composites are shown in Figure 64 and Figure 65, respectively. It can be seen that the composites presented an increase of approximately 20 % in flexural modulus when compare to neat PP while the flexural strength was 10 % higher. None of the samples broke during the flexural test, resulting in the same strain at break (0.05) for all of them.

The Tukey test (significance level of 5%) was applied to evaluate if the difference between the results of the different composites was relevant. However, the results did not show significant differences

between them. The Tukey test is a popular method of comparing treatment averages and determining if the differences are statistically significant. It uses the variability of all results simultaneously to compare sample means pairwise at a fixed significance level (α). It is usually performed after the analysis of variance of single-factor experiments [79].

These results demonstrate that the cakes obtained with the lab-scale drum filtration system behave as effective reinforcement in the PP matrix, giving rise to a significant improvement in material stiffness. A higher increase in flexural modulus was expected in the samples where MAPP was added, as described by several previous studies [23], [29], [37], [48]. However, no significant increase in flexural modulus or flexural strength was observed in this project when 1wt.% of MAPP was added. Perhaps the relatively poor dispersion of the fiber in the direct injection process was not optimal to reveal the benefits of MAPP. Another relevant aspect is that the contribtion of MAPP tends to more relevant on tensile strengh and not on flexural strengh. Although the extruded sample with MAPP did not present significantly improved mechanical properties when compared to the sample obtained through direct injection, the material was more homogenous, as indicated by the lower standard deviation of the mechanical properties as well as by SEM (Figure 70 and Figure 71) and photography images (Figure 62 and Figure 63).

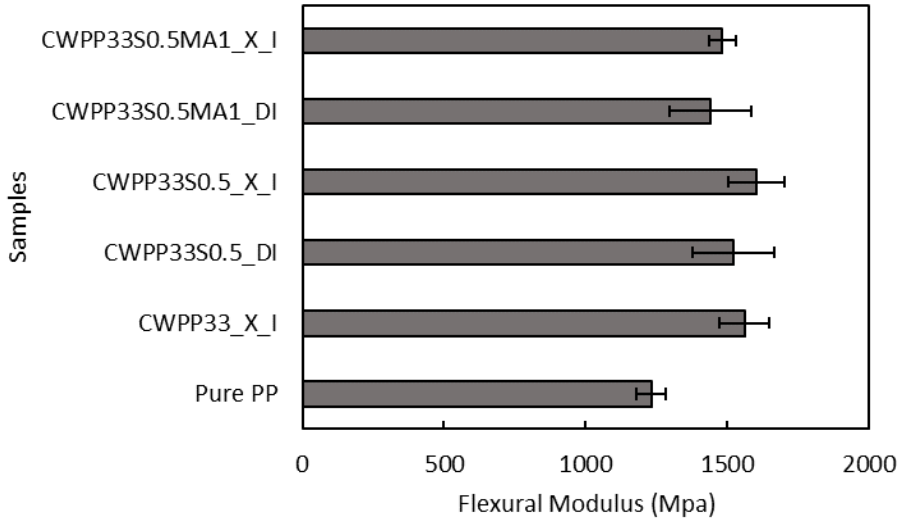

Figure 64: Flexural modulus (MPa) test results.

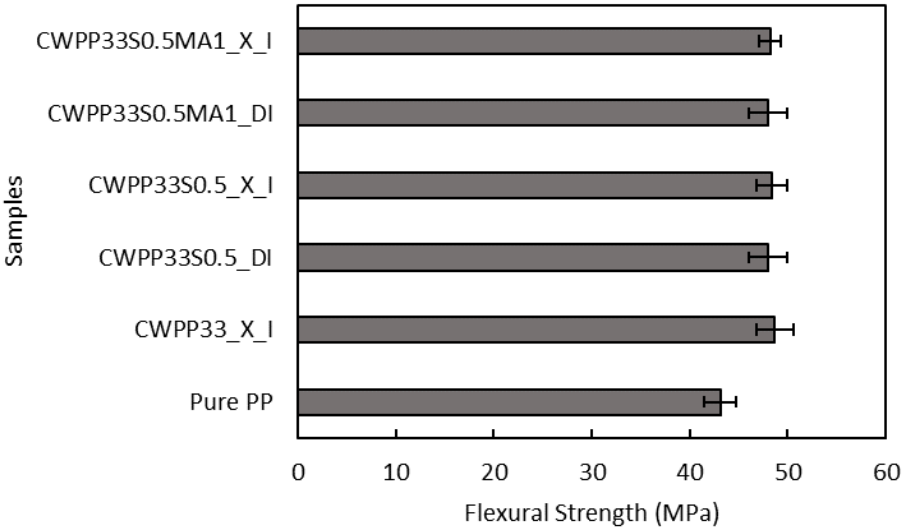

Figure 65: Flexural strength (MPa) test results.

The impact strength results for pure PP and the composites are shown in Figure 66. The addition of cellulose fibers to the PP matrix causes a small reduction in impact strength. Several authors have reported similar behaviour [1], [9], [27], [28]. This behaviour can be attributed to fiber agglomeration promoting stress concentrations which in turn lead to crack formation, propagation and failure upon an impact.

Composite with dispersed phase may require less energy to break during the impact test [82], [83]. The different processes and additives used in composite production had a slight effect on impact strength, although impact strength tended to decrease as more additives were incorporated.

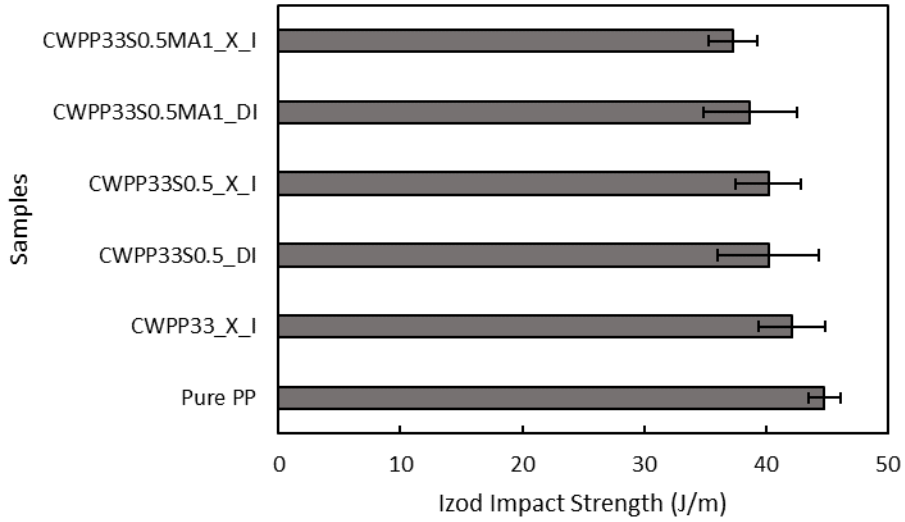

Figure 66: Izod impact (J/m) test results.

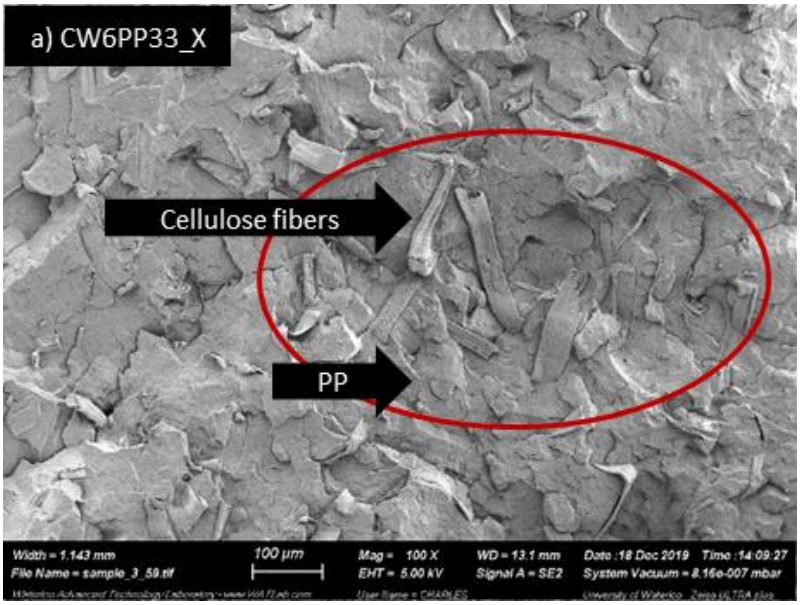

Figure 67: SEM of CW6PP33-X cake (cross-sectional view).

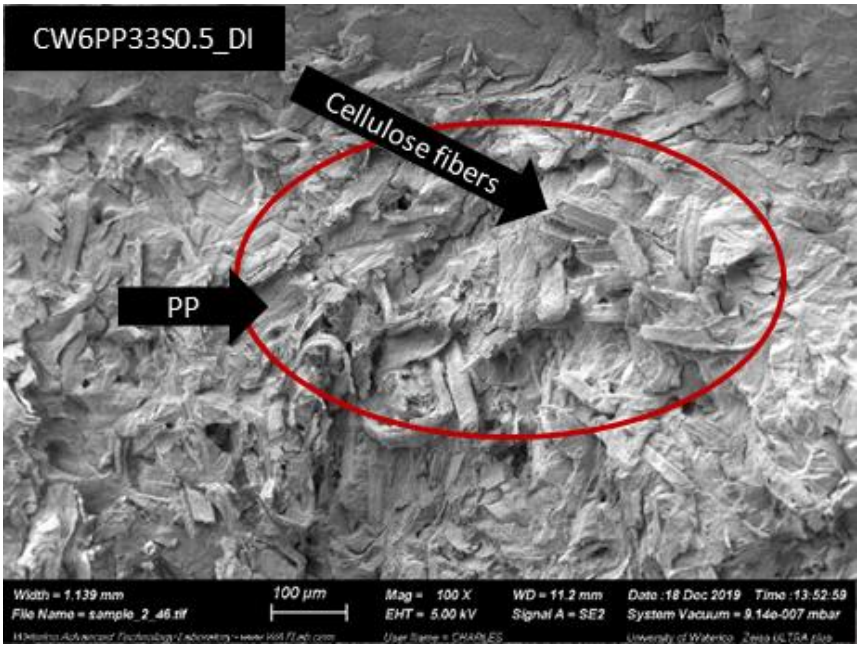

Figure 68: SEM of CW6PP33S0.5_DI cake (cross-sectional view).

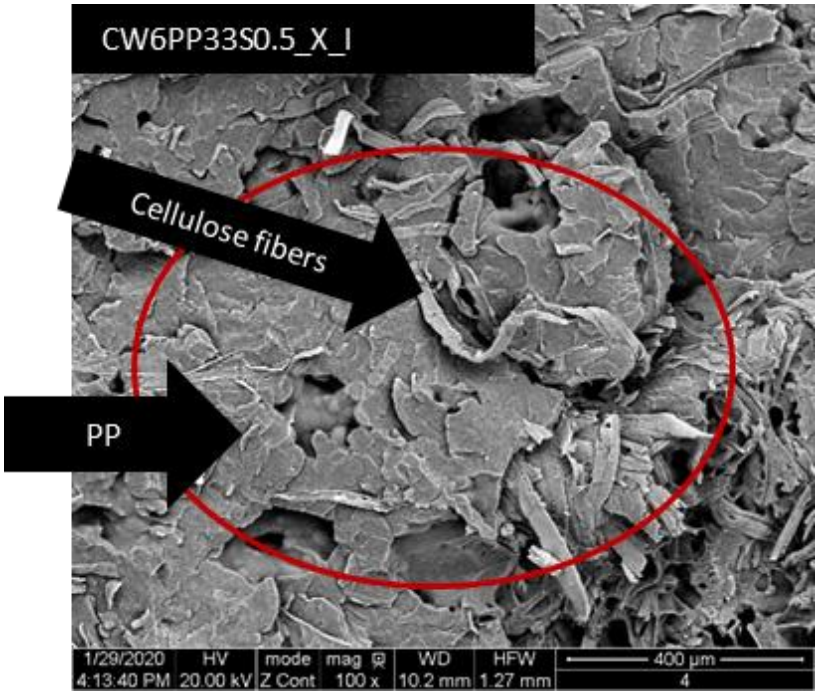

Figure 69: SEM of CW6PP33-X_I cake (cross-sectional view).

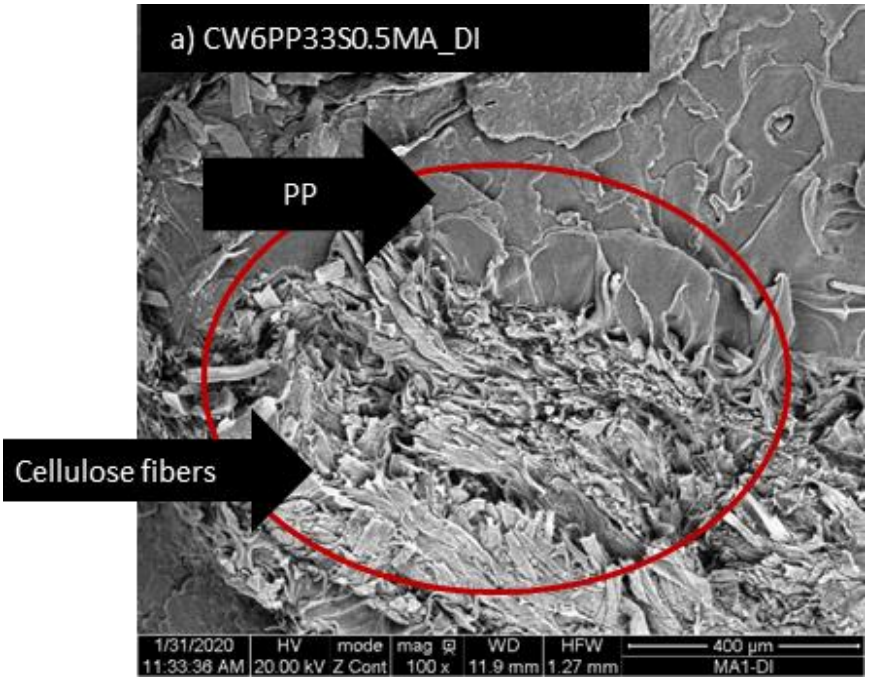

Figure 70: SEM of CW6PP33S0.5MA_DI cake (cross-sectional view).

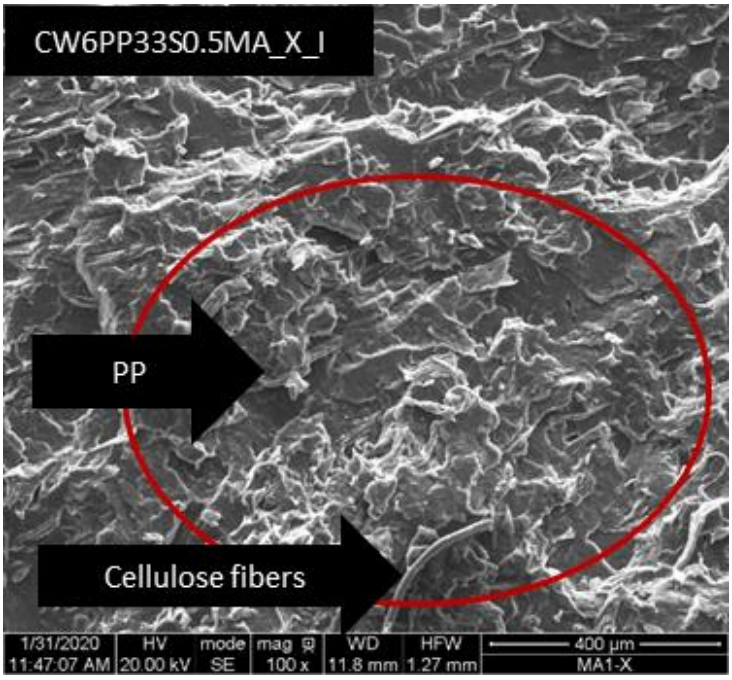

Figure 71: SEM of CW6PP33S0.5MA_X_I cake (cross-sectional view).

Chapter 6: Conclusion and Recommendation

6.1 Conclusion

The objectives of this study were:

1. Assemble a continuous drum filtration system in laboratory scale as a research tool;
2. Evaluate the filtration rate and visual aspect of the cake;
3. Use the continuous filtration system to obtain cakes with cellulose and PP fibers;
4. Evaluate the processability of the cellulose cakes in injection moulding (with or without prior extrusion).

1. The project was elaborated with the purchase of a laboratory scale vacuum drum filter, which was later modified extensively. An auxiliary package was designed and added to the drum filter. Moreover, the drum filter was modified to better suit the process and to match filter media used in the pulp industry.

2. The variables used to evaluate the filtration rate and visual aspect of the samples were: vacuum, rotation speed and consistency. The rotation speeds used in this study had very little influence on the filtration rate and uniformity of the cellulose cakes. However, filtration rate was highly affected by consistency as well as by the vacuum pressure applied to the drum filter. Moreover, an increase in these parameters lead to an increase in filtration rate. Uniformity of the cellulose cake was only affected by vacuum pressure. Only high vacuum levels resulted in uniform cakes that were evaluated as good in terms of visual aspect rating. These parameters were selected to produce a reference cake named CW6. The levels of the parameters were: high vacuum level (0.11 bar), high consistency (0.7 wt-%), and low rotation (3.8 rpm).

3. The continuous filtration system was used to produce other cakes based on the CW6 cake, but with different amounts if PP fiber and cellulose. The consistency of the slurry was maintained constant. The sample with 33 wt% of PP fiber was the preferred (CW6PP-33) because the

overall performance during filtration assessed as good visual aspect ranking and higher PP fiber content. Mixtures with higher PP contents (50 wt%) obstructed the system making it impossible to produce samples. With the aim of further improving CW6PP-33, a surfactant (debonder) was tested to produce sample CW6PP33S0.5. The role of the debonder was to reduce the cellulose inter-fiber bonding strength.

4. Thermoplastic composites were prepared with 3 different cakes (CW6, CW6PP33, CW6PP33S0.5) as well as dry cellulose. PP pellets were mixed in with cakes (maintaining a cellulose content of 10 wt% for all composites). The composites were prepared by means of injection molding, with or without prior extrusion. The results showed that composites could not be obtained with the CW6 cake, nor could they be obtained with dry cellulose (from cellulose sheet). The presence of PP fiber in cakes enabled the production of composite samples by means of extrusion compounding followed by injection molding. Without extrusion, however, a composite could not be produced.

   The composite samples obtained with CW6PP33S0.5 cakes (which contained the surfactant) were successfully processed with and without extrusion prior to injection molding. In an attempt to improve the interface between the cellulose and the PP matrix, a coupling agent (MAPP) was mixed in with the CW6PP33S0.5 cakes and additional PP pellets. The resulting mixture was labeled CW6PP33S0.5MA. Composites with this mixture were successfully moulded with and without prior extrusion. However, these composites did not present a significant increase in flexural modulus.

In summary, the approach to produce cellulose and PP fiber cakes with the lab-scale rotary drum filtration system is effective for mixing cellulose and PP fibers. This is an advantage because PP fibers could be easily added to the cellulose slurry during its manufacturing with minimal cost and minor

adjustments to the dewatering process. These cellulose cakes with PP fiber and additives were successfully processed with injection molding without the need for extrusion compounding. This outcome could have significant impact in the production of sustainable thermoplastics with cellulose pulp because it solves the problem of mixing cellulose and polypropylene while removing the need for extrusion.

Composites obtained using extrusion were more homogeneous with respect to fiber dispersion than those obtained simply by means of direct injection molding. However, the former did not present significant differences with respect to mechanical properties, which indicates that the extrusion process can be eliminated to reduce costs in industrial scale applications. Composites like these can be used in automotive applications, including for moulded internal parts.

6.2 Recommendations for Future Work

Improve fiber dispersion – The results of this study showed that the filtration and composite preparation processes can be further optimized. This could bring about better fiber dispersion in the PP matrix, which could in turn improve the mechanical properties of resulting composites.

Effect of PP fiber on consistency – It was observed that contents of PP fiber higher than 33 % caused clogging of pipes in the filtration system. It would be desirable to investigate other means to enable filtration of cakes with maybe 50% of PP fiber because it could be beneficial for the processability of the composites.

Additives - The use of surfactants (debonder) and compatibilizers (coupling agent) were important to enable the processability of cakes into composites. It would be interesting to investigate of other types of debonder and perhaps other types of polymer fibers which could have a beneficial contribution to the processability. This could be an additional factor in eliminating the need for prior extrusion before moulding.

Other tests - Depending on the application, other tests beyond the flexural strength and impact strength tests used in this project, should be carried out. Such tests include tensile testing, water absorption and heat deflection temperature, among others.

Bibliography

[1] H. Ku, H. Wang, N. Pattarachaiyakoop, and M. Trada, "A review on the tensile properties of natural fiber reinforced polymer composites," *Compos. Part B Eng.*, vol. 42, no. 4, pp. 856–873, 2011.

[2] L. Mohammed, M. N. M. Ansari, G. Pua, M. Jawaid, and M. S. Islam, "A review on natural fiber reinforced polymer composite and its applications," *Int. J. Polym. Sci.*, vol. 2015, pp. 1–15, 2015.

[3] A. K. Mohanty, M. Misra, and L. T. Drzal, *Natural Fibers, Biopolymers, and Biocomposites*, 1st ed. Baton Rouge: CRC Press, 2005.

[4] A. K. Diallo, C. Jahier, R. Drolet, B. Tolnai, and D. Montplaisir, "Cellulose filaments reinforced low-density polyethylene," *Polym. Compos.*, vol. 40, no. 1, pp. 16–23, 2019.

[5] D. K. Rajak, D. D. Pagar, P. L. Menezes, and E. Linul, "Fiber-reinforced polymer composites: manufacturing, properties, and applications," *Polymers (Basel).*, vol. 11, no. 10, p. 1667, Oct. 2019.

[6] H. Abramovich, *Introduction to composite materials*. IntechOpen, 2017.

[7] H. Quan, Z. M. Li, M. B. Yang, and R. Huang, "On transcrystallinity in semi-crystalline polymer composites," *Composites Science and Technology*, vol. 65, no. 7–8. pp. 999–1021, Jun-2005.

[8] C. Scarponi and C. S. Pizzinelli, "Interface and mechanical properties of natural fibres reinforced composites: a review," *Int. J. Mater. Prod. Technol.*, vol. 36, no. 1–2, pp. 278–303, 2009.

[9] N. E. Zafeiropoulos, Ed., *Interface Engineering of Natural Fibre Composites for Maximum Performance*, 1st ed. Oxford: Woodhead Pub, 2011.

[10] A. R. Sanadi, D. F. Caulfield, and R. M. Rowell, "Reinforcing polypropylene with natural fibers," *Plast. Eng.*, vol. 50, no. 4, p. 27, 1994.

[11] M. A. López-Manchado, J. Biagitti, and J. M. Kenny, "Comparative study of the effects of different fibers on the processing and properties of ternary composites based on PP-EPDM blends," *Polym. Compos.*, vol. 23, no. 5, pp. 779–789, 2002.

[12] J. L. Thomason and M. A. Vlug, "Influence of fibre length and concentration on the properties of glass fibre-reinforced polypropylene: 4. Impact properties," *Compos. Part A Appl. Sci. Manuf.*,

vol. 28, no. 3, pp. 277–288, 1997.

[13] Y. Yoo, M. W. Spencer, and D. R. Paul, “Morphology and mechanical properties of glass fiber reinforced Nylon 6 nanocomposites,” *Polymer (Guildf).*, vol. 52, no. 1, pp. 180–190, Jan. 2011.

[14] J. Himani and J. Purnima, “Development of glass fiber, wollastonite reinforced polypropylene hybrid composite: Mechanical properties and morphology,” *Mater. Sci. Eng. A*, vol. 527, no. 7, pp. 1946–1951, 2010.

[15] T. Bárány, T. Czigány, and J. Karger-Kocsis, “Application of the essential work of fracture concept for polymers, related blends and composites: A review,” *Prog. Polym. Sci.*, vol. 35, no. 10, pp. 1257–1287, 2010.

[16] G. He, F. Zhang, L. Huang, J. Li, and S. Guo, “Evaluation of the fracture behaviors of multilayered propylene-ethylene copolymer/polypropylene homopolymer composites with the essential work of fracture,” *J. Appl. Polym. Sci.*, vol. 131, no. 15, Aug. 2014.

[17] A. M. Sharma, “Mechanical behaviour, water absorption and morphology of wheat straw, talc, mica and wollastonite filled polypropylene composites,” University of Waterloo, Waterloo, Ont, 2012.

[18] W. Steen and R. Clark, “Talc in Polypropylene,” in *Handbook of Polypropylene and Polypropylene Composites*, I. Marcel Dekker, Ed. New York, 2003, pp. 1–30.

[19] L. Lapcik, P. Jindrova, B. Lapcikova, R. Tamblyn, R. Greenwood, and N. Rowson, “Effect of the talc filler content on the mechanical properties of polypropylene composites,” *J. Appl. Polym. Sci.*, vol. 110, no. 5, pp. 2742–2747, 2008.

[20] S. Maiti and K. Sharma, “Studies on polypropylene composites filled with talc particles,” *J. Mater. Sci.*, vol. 27, no. 17, pp. 4605–4613, 1992.

[21] J. Karger-Kocsis, *Polypropylene: Structure, Blends and Composites*, 1st ed. London: Chapman & Hall, 1993.

[22] B. Kaynak, M. Spoerk, A. Shirole, W. Ziegler, and J. Sapkota, “Polypropylene/cellulose composites for material extrusion additive manufacturing,” *Macromol. Mater. Eng.*, vol. 303, no. 5, p. 1800037, 2018.

[23] N. Saba, M. Jawaid, O. Y. Alothman, and M. T. Paridah, “A review on dynamic mechanical

properties of natural fibre reinforced polymer composites," *Constr. Build. Mater.*, vol. 106, pp. 149–159, 2016.

[24] R. Malkapuram, V. Kumar, and Y. S. Negi, "Recent development in natural fiber reinforced polypropylene composites," *J. Reinf. Plast. Compos.*, vol. 28, no. 10, pp. 1169–1189, 2009.

[25] K. Suzuki, Y. Homma, Y. Igarashi, H. Okumura, and H. Yano, "Effect of preparation process of microfibrillated cellulose-reinforced polypropylene upon dispersion and mechanical properties," *Cellulose*, vol. 24, no. 9, pp. 3789–3801, 2017.

[26] L. Huang, Q. Wu, Q. Wang, R. Ou, and M. Wolcott, "Solvent-free pulverization and surface fatty acylation of pulp fiber for property-enhanced cellulose/polypropylene composites," *J. Clean. Prod.*, vol. 244, p. 118811, 2020.

[27] A. Arbelaiz and I. Mondragon, "Testing the effect of processing and surface treatment on the interfacial adhesion of single fibres in natural fibre composites," in *Interface engineering of natural fibre composites for maximum performance*, 2011, pp. 146–185.

[28] L. Ma, L. J. He, and S. Y. Shao, "Study on effect of surface treating method on mechanical behavior ofthree plant fiber reinforced polypropylene composites," *Polym. Polym. Compos.*, vol. 25, no. 1, pp. 93–102, 2017.

[29] T. Sullins, S. Pillay, A. Komus, and H. Ning, "Hemp fiber reinforced polypropylene composites: The effects of material treatments," *Compos. Part B Eng.*, vol. 114, pp. 15–22, 2017.

[30] C. E. Carraher, *Introduction to Polymer Chemistry*, 3rd ed. Boca Raton, FL: CRC Press, 2013.

[31] M. Lewin, *Handbook of Fiber Chemistry*, 3rd ed., vol. 16. Boca Raton, FL: CRC, Taylor & Francis, 2007.

[32] Y. Lin *et al.*, "Structural evolution of hard-elastic isotactic polypropylene film during uniaxial tensile deformation: the effect of temperature," *Macromolecules*, vol. 51, no. 7, pp. 2690–2705, 2018.

[33] E. J. Baltá-Calleja and H.-G. Kilian, "A novel concept in describing elastic and plastic properties of semicrystalline polymers: polyethylene," *Colloid Polym. Sci.*, vol. 263, no. 9, pp. 697–707, Sep. 1985.

[34] W. D. Callister, *Fundamentals of Materials Science and Engineering: an Integrated Approach*,

4th ed. Hoboken, NJ: Wiley, 2012.

[35] J. Holbery and D. Houston, “Natural-fiber-reinforced polymer composites in automotive applications,” *JOM*, vol. 58, no. 11, pp. 80–86, 2006.

[36] A. Patil, A. Patel, and R. Purohit, “An overview of polymeric materials for automotive applications,” *Mater. Today Proc.*, vol. 4, no. 2, pp. 3807–3815, 2017.

[37] A. Ali *et al.*, “Hydrophobic treatment of natural fibers and their composites - a review,” *J. Ind. Text.*, vol. 47, no. 8, pp. 2153–2183, 2018.

[38] E. Malmström and A. Carlmark, “Controlled grafting of cellulose fibres - an outlook beyond paper and cardboard,” *Polym. Chem.*, vol. 3, no. 7, pp. 1702–1713, 2012.

[39] E. C. Lengowski, E. A. Bonfatti Júnior, M. M. Nishidate Kumode, M. E. Carneiro, and K. G. Satyanarayana, “Nanocellulose in the paper making,” in *Sustainable Polymer Composites and Nanocomposites*, no. 167, Springer International Publishing, 2019, pp. 1027–1066.

[40] J. N. Stephenson, *Pulp and Paper Manufacture.*, 1st ed. New York: McGraw-Hill, 1950.

[41] R. C. P. Oliveira, M. Mateus, and D. M. F. Santos, “Chronoamperometric and chronopotentiometric investigation of Kraft black liquor,” *Int. J. Hydrogen Energy*, vol. 43, no. 35, pp. 16817–16823, 2018.

[42] F. M. Bolam, *Fundamentals of Papermaking Fibres: Transactions of the Symposium*. London: Technical Section, British Paper and Board Makers’ Assn, 1961.

[43] H. Zhao, J. H. Kwak, Z. Conrad Zhang, H. M. Brown, B. W. Arey, and J. E. Holladay, “Studying cellulose fiber structure by SEM, XRD, NMR and acid hydrolysis,” *Carbohydr. Polym.*, vol. 68, no. 2, pp. 235–241, 2007.

[44] G. Siqueira, J. Bras, and A. Dufresne, “Cellulosic bionanocomposites: A review of preparation, properties and applications,” *Polymers (Basel).*, vol. 2, no. 4, pp. 728–765, 2010.

[45] R. J. Moon, A. Martini, J. Nairn, J. Simonsen, and J. Youngblood, *Cellulose nanomaterials review: structure, properties and nanocomposites*, vol. 40, no. 7. 2011.

[46] S. Kalia *et al.*, “Cellulose-based bio- and nanocomposites: a review,” *Int. J. Polym. Sci.*, vol. 2011, 2011.

[47] I. Pulkkinen, J. Fiskari, and V. Alopaeus, “The effect of hardwood fiber morphology on the

hygroexpansivity of paper," *BioResources*, vol. 4, no. 1, pp. 126–141, 2009.

[48] M. Jawaid and H. P. S. Abdul Khalil, "Cellulosic/synthetic fibre reinforced polymer hybrid composites: A review," *Carbohydr. Polym.*, vol. 86, no. 1, pp. 1–18, Aug. 2011.

[49] D. White *et al.*, "Effects of loblolly pine wood and pulp properties on sheet characteristics," *Tappi J.*, vol. 10, pp. 36–42, Feb. 2011.

[50] I. Filipova *et al.*, "Comparison of the properties of wood and pulp fibers from lodgepole pine (*Pinus contorta*) and scots pine (*Pinus sylvestris*)," *Bioresources*, vol. 7, pp. 1771–1783, Feb. 2012.

[51] R. Wimmer, G. Downes, R. Evans, and J. French, "Effects of site on fibre, kraft pulp and handsheet properties of *Eucalyptus globulus*," *Ann. For. Sci.*, vol. 65, no. 6, p. 602, 2008.

[52] R. C. Francis, R. B. Hanna, S.-J. J. Shin, A. F. Brown, and D. E. Riemenschneider, "Papermaking characteristics of three Populus clones grown in the north-central United States," *Biomass and Bioenergy*, vol. 30, no. 8, pp. 803–808, Aug. 2006.

[53] M. Hietala and K. Oksman, "Pelletized cellulose fibres used in twin-screw extrusion for biocomposite manufacturing: fibre breakage and dispersion," *Compos. Part A Appl. Sci. Manuf.*, vol. 109, pp. 538–545, 2018.

[54] A. D. L. Subasinghe, R. Das, and D. Bhattacharyya, "Fiber dispersion during compounding/injection molding of PP/kenaf composites: flammability and mechanical properties," *Mater. Des.*, vol. 86, pp. 500–507, 2015.

[55] H. Jakubowski, "Structure & Reactivity in Chemistry: Introduction to Biomolecules." [Online]. Available: http://employees.csbsju.edu/hjakubowski/classes/ch125/IB1_IMF_Lipid_Aggregates.html. [Accessed: 20-Jan-2020].

[56] J.-L. Salager, "Surfactants types and uses," Mérida, Venezuela, 2002.

[57] D. Leckband and J. Israelachvili, "Intermolecular forces in biology," *Q. Rev. Biophys.*, vol. 34, no. 2, pp. 105–267, May 2001.

[58] N. A. Ivanova and V. M. Starov, "Wetting of low free energy surfaces by aqueous surfactant solutions," *Curr. Opin. Colloid Interface Sci.*, vol. 16, no. 4, pp. 285–291, 2011.

[59] D. Brutin and V. Starov, “Recent advances in droplet wetting and evaporation,” *Chem. Soc. Rev.*, vol. 47, no. 2, pp. 558–585, 2018.

[60] J. Peters and G. E. Croft, “Pulp containing hydrophilic debonder and process for its application,” 4432833, 1984.

[61] T. Seyidoglu and U. Yilmazer, “Modification and characterization of bentonite with quaternary ammonium and phosphonium salts and its use in polypropylene nanocomposites,” *J. Thermoplast. Compos. Mater.*, vol. 28, no. 1, pp. 86–110, 2015.

[62] B. Perlmutter, *Solid-Liquid Filtration: Practical Guides in Chemical Engineering*. Elsevier, 2015.

[63] N. P. Cheremisinoff, “Industrial liquid filtration equipment,” in *Fibrous Filter Media*, P. J. Brown and C. L. B. T.-F. F. M. Cox, Eds. Woodhead Publishing, 2017, pp. 27–50.

[64] B. Perlmutter, “Choosing a fine-particle filtration system,” *Chem. Eng. Prog.*, vol. 110, no. 12, pp. 35–39, 2014.

[65] N. P. Cheremisinoff, *Liquid Filtration*, 2nd ed. Boston: Elsevier, 1998.

[66] K. S. Sutherland and G. Chase, *Filters and Filtration Handbook*, 5th ed. Elsevier, 2007.

[67] F. J. Merchel III, M. A. Tardie, and R. C. Short, “Rotary drum filtering apparatus,” 10035088, 31-Jul-2018.

[68] R. Boiocchi *et al.*, “Dynamic model validation and advanced polymer control for rotating belt filtration as primary treatment of domestic wastewaters,” *Chem. Eng. Sci.*, vol. 217, p. 115510, 2020.

[69] Dorzammir, “Rotary Drum Vaccum Filter Scraper Discharge,” *Dorzammir*, 2018. [Online]. Available: https://imgbin.com/png/LRNV5msL/rotary-vacuum-drum-filter-suction-filtration-filter-press-png. [Accessed: 20-Apr-2019].

[70] L. Simon, “Fundamentals of Nanotechnology: Nanocomposites,” Waterloo, 2018.

[71] P. M. Wambua and R. Anandjiwala, “A review of performs for the composites industry,” *J. Ind. Text.*, vol. 40, no. 4, pp. 310–333, 2011.

[72] N. Tjernlund, “Investigation of pulp dewatering–relating freeness to filtration properties,” Chalmers University of Technology, 2013.

[73] S. A. Khristianovich, “Fundamentals of filtration theory,” *J. Min. Sci.*, vol. 27, no. 1, pp. 1–15, 1991.

[74] F. M. Tiller and M. Shirato, “The role of porosity in filtration: VI. New definition of filtration resistance,” *AIChE J.*, vol. 10, no. 1, pp. 61–67, 1964.

[75] A. Rushton, A. S. Ward, and R. G. Holdich, *Solid-Liquid Filtration and Separation Technology*. Wiley Blackwell, 2008.

[76] T. J. Donohue and C. M. Wensrich, “Improving permeability prediction for fibrous materials through a numerical investigation into pore size and pore connectivity,” *Powder Technol.*, vol. 195, no. 1, pp. 57–62, 2009.

[77] C. Kleinstreuer, *Modern Fluid Dynamics: Basic Theory and Selected Applications in Macro- and Micro-Fluidics*, vol. 87. Dordrecht: Springer Netherlands, 2010.

[78] B. Sarkar, M. Megharaj, Y. Xi, and R. Naidu, “Structural characterisation of Arquad® 2HT-75 organobentonites: Surface charge characteristics and environmental application,” *J. Hazard. Mater.*, vol. 195, pp. 155–161, Nov. 2011.

[79] D. C. Montgomery, *Design and Analysys of Experiments*, 8th ed. John Wiley & Sons, 2013.

[80] A. K. Mohanty, M. Misra, and L. T. Drzal, “Surface modifications of natural fibers and performance of the resulting biocomposites: An overview,” *Compos. Interfaces*, vol. 8, no. 5, pp. 313–343, 2001.

[81] H. Gupta, K. K. Kanaujia, S. M. A. Rizvi, and R. Shukla, “A review on the mechanical properties of natural fibre reinforced polypropylene composites,” *Int. Res. J. Eng. Technol.*, vol. 06, no. 06, pp. 337–342, 2019.

[82] M. A. Khan, J. Ganster, and H.-P. Fink, “Hybrid composites of jute and man-made cellulose fibers with polypropylene by injection moulding,” *Compos. Part A Appl. Sci. Manuf.*, vol. 40, no. 6–7, pp. 846–851, 2009.

[83] J. L. Thomason and J. L. Rudeiros-Fernández, “A review of the impact performance of natural fiber thermoplastic composites,” *Front. Mater.*, vol. 5, p. 60, 2018.

[84] N. P. Chopey and T. G. Hicks, Eds., *Handbook of Chemical Engineering Calculations*. New York: McGraw-Hill, 1984.

Appendix A - Examples of Calculation

The rotary vacuum drum filter shown in Figure 72 is used for filtering, cleaning, drying and discharging a cake. The following calculations are important in this research because they will be used in the design of the laboratory filter drum [25].

The following values and parameters are assumed to be used in subsequent calculations to serve as an example for how the operation of a drum filter can be assessed [25]:

- Cake mass W_c (in $\text{lb}_\text{m}/\text{ft}^2$) is $7.2 \times L$, where L is cake thickness in inches;
- Maximum submergence is 126°; effective submergence is 108°;
- Maximum washing arc is 104°; suction (initial drying) arc is 27°;
- Discharge and resub-mergence arc is 90°;
- Minimum cake thickness is 1/8 in (0.0032 m).

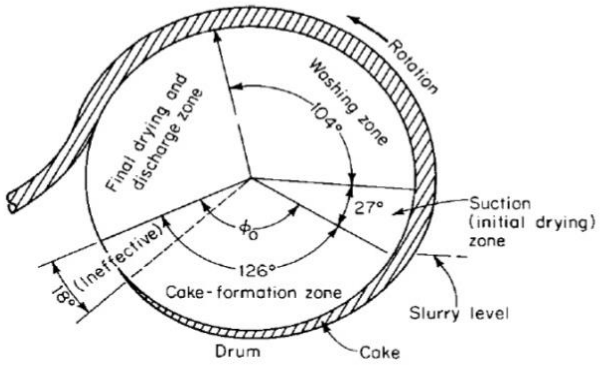

Figure 72: Rotary vacuum drum filter [84]

Cake mass calculation

Compute the filtration time, given a thickness of 0.30 in

$$W_c = 7.2 \times L = 7.2 \times 0.30 = 2.16\ \text{lb}_\text{m}/\text{ft}^2$$

Filtration time

According to Figure 73, with cake mass (W_c) equal to 2.16 lb_m/ft^2, filtration time is approximately 0.26 min.

Filtration rate

$$\text{Filtration rate} = \frac{W_c}{\text{filtration time}} = \frac{2.16}{0.26} \times 60 = 499 \frac{\text{lb}_\text{m}}{\text{h ft}^2}$$

Minimum cycle for cake build-up.

Effective submergence = 108°, which is equal to 30 % of the cylinder's circumference.

The minimum cycle based on cake build-up is filtration time divided by fraction (%) of cylinder circumference.

$$\text{Minimum cycle } = \frac{0.26}{0.3} = 0.87 \text{ min/r}$$

Representing 1.15 r/min.

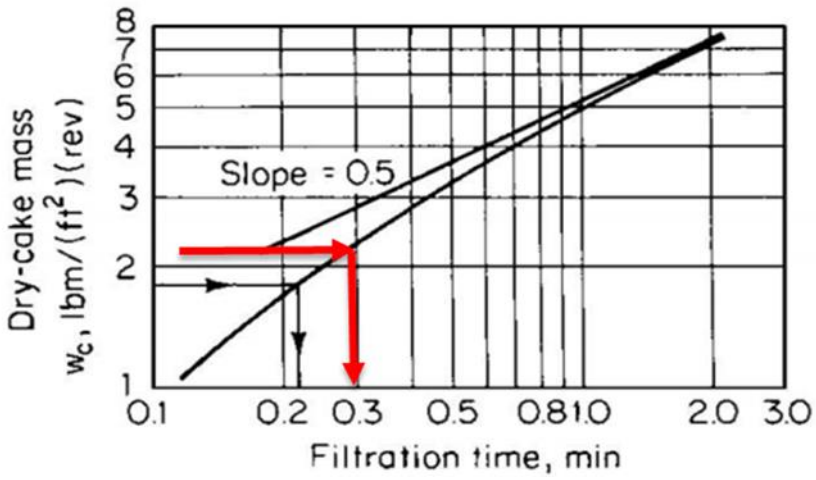

Figure 73: Dry cake mass versus filtration time [25]

Appendix B – Calculation of the Cake from the Lab-Scale Rotary Drum Filtration System.

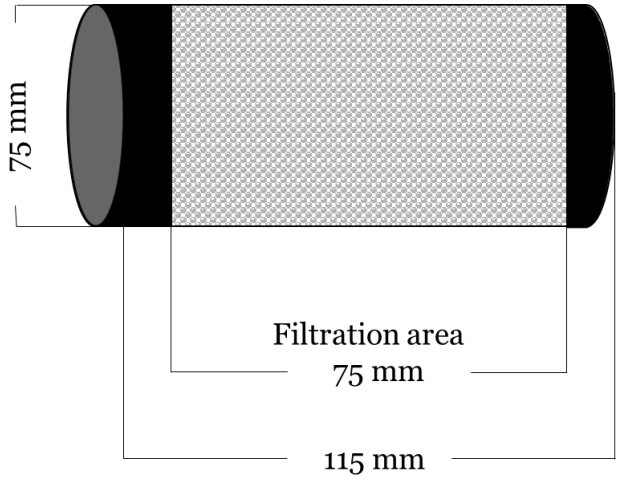

Figure 74: Dimensions of the lab-scale rotary vacuum drum filter filtration system.

Cake demonstration – CW6

Mass of dry solids (M_s)= 31.09 g

Effective submergence (Es) = 180°

Vacuum time (when the filter is submerged, t_V min) = 60 s

A_{cEs} = cylinder area effective submergence

$A_c = 2\pi\ r\ (\ r + h\ )$ ⟶ Ac = 26,5072.5 mm^2 ⟶ A_{cEs}= 132.5363 cm^2

$$\text{Filtration rate} = \frac{M_s}{A_s \times t_V} \qquad \text{Filtration rate} = \frac{31.09\ (g)}{132.5363\ (cm^2) \times 1(min)}$$

Filtration rate = 0.2345 ($g/cm^2.min$)

$$\text{Filtration time} = \frac{t_V}{\frac{rpm}{Es}} \qquad \text{Filtration time} = \frac{60\ (s)}{3.8\ (rpm) \times \frac{360°}{180°}}$$

Filtration time = 7.9 s

Appendix C – Figures Copyright

Figure 2)

Copyright

Copyright © 2015 Layth Mohammed et al. This is an open access article distributed under the Creative Commons Attribution License, which permits unrestricted use, distribution, and reproduction in any medium, provided the original work is properly cited.

Figure 4 and 5)

SPRINGER NATURE LICENSE
TERMS AND CONDITIONS

Apr 16, 2020

This Agreement between University of Waterloo -- Douglas Casetta ("You") and Springer Nature ("Springer Nature") consists of your license details and the terms and conditions provided by Springer Nature and Copyright Clearance Center.

License Number	4810590491874
License date	Apr 16, 2020
Licensed Content Publisher	Springer Nature
Licensed Content Publication	Springer eBook
Licensed Content Title	Classification of Composite Materials
Licensed Content Author	Holm Altenbach, Johannes Altenbach, Wolfgang Kissing
Licensed Content Date	Jan 1, 2018
Type of Use	Thesis/Dissertation
Requestor type	academic/university or research institute
Format	electronic
Portion	figures/tables/illustrations
Number of figures/tables/illustrations	2

Figure 6)

ELSEVIER LICENSE
TERMS AND CONDITIONS

Apr 16, 2020

This Agreement between University of Waterloo -- Douglas Casetta ("You") and Elsevier ("Elsevier") consists of your license details and the terms and conditions provided by Elsevier and Copyright Clearance Center.

License Number	4810600269996
License date	Apr 16, 2020
Licensed Content Publisher	Elsevier
Licensed Content Publication	Elsevier Books
Licensed Content Title	Interface Engineering of Natural Fibre Composites for Maximum Performance
Licensed Content Author	A. Arbelaiz,I. Mondragon
Licensed Content Date	Jan 1, 2011
Licensed Content Pages	40
Start Page	146
End Page	185
Type of Use	reuse in a thesis/dissertation

Figure 7)

SPRINGER NATURE LICENSE
TERMS AND CONDITIONS

Apr 16, 2020

This Agreement between University of Waterloo -- Douglas Casetta ("You") and Springer Nature ("Springer Nature") consists of your license details and the terms and conditions provided by Springer Nature and Copyright Clearance Center.

License Number	4810601212769
License date	Apr 16, 2020
Licensed Content Publisher	Springer Nature
Licensed Content Publication	Cellulose
Licensed Content Title	Effect of preparation process of microfibrillated cellulose-reinforced polypropylene upon dispersion and mechanical properties
Licensed Content Author	Katsuhito Suzuki et al
Licensed Content Date	Jun 22, 2017
Type of Use	Thesis/Dissertation
Requestor type	academic/university or research institute
Format	electronic
Portion	figures/tables/illustrations

Figure 8)

ELSEVIER LICENSE
TERMS AND CONDITIONS

Apr 16, 2020

This Agreement between University of Waterloo -- Douglas Casetta ("You") and Elsevier ("Elsevier") consists of your license details and the terms and conditions provided by Elsevier and Copyright Clearance Center.

License Number	4810800294523
License date	Apr 16, 2020
Licensed Content Publisher	Elsevier
Licensed Content Publication	Progress in Polymer Science
Licensed Content Title	Composites reinforced with cellulose based fibres
Licensed Content Author	A.K Bledzki,J Gassan
Licensed Content Date	May 1, 1999
Licensed Content Volume	24
Licensed Content Issue	2
Licensed Content Pages	54
Start Page	221
End Page	274
Type of Use	reuse in a thesis/dissertation

Figure 9)

ELSEVIER LICENSE
TERMS AND CONDITIONS

Apr 16, 2020

This Agreement between University of Waterloo -- Douglas Casetta ("You") and Elsevier ("Elsevier") consists of your license details and the terms and conditions provided by Elsevier and Copyright Clearance Center.

License Number	4810800837030
License date	Apr 16, 2020
Licensed Content Publisher	Elsevier
Licensed Content Publication	Composites Part B: Engineering
Licensed Content Title	Hemp fiber reinforced polypropylene composites: The effects of material treatments
Licensed Content Author	Theresa Sullins,Selvum Pillay,Alastair Komus,Haibin Ning
Licensed Content Date	Apr 1, 2017
Licensed Content Volume	114
Licensed Content Issue	n/a
Licensed Content Pages	8
Start Page	15
End Page	22
Type of Use	reuse in a thesis/dissertation

Figure 11)

16/04/2020 RightsLink Printable License

JOHN WILEY AND SONS LICENSE
TERMS AND CONDITIONS

Apr 16, 2020

This Agreement between University of Waterloo -- Douglas Casetta ("You") and John Wiley and Sons ("John Wiley and Sons") consists of your license details and the terms and conditions provided by John Wiley and Sons and Copyright Clearance Center.

License Number	4810831424101
License date	Apr 16, 2020
Licensed Content Publisher	John Wiley and Sons
Licensed Content Publication	Journal of Polymer Science
Licensed Content Title	Polymer materials science, Jerold M. Schultz, Prentice-Hall, Englewood Cliffs, N.J., 1974, 524 pp.
Licensed Content Author	Ian R. Harrison
Licensed Content Date	Mar 11, 2003
Licensed Content Volume	12
Licensed Content Issue	10
Licensed Content Pages	2

Figure 12)

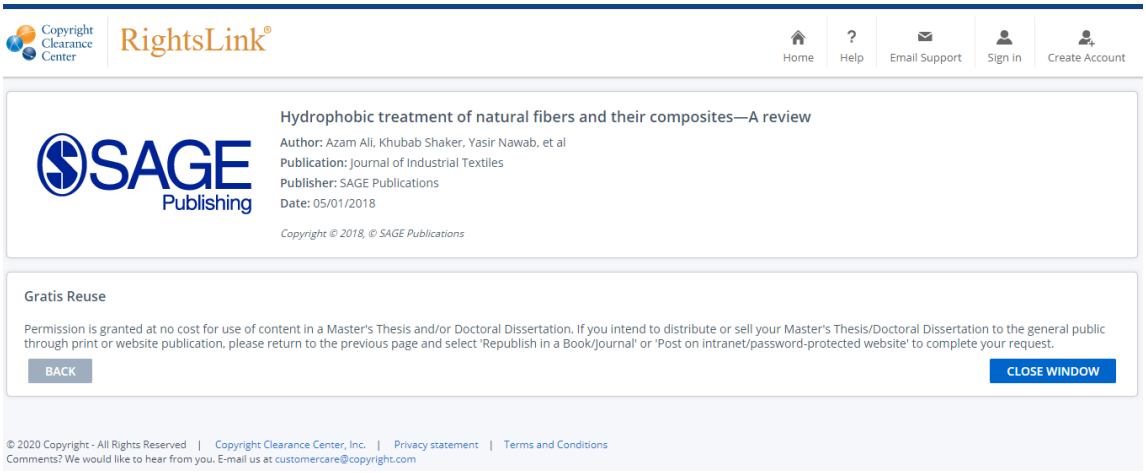

Figure 13)

© 2015 The Author(s). Licensee IntechOpen. This chapter is distributed under the terms of the Creative Commons Attribution 3.0 License, which permits unrestricted use, distribution, and reproduction in any medium, provided the original work is properly cited.

Figure 14)

This site is written and maintained by Henry Jakubowski as part of a Structure & Reactivity in Organic, Biological and Inorganic Chemistry written by Chris P. Schaller, Ph.D., College of Saint Benedict / Saint John's University. It is freely available for educational use.

Structure & Reactivity in Organic, Biological and Inorganic Chemistry by Chris Schaller is licensed under a Creative Commons Attribution-NonCommercial 3.0 Unported License.

Send corrections for this chapter to hjakubowski@csbsju.edu

Figure 15)

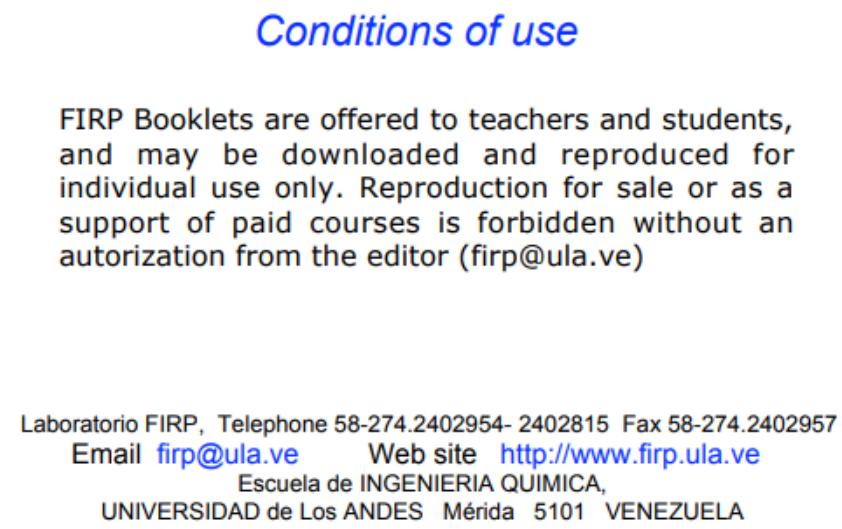

Conditions of use

FIRP Booklets are offered to teachers and students, and may be downloaded and reproduced for individual use only. Reproduction for sale or as a support of paid courses is forbidden without an autorization from the editor (firp@ula.ve)

Laboratorio FIRP, Telephone 58-274.2402954- 2402815 Fax 58-274.2402957
Email firp@ula.ve Web site http://www.firp.ula.ve
Escuela de INGENIERIA QUIMICA,
UNIVERSIDAD de Los ANDES Mérida 5101 VENEZUELA

Figure 16)

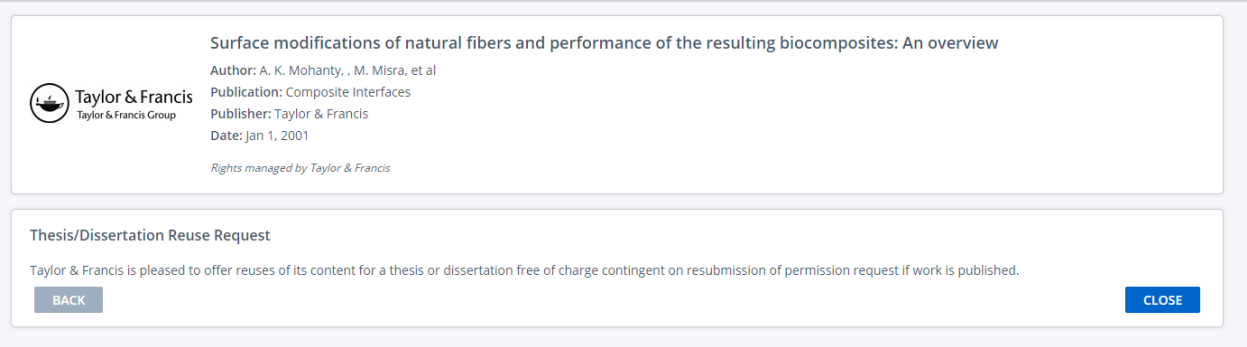

Taylor & Francis
Taylor & Francis Group

Surface modifications of natural fibers and performance of the resulting biocomposites: An overview

Author: A. K. Mohanty, , M. Misra, et al
Publication: Composite Interfaces
Publisher: Taylor & Francis
Date: Jan 1, 2001

Rights managed by Taylor & Francis

Thesis/Dissertation Reuse Request

Taylor & Francis is pleased to offer reuses of its content for a thesis or dissertation free of charge contingent on resubmission of permission request if work is published.

BACK CLOSE

Figure 18)

https://imgbin.com/png/LRNV5msL/rotary-vacuum-drum-filter-suction-filtration-filter-press-png

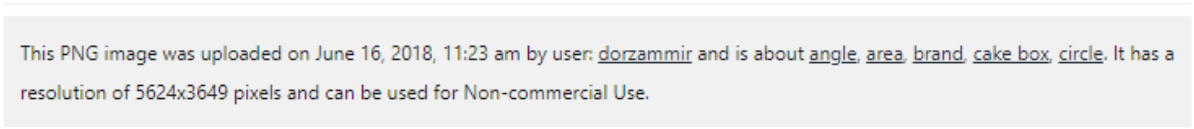

Figure 19)

https://commons.wikimedia.org/wiki/File:Filtro_a_tamburo_tipo_Oliver.svg

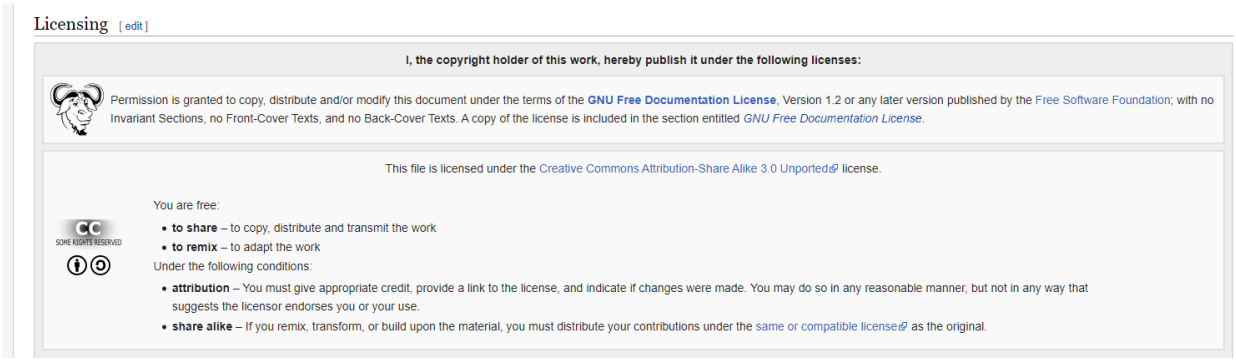

Figures : 21, 22, 23, 24, and 25)

17/04/2020 RightsLink Printable License

ELSEVIER LICENSE
TERMS AND CONDITIONS

Apr 17, 2020

This Agreement between University of Waterloo -- Douglas Casetta ("You") and Elsevier ("Elsevier") consists of your license details and the terms and conditions provided by Elsevier and Copyright Clearance Center.

License Number	4811380856769
License date	Apr 17, 2020
Licensed Content Publisher	Elsevier
Licensed Content Publication	Elsevier Books
Licensed Content Title	Solid-Liquid Filtration
Licensed Content Author	Barry A. Perlmutter
Licensed Content Date	Jan 1, 2015
Licensed Content Pages	20
Start Page	1
End Page	20
Type of Use	reuse in a thesis/dissertation
Portion	figures/tables/illustrations
Number of figures/tables/illustrations	6